



Theses and Dissertations

2004-03-18

High-Torque Capacity Compliant Centrifugal Clutches

Ryan G. Weight
Brigham Young University - Provo

Follow this and additional works at: <https://scholarsarchive.byu.edu/etd>



Part of the [Mechanical Engineering Commons](#)

BYU ScholarsArchive Citation

Weight, Ryan G., "High-Torque Capacity Compliant Centrifugal Clutches" (2004). *Theses and Dissertations*. 10.

<https://scholarsarchive.byu.edu/etd/10>

This Thesis is brought to you for free and open access by BYU ScholarsArchive. It has been accepted for inclusion in Theses and Dissertations by an authorized administrator of BYU ScholarsArchive. For more information, please contact scholarsarchive@byu.edu, ellen_amatangelo@byu.edu.

HIGH-TORQUE CAPACITY COMPLIANT
CENTRIFUGAL CLUTCHES

by

Ryan G. Weight

A thesis submitted to the faculty of

Brigham Young University

in partial fulfillment of the requirements for the degree of

Master of Science

Department of Mechanical Engineering

Brigham Young University

April 2004

BRIGHAM YOUNG UNIVERSITY

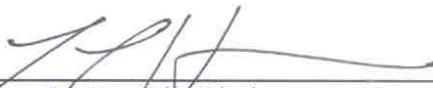
GRADUATE COMMITTEE APPROVAL

of a thesis submitted by

Ryan G. Weight

This thesis has been read by each member of the following graduate committee and by majority vote has been found to be satisfactory.

12 March 2004
Date


Larry L. Howell, Chair

12 March '04
Date


Spencer P. Magleby

12 MARCH 2004
Date


Robert H. Todd

BRIGHAM YOUNG UNIVERSITY

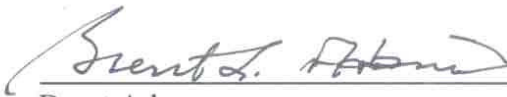
As chair of the candidate's graduate committee, I have read the thesis of Ryan G. Weight in its final form and have found that (1) its format, citations, and bibliographical style are consistent and acceptable and fulfill university and department style requirements; (2) its illustrative materials including figures, tables, and charts are in place; and (3) the final manuscript is satisfactory to the graduate committee and is ready for submission to the university library.

12 March 2004
Date



Larry L. Howell
Chair, Graduate Committee

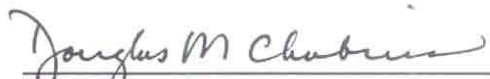
Accepted for the Department



Brent Adams
Graduate Coordinator

Accepted for the College

ogy



Douglas M. Chabries
Dean, College of Engineering and Technol-

ABSTRACT

HIGH-TORQUE CAPACITY COMPLIANT CENTRIFUGAL CLUTCHES

Ryan G. Weight

Department of Mechanical Engineering

Master of Science

This thesis developed high-torque-capacity floating opposing arm clutches that are manufactured with standard economical manufacturing processes, while maintaining critical performance characteristics. Contact engagement speed and torque capacity models were created for the Hoffco-Comet, floating-opposing-arm (FOA), and floating 1 (F1) clutches. Sensitivity analyses were performed to identify key design parameters. A robust compliant FOA clutch was designed by minimizing the tolerance for both contact engagement speed and torque capacity. The robust design insures that the clutch will operate within the prescribed application constraints. Additional modeling showed that using a layered clutch would significantly tighten the contact engagement speed and torque performance tolerances. The riveted layered clutch reduced engagement and torque tolerances by 83% in comparison to a single layer clutch. Two versions of the multi-layer FOA clutch were fabricated. Each clutch consisted of 10 layers and assembled into the drum of the benchmark clutch. Testing showed that the MFOA clutch's torque-speed characteristics performed comparable to the benchmark clutch. In addition, testing validated the torque-speed models and showed the validity of using multiple layers for future manufacturing.

ACKNOWLEDGEMENTS

This research was supported by funding from the Utah Center of Excellence Program and BYU's Compliant Mechanisms Research group. These programs are gratefully acknowledged for their help. I would like to acknowledge the continuous help and support of Dr. Larry Howell. He has dedicated countless hours to training, guiding, and teaching me. His impact on me extends beyond the engineering classroom and laboratory. I would also like to acknowledge the help of the Mechanical Engineering Faculty and staff. They have been an immense help to me and have always been there. Especially the help of Dr. Spencer Magleby and Dr. Robert Todd for their support and direction with regards to this work. The help of Kevin Cole, Derek Wright, and Blake Dyer in development and testing the Multi Layered Floating Opposing Arm Clutch is appreciated and acknowledged. I would also like to thank my wonderful parents and siblings. They have truly inspired me to greater heights. I am thankful for their support and motivation. Most of all, I would like to thank my Heavenly Father for His help and guidance throughout my scholastic endeavors.

Table of Contents

CHAPTER 1 Introduction.....	1
1.1 Problem.....	1
1.2 Thesis Objective	2
1.3 Benefits of Centrifugal Clutches.....	3
1.4 Thesis Contributions.....	4
1.5 Thesis Outline	6
CHAPTER 2 Literature Review	7
2.1 Clutches	7
2.1.1 Traditional Centrifugal Clutches	8
2.1.2 Compliant Clutches	10
2.1.3 Benefits of Centrifugal Clutches	12
2.1.4 Undesirable Characteristics	13
2.1.5 Clutch Patents	13
2.2 Theoretical Analysis of Clutches	14
2.2.1 Basic Operating Principles	14
2.2.2 Standard Centrifugal Clutch Comparison Method	17
2.2.3 Self-Locking / Self-Energizing Characteristic of Clutches	17
2.2.4 Specific Applications.....	19
2.2.5 Floating-Opposing-Arm Clutch Model	19
2.2.6 Friction.....	21
2.3 Implementing Compliant Mechanism Theory	22
2.3.1 Compliant Mechanisms.....	22
2.4 Manufacturing Considerations.....	24
2.5 Results of Preliminary Testing	26
2.5.1 Ground Tiller Application	26
2.5.2 Go-Kart Application	29
2.5.3 Preliminary Test Problems	30
CHAPTER 3 Research Methodology	31
3.1 FOA Modeling	32
3.2 Testing	32
3.2.1 Benchmarking.....	32
3.2.2 Prototypes	33
3.2.3 Measured Test Data	34

3.3 Evaluation Criteria	34
3.3.1 Torque Capacity	34
3.3.2 Accuracy of Engagement.....	34
3.3.3 Smoothness of Engagement.....	35
3.3.4 Manufacturability of the Clutch.....	35
3.3.5 Performance Sensitivity	36
3.4 Clutch Testing	36
3.4.1 Test Setup	36
3.4.2 Data Measurements	38
3.4.3 Test Procedures.....	38
3.4.4 Error Sources	39
3.5 Comparing FOA Clutch to Benchmark Clutch.....	40
CHAPTER 4 Models for Centrifugal Clutches	43
4.1 Hoffco-Comet 4 inch Go-Kart Clutch	43
4.1.1 Contact Engagement Speed Model.....	44
4.1.2 Torque Model	45
4.2 Floating-Opposing-Arm Clutch.....	47
4.2.1 Contact Engagement Speed Model.....	48
4.2.2 Torque Model	50
4.3 Floating 1 (F1) Clutch.....	52
4.3.1 Engagement Model.....	53
4.3.2 Torque Model	57
CHAPTER 5 Minimizing Performance Tolerances	61
5.1 Manufacturing Issues for Compliant Mechanisms.....	61
5.1.1 Advantages of the Hybrid Process	64
5.1.2 Disadvantages of the Hybrid Process	65
5.2 Sensitivity of Key Parameters	66
5.2.1 Numerical Derivatives	66
5.2.2 Manufacturing and Design Tolerances	69
5.2.3 Performance Tolerances	70
5.2.4 Accuracy of Performance Tolerance Modeling.....	73
5.2.5 Robust Clutch Design	75
5.2.6 Basic Parameter-Performance Relationships.....	78
5.3 Performance of Layers.....	79
5.3.1 Benefits of Multiple Layers	79
5.3.2 Monte-Carlo Simulations for Multiple Layers	80
5.4 Summary	83
CHAPTER 6 Testing	85
6.1 Test Setup	85

6.2 Benchmarking (Hoffco-Comet) Testing	87
6.2.1 Contact Engagement Speed (Comet).....	88
6.2.2 Torque Capacity (Comet)	89
6.2.3 Observations of Benchmark Testing	90
6.3 Multi-layer Floating Opposing Arm (MFOA) Testing	90
6.3.1 Contact Engagement Speed (MFOA).....	92
6.3.2 Torque Capacity (MFOA)	94
6.3.3 Observations of MFOA Testing	95
6.4 Comparison of Comet Clutch to the MFOA Clutch.....	97
6.4.1 Contact Engagement	97
6.4.2 Torque Capacity	97
6.5 Results of Layered Approach	100
6.6 Summary	100
CHAPTER 7 Conclusions and Recommendations	103
7.1 Contributions	103
7.1.1 Modeling of Comet, FOA, and F1 Clutches.....	103
7.1.2 Parameter Sensitivity Analysis.....	104
7.1.3 Minimizing Engagement & Torque Performance Tolerances	104
7.1.4 Simulation of Free Floating and Riveted Layer Clutches	105
7.1.5 Testing of two Multi-layer Floating Opposing Arm Clutches	105
7.2 Summary of Keys to Future FOA Clutches Design	106
7.3 Recommendations	107
7.3.1 Fatigue Testing	107
7.3.2 Accurately Determine the Coefficient of Friction	107
7.3.3 Benchmark Costs of Manufacturing.....	107
7.3.4 Dynamics of the Clutch System	108
7.3.5 Create a Multi-Engagement Speed Clutch	108
7.4 Conclusions	108
REFERENCES	109
APPENDIX A Sensitivity of Key Design Parameters	113
A.1 Design Parameters for 4 inch FOA Clutch	113
A.2 Floating 1 (F1) Clutch's Sensitivity	114
A.3 Sensitivity of the 2 1/8 inch FOA Clutch.....	115
A.4 FOA Sensitivity Chart when = 20 degrees	116
A.5 FOA Performance Tolerance Verification	117
A.6 FOA Robust Design Parameter	119
A.7 FOA Performance Frequency Chart	120
A.8 Monte Carlo Layer Simulation	121

APPENDIX B Test Set-up and Test Results	123
B.1 Dynamometer	123
B.2 Benchmark Clutch	124
B.2.1 Benchmark Contact Engagement Speed Data	124
B.2.2 Benchmark Engagement Speed Data	126
B.2.3 Benchmark Torque Capacity Data.....	127
B.3 Multi-layer Floating Opposing Arm (MFOA) Clutch.....	131
B.3.1 MFOA Model Parameter Values	131
B.3.2 MFOA vA SHA Contact Engagement Speed Data	132
B.3.3 MFOA vA LHA Contact Engagement Speed Data	135
B.3.4 MFOA vB SHA Contact Engagement Speed Data	136
B.3.5 MFOA vB LHA Contact Engagement Speed Data	138
B.3.6 MFOA vA SHA Torque Capacity Data.....	140
B.3.7 MFOA vB LHA Torque Capacity Data.....	142

List of Figures

Figure 1.1	Compliant floating-opposing-arm clutch (FOA) designed by Crane et al.	2
Figure 1.2	Four main components of a centrifugal clutch.	4
Figure 2.1	(a) Connected Shoe Clutch (b) Floating Shoe Clutch and (c) Flexible Trailing Shoe Clutch.....	9
Figure 2.2	Two types of existing compliant clutches: (a) Compliant C4 clutch and (b) Compliant S-clutch.	10
Figure 2.3	Various clutch designs developed by Crane et al. (a) Floating 1 Clutch (b) Floating-Opposing-Arm Clutch (c) Grounded-Opposing Arm clutch and (d) Split-Arm Clutch	11
Figure 2.4	(a) St. John's [10] patented connected shoe clutch. (b) Nagashima's [11] patented floating shoe clutch.....	13
Figure 2.5	Various patented one piece s-clutch designs. (a) Dietzsh et. al. [20] (b) Ruddy [17] and (c) Sageshima [18].....	14
Figure 2.6	(a) Body rotating at a constant angular velocity. (b) The motion equations using the standard form of Newton's Second Law. (c) The motion equations using D'Alembert's Principle and centrifugal forces are shown.	15
Figure 2.7	Friction force that transmits torque between the shoe clutch and drum.	16
Figure 2.8	Forces acting on a clutch, which may cause self-locking.....	18
Figure 2.9	FOA clutch with its PRBM	20
Figure 2.10	Comparison between (a) compliant crimping mechanism developed by AMP Inc., and its (b) rigid-body counterpart [1].	22
Figure 2.11	(a) Compliant overrunning clutch and (b) Equivalent rigid-body design shown disassembled.....	23
Figure 2.12	The hybrid process used on compliant overrunning clutch.....	25
Figure 2.13	Two 2 1/8 inch clutches used in a ground tiller (a) Floating-opposing-arm clutch (b) Connected shoe clutch.....	27
Figure 2.14	Friction between clutch and clutch fixture made the clutch not disengage from the drum.	29
Figure 3.1	FOA clutch design to fit in the Comet (benchmark) clutch's drum.....	33
Figure 3.2	Sample data taken from the testing Comet's 2 1/8 clutch. a) Torque vs. rpm data when the clutch is slipping (b) Large spike represents an aggressive engagement.....	35
Figure 3.3	Main factors that affect the manufacturability of the FOA clutch.	36
Figure 3.4	Set-up for testing the clutch's engagement accuracy and characteristics, as well as the clutch's torque capacity. (a) Actual pictures and (b) Top view schematic of testing apparatus.....	37
Figure 4.1	Model parameters of the Hoffco-Comet 4 inch clutch.....	44
Figure 4.2	Floating-Opposing-Arm (FOA) clutch with key design parameters.	47
Figure 4.3	The design parameters of this section of a FOA segment is used to solve for the contact engagement speed.....	48

Figure 4.4	Force and moment equilibrium diagrams for the FOA clutch that are used to solve for torque capacity.....	51
Figure 4.5	The Floating 1 (F1) clutch with key design parameters.	53
Figure 4.6	Force and moment diagrams for (a) half a segment and (b) one segment of the F1 clutch.....	55
Figure 5.1	Key parameters for manufacturing process capabilities of compliant mechanisms. (a) shows the thickness, length and depth of the flexible segment and (b) shows how the thickness of the flexible segment relates to the FOA clutch.	62
Figure 5.2	FOA clutch shown with multiple layers that float on hub.....	63
Figure 5.3	Drum profile due to manufacturing process.	65
Figure 5.4	FOA clutch's design parameters.....	66
Figure 5.5	The FOA clutch's most sensitive clutch parameters for (a) Contact Engagement Speed and (b) Torque Capacity. Sensitivities are the same as those found in Table 5.3	68
Figure 5.6	α is the angle that determines how much of the clutch's surface engages with the drum.....	69
Figure 5.7	Percent contribution of design parameters to the (a) contact engagement speed and (b) torque capacity for the FOA clutch.....	72
Figure 5.8	Cause-effect relationship between design parameters and engagement & torque performance.	78
Figure 5.9	Different layered clutches: a) Free-floating and b) Riveted.	80
Figure 5.10	Frequency chart for the single layer clutch: (a) contact engagement speed and (b) torque capacity.	81
Figure 5.11	The (a) free floating layer clutch's engagement and torque are based on individual layer parameters, while the (b) riveted layer clutch's engagement and torque are based on the average parameter values for all layers and the smallest clearanc.	82
Figure 6.1	Set-up for testing the clutch's engagement accuracy and characteristics, as well as the clutch's torque capacity. (a) Actual pictures and (b) Top view schematic of testing apparatus.....	86
Figure 6.2	Hoffco-Comet 4 inch go-kart clutch. Consist of 6 shoes held together by a spring wrapped around the groove.	87
Figure 6.3	Contact engagement speed (2055 rpm) and smoothness of engagement for the Comet 4 inch go-kart clutch: (a) smooth engagement and (b) mild rough engagement.....	88
Figure 6.4	Maximum torque capacity of Comet clutch. Max torque capacity occurs when the clutch slips on the hub (Pt A).	89
Figure 6.5	Plotted torque values where Comet clutch slipped and other torque values along with predicted values from model.	90
Figure 6.5	The (a) shoe and (b) drum wear of the Comet clutch. Only half of the shoe engages with the drum because the spring wraps around the shoe a little off center.	91
Figure 6.6	MFOA clutch assembled into a Comet drum. The clutch consist of 10 layers of spring steel: each 0.062" thick.....	91
Figure 6.7	Contact engagement speed (2436 & 2224) and smooth engagement for the (a) MFOA vA LHA clutch and (b) MFOA vB LHA clutch.....	92

Figure 6.8	Contact engagement speed (2364 & 2102) and rough engagement for the (a) MFOA vA SHA clutch and (b) MFOA vB SHA clutch.	93
Figure 6.9	(a) Loading of the MFOA vA SHA clutch. (b) Torque points for the MFOA vA SHA clutch that are limited by the engine's output torque.	94
Figure 6.10	(a) Measured torque values that are below the torque curve because of the engine output limitation. No clutch slippage occurred at these points (b) FOA model's estimated torque values when the COF is 0.55.....	95
Figure 6.11	The (a) shoe and (b) drum wear of the MFOA vA clutch.....	96
Figure 6.12	Impression marks left by the clutch on the short hub arms.	96
Figure 6.13	The MFOA vB LHA slipping at 2500 rpm and 8 ft-lbs	98
Figure 6.14	Experimental data in relation to the model data for all three different designs (Comet, MFOA vA, & MFOA vB) with various coefficients of friction	99

List of Tables

TABLE 2.1	Preliminary test results for a 2 1/8 inch clutch.	27
TABLE 3.1	Description of the Hoffco-Comet's benchmark clutch.	33
TABLE 5.1	Process capabilities for compliant mechanisms as they relate to the small-length flexural pivots found on the FOA clutch.	62
TABLE 5.2	Two new process capabilities for compliant mechanisms	62
TABLE 5.3	Parameter sensitivities for the FOA clutch using central difference method to calculate numerical derivatives.	68
TABLE 5.4	Performance tolerances for several scenarios with the 4 inch and 2 inch FOA clutch.	71
TABLE 5.5	Percent difference between the estimated performance tolerance and that of the Monte-Carlo simulation.	73
TABLE 5.6	Performance tolerance results and percent rejects for various manufacturing processes.	74
TABLE 5.7	Design parameters and corresponding sensitivity values for the optimal solution in minimizing torque capacity performance tolerance.	76
TABLE 5.8	Parameter sensitivity values for the FOA clutch after minimizing performance tolerances.	77
TABLE 5.9	Change in torque performance tolerance with changes in μ and σ	77
TABLE 5.10	Torque performance tolerance for the three types of FOA layered clutches.	83
TABLE 6.1	(a) Torque slippage points where clutch slips and (b) torque values that are under torque curve.	90
TABLE 6.2	MFOA's measured contact engagement speeds. In addition, the predicted and adjusted predicted values are compared to the experimental values.	93
TABLE 6.3	Comet and MFOA clutch's measured contact engagement speeds.	97
TABLE 6.4	Torque capacity of the five clutches at 2400 and 3600 rpm.	100

1.1 Problem

Compliant mechanism technology has been around for centuries, yet has only recently been accurately modeled, thereby enabling better working mechanisms to be created. This technology has many benefits over traditional rigid-body technology mainly due to cost reduction and improved performance characteristics [1]. Because of new modeling capabilities, this new technology can be more readily implemented in existing products.

Crane et al. [2] researched how to implement compliant mechanism technology into the arena of centrifugal clutches. After reviewing existing centrifugal clutch designs, Crane was able to use the compliance potential criteria developed by Roach and Howell [3] and Berglund [4] to identify which centrifugal clutch concepts were most adaptable to compliant mechanisms. Crane then created and prototyped several novel compliant centrifugal clutches out of polypropylene and tested their torque-speed characteristics.

One of the new clutch designs was the innovative compliant floating-opposing-arm clutch (FOA) [2,5,6]. (see Figure 1.1) This clutch consists of three main parts; the hub, the floating shoes (clutch), and the drum. While traditional clutches may contain various pin-joints and springs, the compliant FOA clutch relies on flexible segments to act as

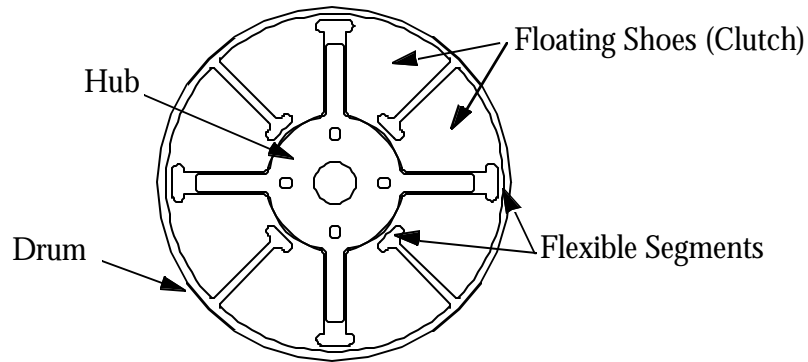


Figure 1.1 Compliant floating-opposing-arm clutch (FOA) designed by Crane et al.

pin-joints and to create a restitution spring force. Due to the elimination of pin-joints, the FOA clutch has dramatically decreased part count compared to traditional designs, which presents numerous possibilities to decrease manufacturing and assembly cost while maintaining torque-speed performance.

Even though it is feasible to re-design existing products with this compliant technology, new applications for this technology have generally been difficult to implement in mature industries. The FOA centrifugal clutch is a perfect example of this difficult implementation. The FOA clutch has not yet penetrated the existing market for two main reasons. First, the torque capacity in high-torque applications of an early design performed poorly in comparison to torque capacity of a benchmark clutch as shown in a preliminary test with a go-kart clutch. Secondly, the original FOA clutch design did not address some critical manufacturing issues, such as maintaining critical tolerances on the flexible segments. The results of this thesis helps address these issues.

1.2 Thesis Objective

The objective of this thesis is to develop high-torque-capacity floating opposing arm clutches that are manufactured with standard economical manufacturing processes, while maintaining critical performance characteristics. It is believed that by manufacturing the compliant clutch in multiple layers¹, not only is it feasible to produce these clutches in high volumes, but the engagement and torque performance variations are tight-

ened, therefore allowing the clutch to perform more consistently. The FOA clutch's torque-speed characteristics are very comparable to those of the benchmark clutches. The FOA clutch design is based on Crane's preliminary concept [2,5,6] and includes consideration of manufacturing issues as they relate to compliant mechanisms' functional characteristics. In addition, the high-torque FOA design accounts for performance sensitivity to variations in both design parameters and manufacturing processes and minimizes such variations.

1.3 Benefits of Centrifugal Clutches

There are multiple centrifugal clutch designs such as trailing shoes, floating shoes, mercury clutch, connected shoes, and oil clutch [6,7]. All of these clutches have different components and designs, but the benefits of centrifugal clutches are the same for each. The benefits include:

- Simplicity of design and operation
- Automatic engagement at a pre-determined speed
- Reduction in startup loads on AC motors and combustion engines
- Cushioning of shock loads on drive train components

Even though centrifugal clutches have different components and designs, they all operate under the principle of centrifugal force. The four main components of a centrifugal clutch are the shoes, the drum, the retaining springs, and the hub (see Figure 1.2). The centrifugal clutch's operation begins with the motor-driven hub rotating the shoes. The clutch then transmits torque to the hub by the shoes being radially forced outward due to the shoe mass and the normal acceleration. The retaining springs provide an opposing force to the centrifugal force, which ultimately controls the speed at which the shoes engage the hub, thereby transmitting torque to the driven shaft. More centrifugal clutch basics will be discussed in Chapter 2.

1. Multiple layers refers to manufacturing the clutch in two or more layers. The clutch may then be assembled around a solid hub. When the FOA clutch is made with multiple layers it will be called MFOA.

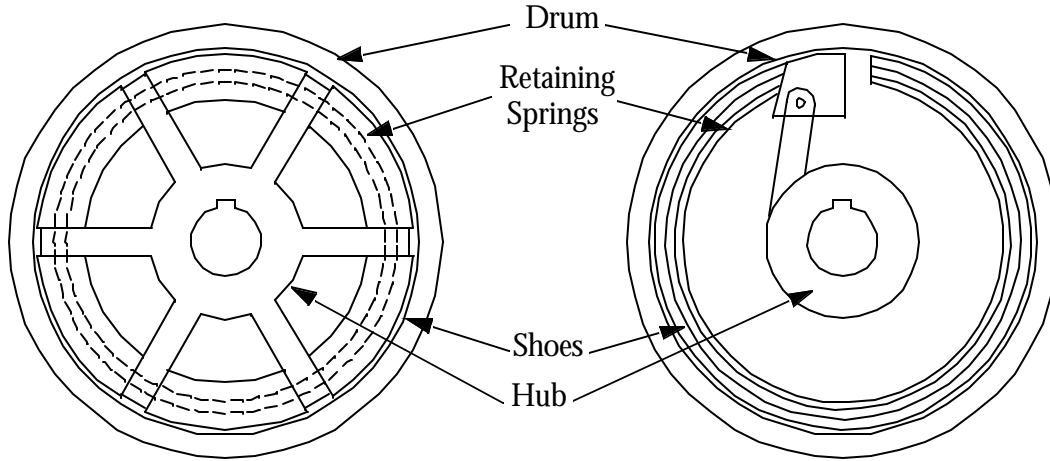


Figure 1.2 Four main components of a centrifugal clutch.

The benefits of centrifugal clutches make it ideal for hundreds of applications. Within the garden equipment market, tens of thousands of clutches are made annually. Even though the clutch is a vital part of much machinery, the basic design has not changed in years. The design constrains the type of manufacturing processes that may be used and therefore it is hard to reduce manufacturing cost without process improvements. The compliant clutch on the other hand has the potential to be fabricated using other manufacturing processes, which provides the potential of substantially reduced assembly and manufacturing costs.

1.4 Thesis Contributions

While Crane et al. developed and tested several new compliant clutch designs, this thesis takes a much closer look into the floating opposing arm (FOA) design for high-torque applications. The model was revisited, clutches were fabricated out of steel, and testing was performed on larger diameter clutches. In addition, the FOA clutch was designed with multiple layers in order to validate the use of alternate, less costly manufacturing processes. Analysis was performed to model and predict the behavior of such layers on the clutch's performance characteristics.

This thesis investigates high-torque-capacity FOA clutches that are manufacturable. The following objectives were critical in achieving the best performing manufacturable clutch:

- *Implement a manufacturing methodology for compliant mechanisms:* Aaron Herring et al. [28] addressed the problems involved in manufacturing compliant mechanisms. This methodology was used to determine the best manufacturing processes for compliant clutches.
- *Develop a model of the clutch's performance sensitivity to key design parameters:* Analysis is performed to find the clutch's performance sensitivity to certain key design parameters. After these design parameters were identified, the design was altered in order to minimize the clutch's sensitivity to those parameters. In this manner, a robust clutch design was obtained.
- *Develop a model of the clutch's performance sensitivity to manufacturing variations:* In addition to finding key design parameters, an analysis was performed to find the effects of manufacturing variations on the clutch's torque-speed performance. A simulation model was created for each clutch design in order to view how manufacturing variations will be mitigated by a multiple layered clutch design.
- *Refine and extend existing clutch models that more accurately predict the performance of high-torque clutch concepts:* The under performance of the compliant go-kart clutch in comparison to the benchmark clutch leads one to believe it is possible to increase the clutch's torque capacity. Models were revisited and expanded for the FOA clutch design by Crane et al. This model was created in order to predict the clutch's performance behavior, and it was a key for analyzing the clutches' performance sensitivity to key design parameters and manufacturing tolerances.
- *Verify models by performance testing:* Since the main objective of this thesis is to develop high-torque-capacity compliant centrifugal clutches, testing will be performed in order to ensure that the new compliant clutch

designs perform comparable to the benchmark clutches. A test set-up will measure the torque-speed behavior of several steel clutches for industry applications. This data will verify the accuracy of the new models and show the feasibility of the layered clutch approach.

In conclusion, these main objectives were critical in developing a high-torque-capacity MFOA clutch that are economically manufactured, while maintaining critical performance characteristics. As a result of this study, a step by step design methodology for compliant clutches was developed.

1.5 Thesis Outline

This thesis is divided into eight chapters. This chapter (Chapter 1) gave a brief background of the accomplishments of previous work, as well as the future progression of compliant clutch design. Chapter 2 covers the current literature on centrifugal clutches, the theoretical analysis of clutches, the theory behind compliant mechanisms, the design-for-manufacture of compliant mechanisms, and results from preliminary tests. Chapter 3 consists of a brief outline of the research methodology for modeling and testing high-torque FOA clutches, as well as clutch evaluation criteria. Chapter 4 outlines high-torque FOA and F1 clutch models, as well as the benchmark Comet clutch model. Following the modeling, Chapter 5 addresses manufacturing considerations with compliant mechanisms and performance sensitivity to variations in manufacturing tolerances and design parameters. In Chapter 6, benchmark testing and model accuracy testing is presented. Finally, Chapter 7 summarizes the contributions made and future research recommendations.

In order to better understand the basis for new Floating-Opposing-Arm (FOA) clutch research, this chapter discusses some of the previous literature on traditional centrifugal clutches. In addition, two previous existing compliant clutches and four novel compliant clutches are presented. Of these four novel compliant clutches, the FOA clutch's model that was created by Crane et. al. is outlined. Research by Herring et. al. on manufacturing issues with compliant mechanisms is also presented. Finally, preliminary test results with the FOA clutch are shown in order to highlight some of the problems with earlier designs.

2.1 Clutches

Since the invention of the electric motor and the internal combustion engine, centrifugal clutches have been a means of transferring power. Centrifugal clutches can be found in inexpensive garden equipment such as string-trimmers, tillers, and chainsaws. They also transmit power in recreation vehicles such as go-karts. In addition, these clutches are found in expensive industrial equipment such as punches, compressors, centrifuges, and presses [7]. Almost all electric motors and internal combustion engines that do not have more expensive hydraulic clutches use centrifugal clutches to disconnect the load from the power source during start-up.

St. John [8] presented rules describing when a centrifugal clutch should be used. He said a centrifugal clutch should be considered (1) when automatic engagement and disengagement are desirable, (2) when motor speed is an adequate clutch control factor, (3) when low costs are desired, (4) when isolation of shock spikes between prime mover (engine) and load is desired, or (5) when high reliability and maintainability is wanted. He also presented rules for design issues. For example, a designer usually wants the engagement speed to be as far below any continuous running condition as possible; preferably more than 600 rpm below [9].

2.1.1 Traditional Centrifugal Clutches

Centrifugal clutches are actuated by centrifugal force, and they transfer torque through frictional contact. Although the same principles are used, different types of clutches use different methods to achieve the necessary speed and torque characteristics. Goodling [7] outlines seven basic clutches, along with their characteristics, benefits, limitations, typical applications and power ranges. The seven clutches are the flexible trailing shoe clutch, the connected shoe clutch, the floating shoe clutch, the mercury clutch, the oil clutch, the ball and cone clutch, and the dry fluid clutch. The three clutches with characteristics similar to the FOA clutch are reviewed. They are the flexible trailing shoe clutch, the connected shoe clutch, and the floating shoe clutch.

Flexible Trailing Shoe Clutch

The flexible trailing shoe clutch consists of a flexible band line with friction material that is pulled by its leading edge (Figure 2.1(c)). As the clutch accelerates, the band is pushed into contact with the drum, and therefore transmits torque. The main characteristic of this clutch is that it is less sensitive to changes in coefficient of friction than most other clutches. For example, a 30% variation in friction coefficient only creates a 5% variation in output torque at a rated speed [7].

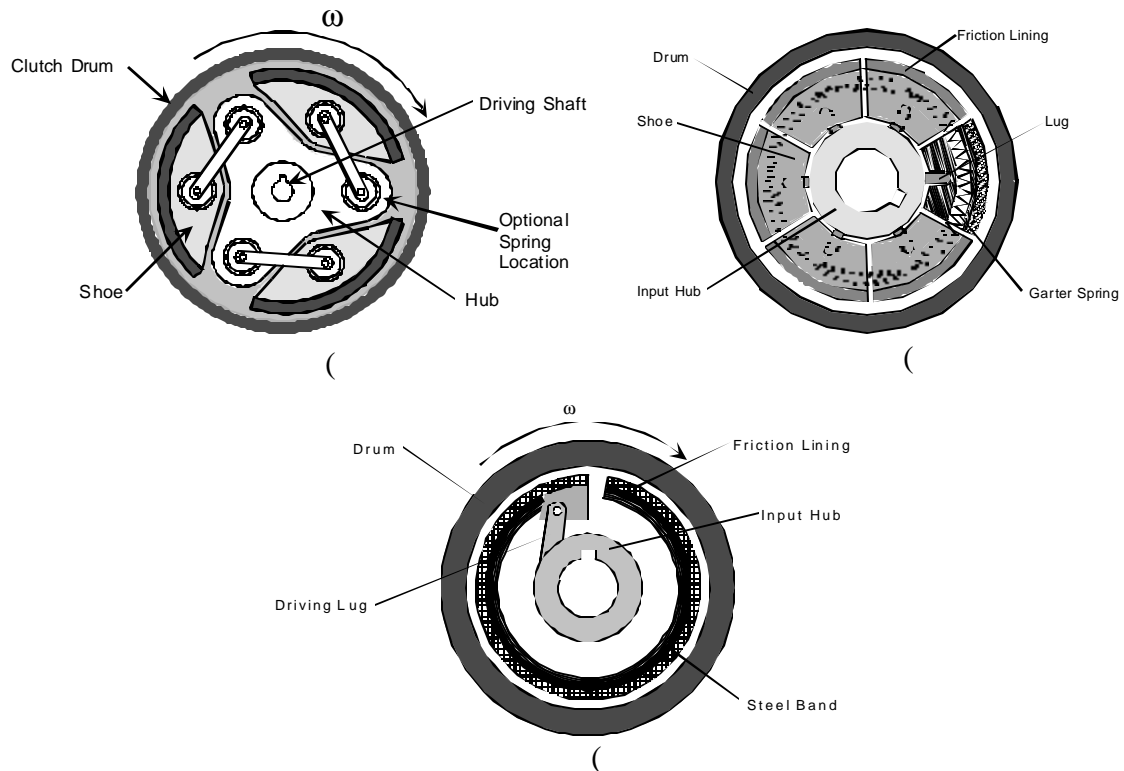


Figure 2.1 (a) Connected Shoe Clutch (b) Floating Shoe Clutch and (c) Flexible Trailing Shoe Clutch

Connected Shoe Clutch

The connected shoe clutch has friction shoes that are attached to a rotating link (Figure 2.1(a)). Normally the link is connected to a spring for a pre-calculated engagement speed. One significant point is that these clutches have different torque characteristics, depending on the direction of rotation. Torque is much higher when the friction force increases the pressure of the shoe on the drums. This higher torque direction is termed as the aggressive or self-energizing mode, while the lower torque direction is known as the non-aggressive mode.

Floating Shoe Clutch

Finally, the floating shoe clutch consists of shoes that slide radially on lugs due to the centrifugal force (Figure 2.1(b)). In addition, there is normally a garter spring that opposes the centrifugal force, which ensures that the shoes engage at the proper speed. This type of clutch operates in the same manner in both rotating directions.

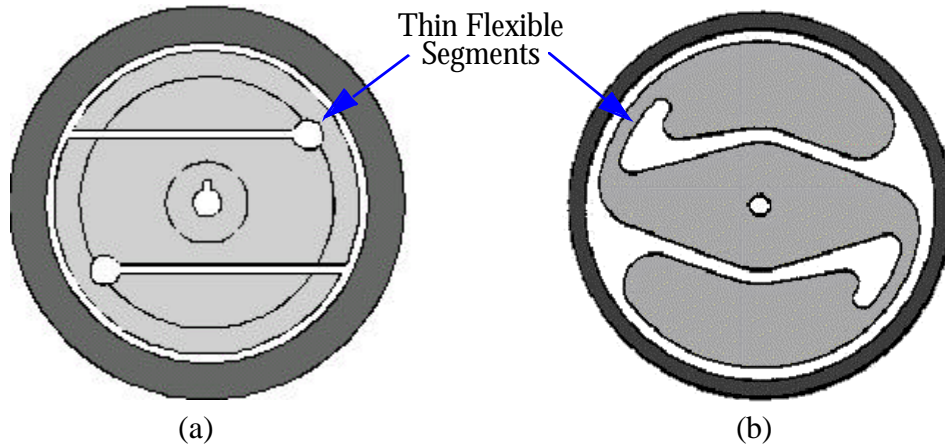


Figure 2.2 Two types of existing compliant clutches: (a) Compliant C4 clutch and (b) Compliant S-clutch.

2.1.2 Compliant Clutches

In addition to these seven clutches, Crane presented two previous existing compliant clutches and four novel compliant centrifugal clutch configurations. Two of the four novel clutches were compliant floating-shoe clutches, one was a flexible trailing shoe, and one was based on a double-slider mechanism. The following sections present the compliant clutches, while their corresponding models may be found in [2].

C⁴ Clutch and S-Clutch

The two previously existing compliant clutches are the conventional compliant centrifugal clutch (C^4) (Figure 2.2(a)) and the S-clutch (Figure 2.2(b)). These clutches are already used in many low-cost applications such as garden equipment and toys, because they can be produced economically in high-volumes. Cost is reduced further because the low torque applications do not require a friction lining to increase coefficient of friction.

The S-clutch and C^4 clutch operate very similarly to the connected shoe clutch. As the driving shaft increases speed (spinning the clutch) the centrifugal force causes the shoes to move radially into the hub. The friction between hub and clutch then drives the load. Similar to the connected shoe clutch, these two clutches have opposing spring forces in the thin-flexible segments, which ensures proper engagement speed. In addition, they

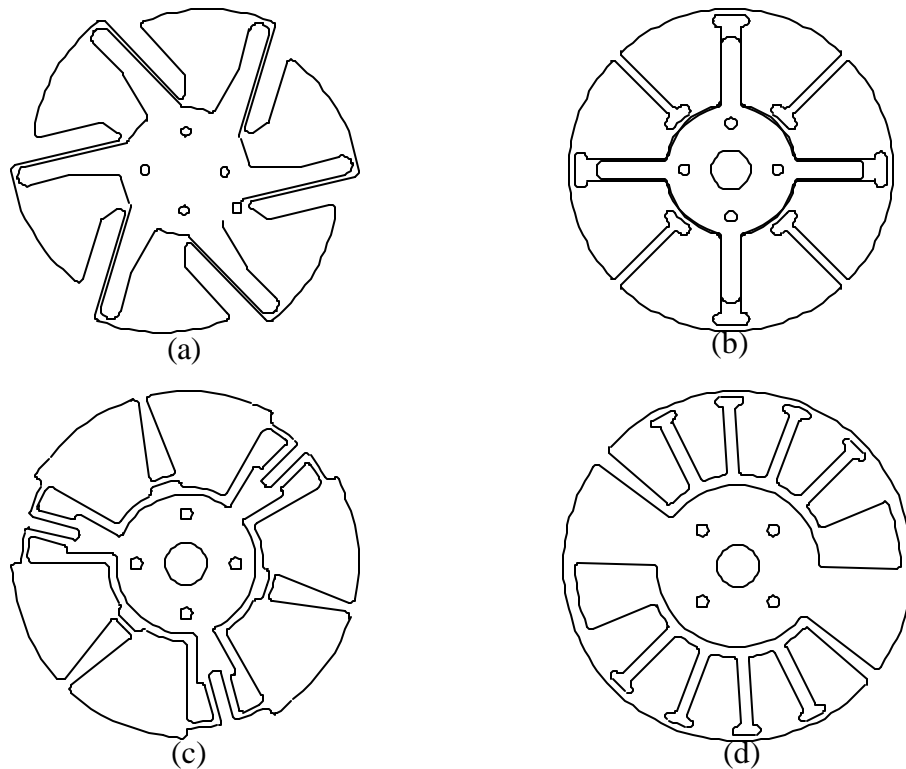


Figure 2.3 Various clutch designs developed by Crane et al. (a) Floating 1 Clutch (b) Floating-Opposing-Arm Clutch (c) Grounded-Opposing Arm clutch and (d) Split-Arm Clutch

exhibit aggressive and non-aggressive performance based on the direction in which the clutch is turned.

Floating 1 Clutch

Crane created a compliant version of the floating shoe clutch (Figure 2.3(a)). The design combines the shoes and the springs of a rigid-body floating-shoe clutch to reduce the part count. The shoes are connected by thin flexible segments that provide spring force. However, the hub rather than the flexible segments bears the torque load. The clutch can be designed to engage at very low speeds using very flexible connecting elements while supporting large torque loads through a stiff hub.

Floating-Opposing-Arm Clutch

The floating-opposing-arm clutch combines both aggressive and non-aggressive shoes in order to maintain high torque transfer without sacrificing smooth engagement.

The FOA clutch is similar to the Floating 1 design and consists of a hub and multiple shoes (Figure 2.3(b)).

Grounded-Opposing-Arm Clutch

The grounded-opposing-arm (GOA) clutch is essentially an FOA clutch that is fixed to the spider lug (Figure 2.3(c)). The GOA exhibits the same characteristics as the FOA clutch. The main drawback is that the load is now transferred through the flexible segments, similar to the S-clutch. This connection between the hub and shoes prohibits a de-coupling of the engagement speed and maximum torque transfer as exhibited in both the FOA and Floating 1 clutch.

Split-Arm Clutch

The split-arm clutch is similar to a flexible trailing shoe clutch (Figure 2.3(d)). As the number of segments increase, the clutch more closely approximates the continuous compliance of a flexible shoe [5].

2.1.3 Benefits of Centrifugal Clutches

Almost all centrifugal clutch literature presents the benefits or advantages of using such clutches. Goodling [7] divides these benefits into start-up and operational performance. When a motor starts up with a centrifugal clutch it draws less power (a decrease from 600% to 200%), takes less time, and has a smoother engagement. The engagement characteristic of centrifugal clutches permits internal combustion engines to idle without transferring torque to the output. During operation, the centrifugal clutch smooths out destructive jerks in the load, which stops the load from damaging costly machines.

Likewise, St. John [8] adds that centrifugal clutches provide automatic engagement and release without peripheral sensors or other equipment, let prime movers carry load only at acceptable torque and speed, and permit slow or rapid load pickup. Similar to Goodling, St. John also says that such clutches permit slippage during extreme shock or overload, which reduces loads on bearings, mountings, shafting, and vibration absorbers.



Figure 2.4 (a) St. John's [10] patented connected shoe clutch. (b) Nagashima's [11] patented floating shoe clutch.

2.1.4 Undesirable Characteristics

Even though centrifugal clutches have many positive attributes as described in the previous section, they also have many undesirable characteristics. St. John [8] explained the critical importance of correctly sizing the clutch for a given application. Undersizing a clutch will cause it to slip, which in turn causes wear, overheating, and premature failure. Over sizing a clutch will damage machine components, contribute to premature engine failure, and cause combustion engines to stall.

2.1.5 Clutch Patents

Industry has been trying to take full advantage of the many benefits that centrifugal clutches offer, while mitigating their undesirable characteristics. St. John [10] created a connected shoe clutch and Nagashima [11] patented a floating shoe clutch. Luerken [12] developed a clutch with greater immunity to the effects of variations in components by using spring configurations which require a relatively long spring extension. Weiss [13] created a clutch with a maximum torque level by using return weights that oppose the pressing force of the centrifugal weight when the speed increases over a certain level. Shimizu & Ogura [14] created an instantaneous (bi-stable) engagement clutch, therefore eliminating slip and prolonging the clutch's life. Shultz [15] patented a bi-directional clutch.

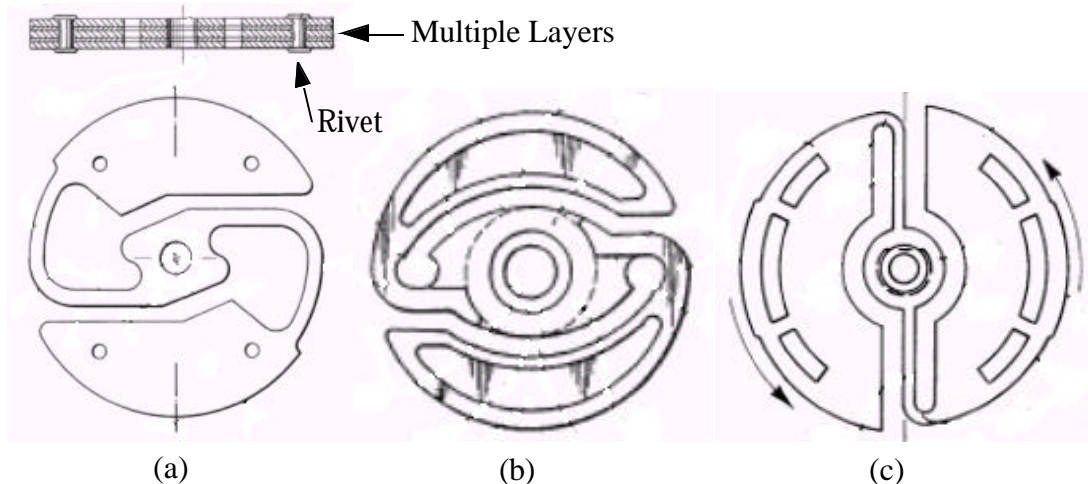


Figure 2.5 Various patented one piece s-clutch designs. (a) Dietzsh et. al. [20] (b) Ruddy [17] and (c) Sageshima [18]

In addition, many designers have tried to take advantage of one piece s-clutches [16,17,18,19]. One interesting s-clutch design was presented by Dietzsh, Henning & Lux [20] which permits low manufacturing costs while obtaining desired precision (Figure 2.5(a)). This design uses multiple layers that are riveted together to form one thick clutch.

2.2 Theoretical Analysis of Clutches

2.2.1 Basic Operating Principles

Since centrifugal clutches are widely used in many applications, their basic operating principles are well defined in many engineering design books [21,22,23,24]. These design books present the necessary equations for determining the forces and torques involved in centrifugal clutches.

The acceleration of a body that is rotating about a center has a centripetal and a tangential component (Figure 2.6(a)). Centripetal or normal acceleration is the acceleration of a rotating body towards the center of the circular motion, and is caused by centrip-

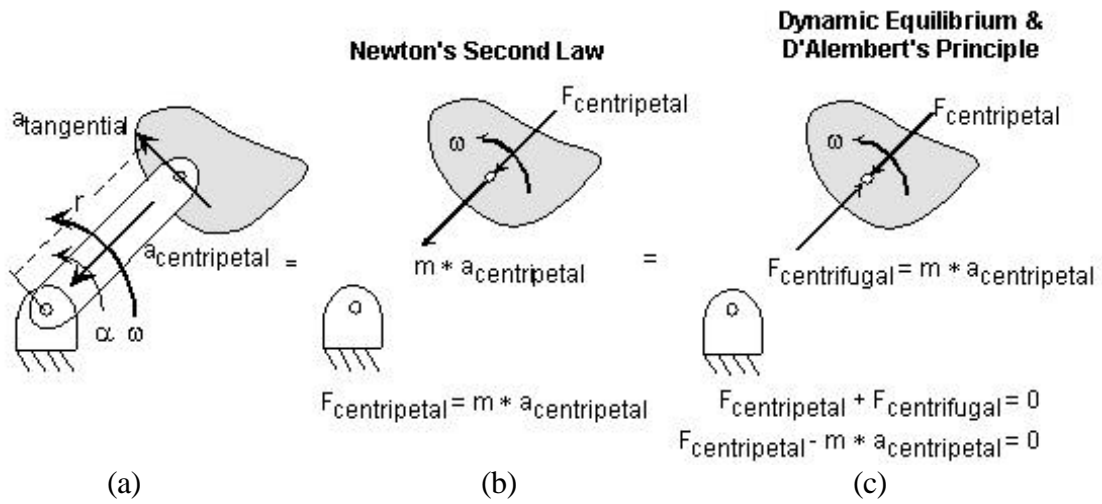


Figure 2.6 (a) Body rotating at a constant angular velocity. (b) The motion equations using the standard form of Newton's Second Law. (c) The motion equations using D'Alembert's Principle and centrifugal forces are shown.

etal force. Tangential acceleration is the acceleration of the body normal to the centripetal acceleration.

$$a_N = r\omega^2 \quad (2.1)$$

$$a_T = r\alpha \quad (2.2)$$

where r is the distance from the center, ω is the radial velocity, and α is the angular acceleration. If the angular velocity is constant then the angular acceleration (α) is equal to zero and equation(2.2) becomes zero. The centrifugal force exerted by the centripetal acceleration is (see Figure 2.6(b))

$$F_{\text{centrifugal}} = ma = mr\omega^2 \quad (2.3)$$

or

$$\Sigma F + (-mr\omega^2) = 0 \quad (2.4)$$

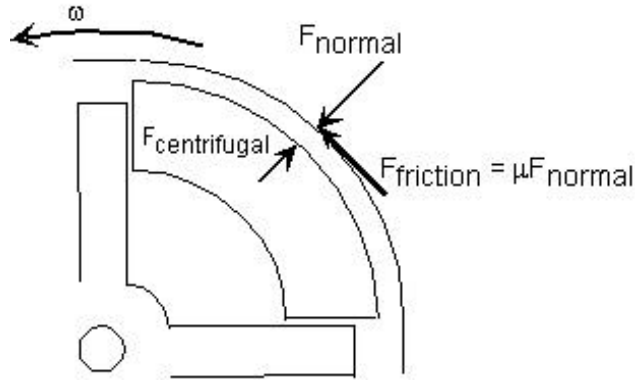


Figure 2.7 Friction force that transmits torque between the shoe clutch and drum.

The term $-mr\omega^2$ is known as an inertial or D'Alembert force. This term is directed opposite to the centripetal acceleration and has units of force. Centrifugal force is the D'Alembert force caused by the centripetal acceleration of a rotating body, or

$$F_{centrifugal} = -mr\omega^2 \quad (2.5)$$

As the centrifugal force pushes the shoes of a clutch radially into the drum (Figure 2.7), friction is created between the clutch and drum. The friction force exerted to the drum is approximated as

$$F_{friction} = \mu F_{normal} \quad (2.6)$$

where $F_{normal} = F_{centrifugal}$ and μ is the coefficient of friction. The transferred torque from clutch to load is

$$T = NrF_{friction} \quad (2.7)$$

where N is the number of shoes and r is the drum's inside radius.

Normally, there are springs attached to the shoes in order to have the clutch engage at a predetermined speed. This would make the normal force equal to

$$F_{normal} = mr\omega^2 - k\lambda \quad (2.8)$$

where k is the spring stiffness and λ is the spring displacement. The springs decrease the applied normal force, and therefore decrease the maximum torque transferred.

As may be seen, the torque capacity of a clutch is dependent on the coefficient of friction, and the centrifugal force. Centrifugal force is proportional to the square of the speed, the radius of the clutch, and the mass of the shoe.

2.2.2 Standard Centrifugal Clutch Comparison Method

In addition to these basic centrifugal clutch equations, Goodling [25] presented the derivation of specific torque equations for different types of centrifugal clutches. St. John [8] developed an equation to standardize torque values for clutch comparison as

$$T_c = T_b(U_0^2 - U_r^2) \quad (2.9)$$

where

T_c = operating torque of clutch at U_0

T_b = basic torque of clutch at 1000rpm without bias springs

U_0 = the operating rpm/1000

U_r = the clutch release rpm/1000

This equation is ideal in comparing centrifugal clutches with totally different design concepts. Crane [5] even used this equation to compare the different compliant clutch designs.

2.2.3 Self-Locking / Self-Energizing Characteristic of Clutches

One characteristic that is common with centrifugal clutches is that of self-energizing or aggressive engagement. South [24] says this phenomena "occurs when the configuration of the brake [or clutch] is such that the friction force generated by the brake [or clutch] reinforces the external actuation force [centrifugal force]."

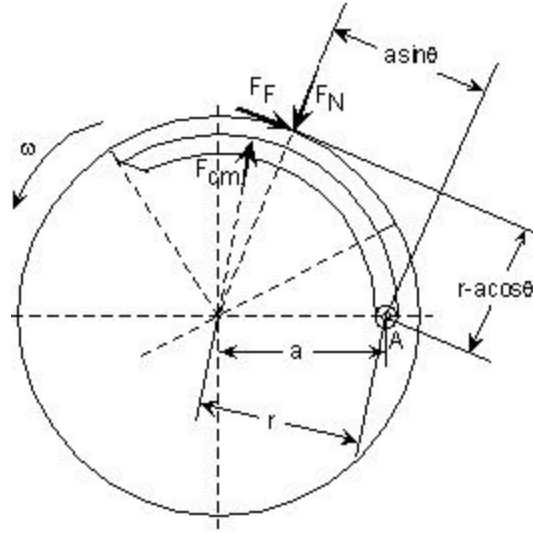


Figure 2.8 Forces acting on a clutch, which may cause self-locking.

When looking at a brake or clutch, Shigley [23] shows that the actuating force F must balance the moment caused by the friction force, as well as the normal force (see Figure 2.8). This equilibrium statement gives

$$F = \frac{M_N - M_F}{c} \quad (2.10)$$

where M_N is the moment of F_N and M_F is the moment of F_F about point A, and c is distance from the pivot point to the actuating force. In the centrifugal clutch case, the actuating force is equal to the centrifugal force acting at the shoe's center of mass.

If $M_N = M_F$ then zero actuating force is needed to engage the brake or clutch, and self-locking is obtained. This self-locking characteristic only holds true for aggressive shoes. Non-aggressive shoes operate with

$$F = \frac{M_N + M_F}{c} \quad (2.11)$$

An aggressive clutch transmits more torque with an impact engagement, while a non-aggressive clutch transmits less torque with a smooth engagement. In addition, a self-energizing shoe is more sensitive to the coefficient of friction (COF). In other words, as the COF changes, the torque varies over a wider range than that of a non-aggressive shoe.

The FOA clutch possesses aggressive and non-aggressive shoes. While there are a few centrifugal clutches with this characteristic, most centrifugal clutches are either aggressive or non-aggressive. The FOA clutch combines the characteristics of both aggressive and non-aggressive clutches.

2.2.4 Specific Applications

Many researchers have taken these equations a step further by applying them to specific applications. Archi [1] designed a centrifugal clutch using two Honda brake shoes. Goodling [25] outlines the relevant equations for modeling the flexible trailing shoe clutch. Dekhanov & Makhtinger [26] created a model for a modern centrifugal separator that has a smooth start and a larger operational torque. Crane [2] created a compliant model for the two existing compliant clutches and for all four novel compliant clutch designs.

2.2.5 Floating-Opposing-Arm Clutch Model

The FOA clutch consists of both aggressive and non-aggressive shoes. The symmetry of the design allows the clutch to be analyzed by modeling the flexible segments as sliders, because they move on radial paths from the axis (Figure 2.9). In addition, each flexible segment provides a torsional spring torque (T).

Before the clutch engages the drum, the displacement of the shoe may be analyzed by only considering one shoe. By taking a summation of the moments on the linkage, it is possible to solve for the relationship between the centrifugal force and the mechanism position. The resulting equation is

$$\vec{r}_{cm} \times \vec{F}_0 + T_1 + T_2 + l \angle \left(\frac{\pi}{2} - \frac{\pi}{n} - \theta \right) \times \vec{F}_{So} = 0 \quad (2.12)$$

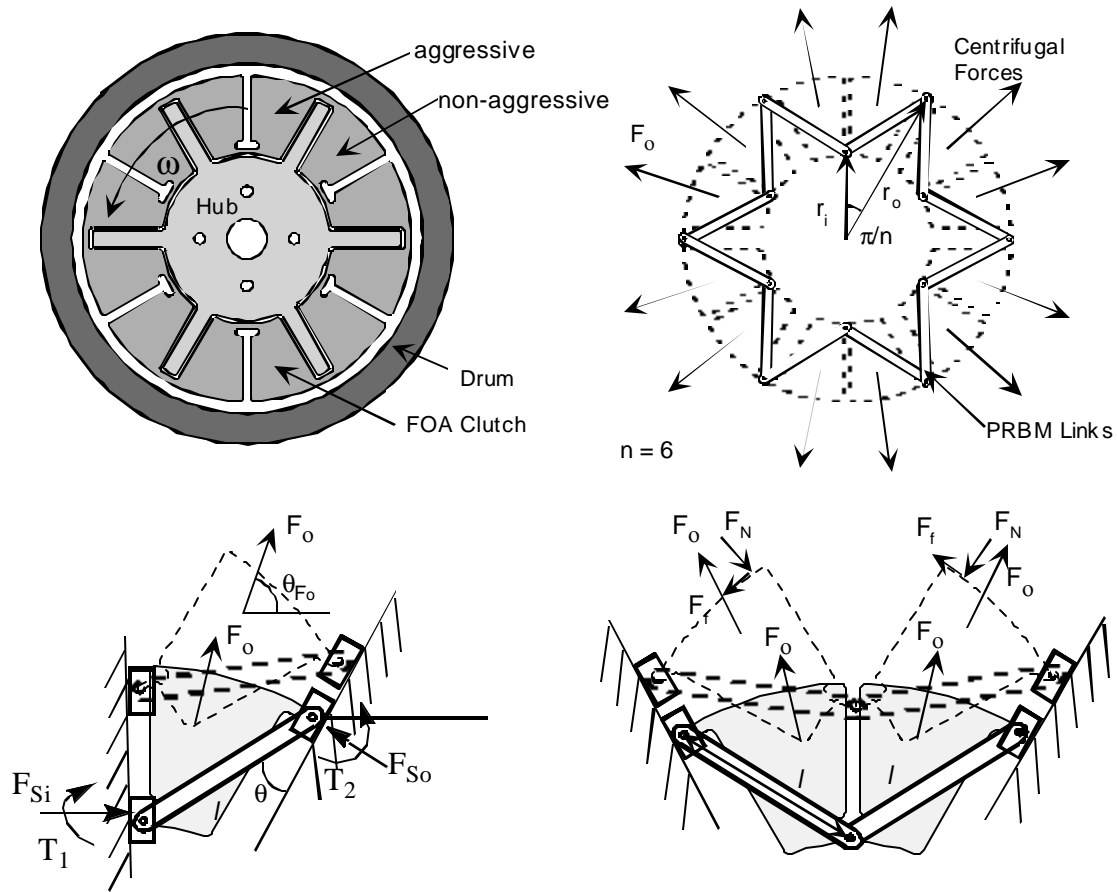


Figure 2.9 FOA clutch with its PRBM

where the variables are defined as

$$l = \sqrt{r_{o_0}^2 + r_{i_0}^2 - 2r_{o_0}r_{i_0}\cos\frac{\pi}{n}} \quad (2.13)$$

$$\theta = \arcsin\left(\frac{r_i \sin\frac{\pi}{n}}{l}\right) \quad (2.14)$$

$$r_o = l\left(\sin\theta \cot\frac{\pi}{n} + \cos\theta\right) \quad (2.15)$$

$$\vec{F}_o = m\omega^2 \vec{r}_{cm} \quad (2.16)$$

$$|\vec{F}_{so}| = \frac{-F_o \sin \theta_{F_o}}{\sin\left(\pi - \frac{\pi}{n}\right)} \quad (2.17)$$

$$\angle \vec{F}_{so} = \pi - \frac{\pi}{n} \quad (2.18)$$

$$T_1 = k_1(\theta_o - \theta) \quad (2.19)$$

$$T_2 = k_2(\theta_o - \theta) \quad (2.20)$$

The variable l is the displacement of the shoe, n is the number of shoes, m is the shoe mass, r_{cm} is the distance to the shoe's center of mass, and F_{S_o} is the reaction force at the outer slider. The torsional spring constants (k) of the flexible segments are equal to $\frac{EI_l}{l}$, where l is the length of the small flexible segment, E is the modulus of elasticity, and I is the moment of inertia of the small flexible segment [1]. Crane assumes that the deflections are sufficiently small, which allows F_o to be solved for directly by equation (2.16).

Once the clutch is engaged, the aggressive and non-aggressive shoes do not load the drum symmetrically, but the position is known. This allows the normal force to be solved for by using force and moment equilibrium equations. After the normal force is solved for, the basic torque equation (2.7) may be used to determine the transferred torque. The FOA clutch's torque transfer is given by

$$T = |F_N| \mu R_{drum} n \quad (2.21)$$

where n is the number of clutch arms and R_{drum} is the inner radius of the drum.

2.2.6 Friction

Friction is a very critical parameter of centrifugal clutches. Friction in centrifugal clutches may be classified as either static or dynamic. Static friction is the largest of the two, because it includes both the resistance to movement of two bodies and the required force to overcome inertia for accelerating one of the bodies relative to the other. Dynamic friction is the force required to maintain relative motion between two objects [27]. Once a

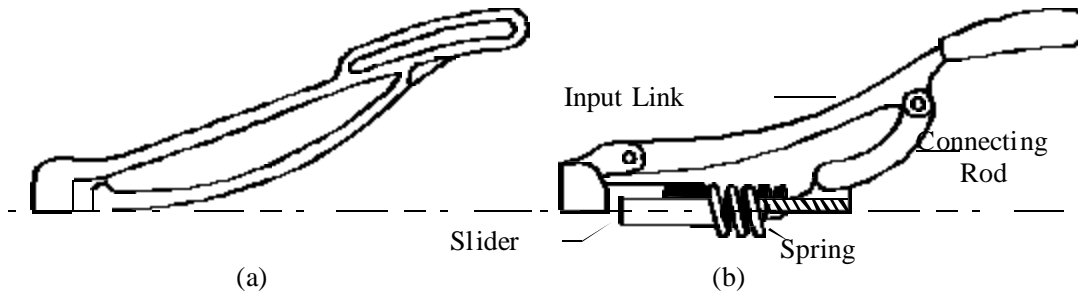


Figure 2.10 Comparison between (a) compliant crimping mechanism developed by AMP Inc., and its (b) rigid-body counterpart [1].

clutch is fully engaged, it is assumed that there is no slip between the clutch and drum, which means static friction exists.

Although friction is commonly discussed as only being dependent on the normal force and not the area, South [24] shows that the coefficient of friction varies with temperature and pressure. The data presented by South matches the observation that the flexible trailing shoe clutch is less sensitive to the coefficient of friction. The flexible trailing shoe clutch has very high surface area that contacts the drum, which helps negate surface irregularities at point contacts.

Another issue that arises with large normal forces over very small surface areas (high pressure) is that of drum scoring. Drum scoring can cause the clutch to lock up, which becomes dangerous in many applications. Designers of clutches should ensure that the normal forces are distributed over enough area to eliminate drum scoring.

2.3 Implementing Compliant Mechanism Theory

2.3.1 Compliant Mechanisms

A mechanism is a mechanical device used to transfer or transform motion, force, or energy. Unlike traditional rigid-link mechanisms, however, compliant mechanisms gain at least some of their mobility from the deflection of flexible members rather than from movable joints only. Figure 2.10 shows a pair of crimpers in both a rigid-link and compliant configurations [1].

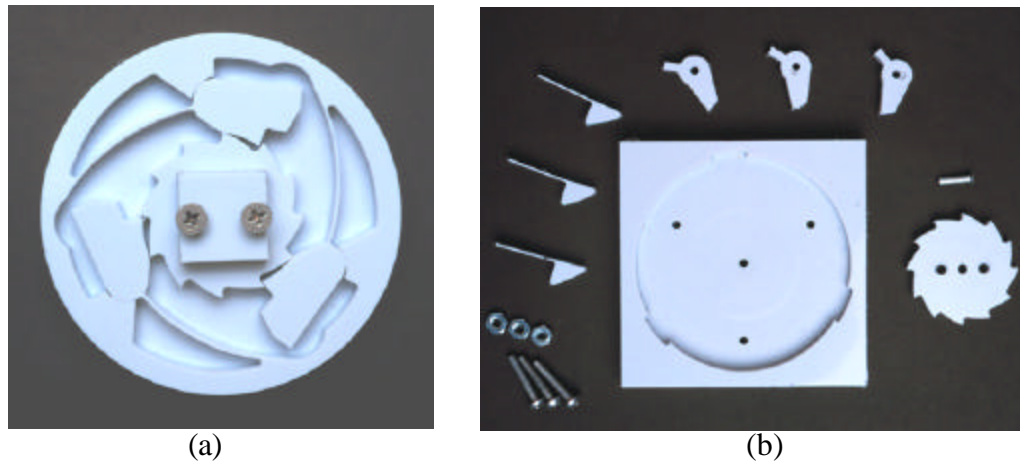


Figure 2.11 (a) Compliant overrunning clutch and (b) Equivalent rigid-body design shown disassembled.

Compliant mechanism technology has many characteristics that make it appealing to existing or new applications. The main two characteristics of compliant mechanisms are cost reduction and performance increase.

Cost reduction is mainly attributed to part-count reduction. Since a compliant mechanism receives some of its motion from the deflection of flexible members rather than from movable joints there is a significant reduction in part count. Figure 2.11 shows a compliant overrunning clutch with an equivalent rigid-body counterpart. As seen, the traditional design has 4 pin joints and a part count of 15, while the compliant design has 1 pin-joint and a part count of 4. Additional cost reduction comes from the fact that with a decrease in part count, it becomes much easier to assemble the final mechanism. No longer do the pin-joints need to be inserted, nor do the springs need to be attached. In addition, the part count reduction leads to a simplification in manufacturing processes, which is another cost savings.

Increased performance can likewise be attributed to part-count reduction. Compliant mechanisms have fewer pin-joints and springs, which reduces the amount of wear, weight, and required maintenance. In addition, pin-joints add additional tolerances, as well as variations, that decrease the precision of the mechanism. By reducing the wear,

weight, and required maintenance, while simultaneously increasing the precision, compliant features are able to increase the reliability of such mechanisms.

In order to be able to take advantage of these two characteristics, it would have to be necessary to have a simple, yet accurate, method of designing compliant mechanisms. Unlike traditional rigid-link mechanisms where their links are considered infinitely rigid, compliant mechanisms rely on deflections for performance. Once the deflection becomes large, linear assumptions do not apply and the full Bernoulli-Euler equation must be used to account for geometric non-linearities.

The Pseudo-Rigid-Body Model (PRBM) sets forth a modeling system which takes a compliant mechanism and transposes it into a traditional rigid body mechanism, which then can be analyzed by traditional kinematic equations. Crane states that "the PRBM approach facilitates design and analysis of these highly nonlinear applications because it de-couples the solution of nonlinear deflections of compliant mechanisms from the solution of nonlinear force-deflection equations." The PRBM is outlined in [1] and will be the main method for creating new torque and speed models.

2.4 Manufacturing Considerations

Herring et al. [28] had an objective to develop a set of manufacturing process tables and charts that represent process capabilities appropriate for compliant mechanisms with long thin beams. These process tables will be applied to the compliant centrifugal clutch, even though it contains small-length flexural pivots instead of long thin beams. The processes were categorized into no-assembly processes (one piece) and partial-assembly processes.

A go-no go matrix was created for producing one piece compliant mechanisms, which contains two criteria; economic high production capability and capability of producing desired geometry. In applying this matrix to the various manufacturing processes only laser cutting, water jet, axial powder compaction, isostatic pressing, die casting, metal injection molding, and impact extrusion passed the test [28].

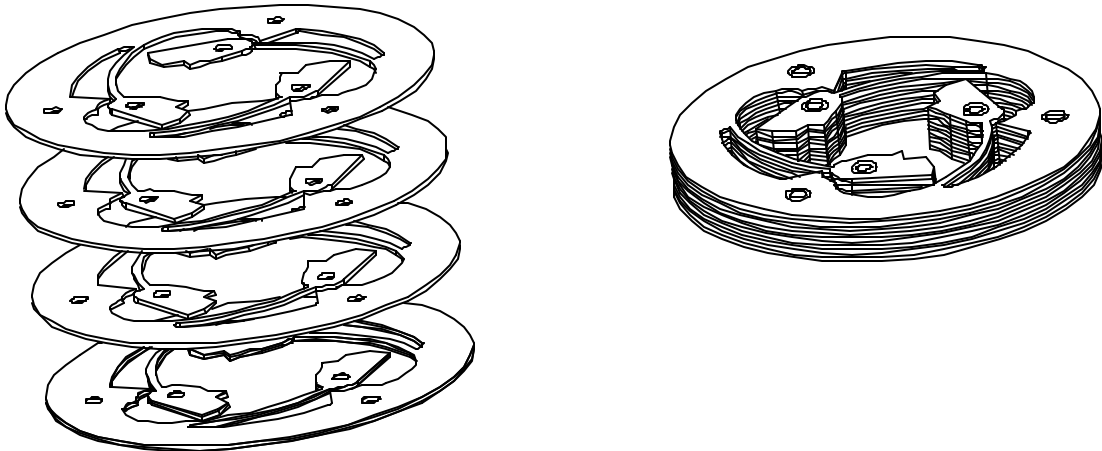


Figure 2.12 The hybrid process used on compliant overrunning clutch.

The findings show that partial-assembly processes are more feasible for compliant mechanism designs. The best process is one that Herring et al. calls a hybrid process. The hybrid process would involve fine-blanking or stamping the part out of sheet metal and then joining the multiple layers together with a mechanical, thermal or chemical process (Figure 2.12).

Multiple criteria were created for judging the partial-assembly processes. The following is a list of each criterion, and how the hybrid process scored within parenthesis.

- Assembly time
 - Part count (high)
 - Assembly complexity (low)
 - Process speed (high)
- Production level compatibility (high)
- Process robustness (high to medium)
- Manufacturing process effect on part functionality (medium)
- Repairability (no)

The only significant discrepancy between the ideal process for compliant mechanisms and this hybrid process is the part count is high instead of low. In general, higher part counts equates to higher assembly and manufacturing cost. This higher part count may be offset

by the low assembly complexity and the high process speed. The assembly process is much less difficult because all parts are the same. Chapter 5 will address these issues more fully as they pertain to the compliant centrifugal clutch.

2.5 Results of Preliminary Testing

Crane et al. [2] was able to fabricate and test multiple clutch designs such as the floating 1 (F1) clutch, the floating-opposing-arm (FOA) clutch, the grounded-opposing-arm (GOA) clutch, and the split-arm clutch. Two types of models were formed for the FOA clutch: the engagement speed model and the torque-capacity model. The error between predicted engagement speed and actual engagement speed was as high as 14%. In addition, the error between predicted operating torque and actual operating torque was as high as 9%. These errors may be attributed to inaccuracies of the model itself, as well as that the tested clutch's material, polypropylene, experiences stress relaxation. In addition, polypropylene's modulus of elasticity varies due to temperature, size, and loading rates [2]. Another factor that increased the error was the test set up procedure in which cotton webbing was attached to the engaging shoes in order to stop the material from melting.

In addition to these tests by Crane et al., preliminary tests have been performed on two other applications: ground tillers and go-karts. The ground tiller application replaced a connected shoe clutch (Figure 2.1 (a)) with an FOA clutch. Similarly, the go-kart application replaced a floating shoe clutch (Figure 2.1 (b)) with a FOA clutch. The following sections will outline these applications, as well as the lessons learned by the testing.

2.5.1 Ground Tiller Application

The ground tiller application consisted of replacing a 2 1/8 inch connected shoe clutch with a FOA clutch.(Figure 2.13). The performance criteria was such that the clutch had to engage at 3500 rpm and transmit at least 12 in-lb at 5000 rpm. Multiple design iterations were done until testing showed that the design fulfilled the performance criteria.

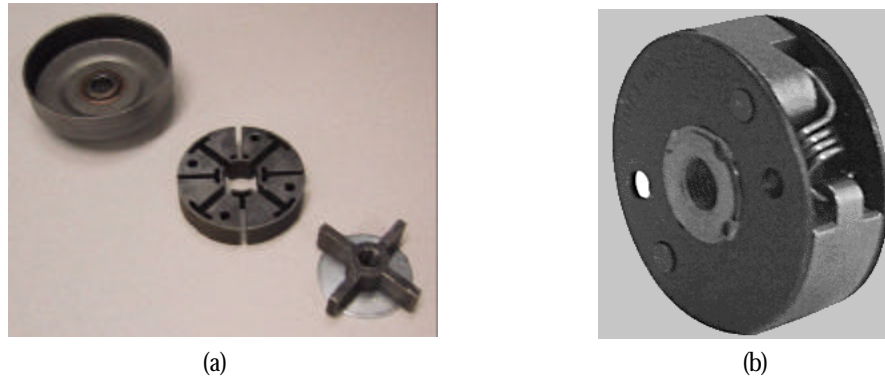


Figure 2.13 Two 2 1/8 inch clutches used in a ground tiller (a) Floating-opposing-arm clutch (b) Connected shoe clutch.

Table 2.1 shows the predicted engagement and torque values, as well as the test results for dynamic slipping torque and engagement speeds. As seen there are discrepancies between predicted and measured values. One source of measured torque error is that it is calculated using dynamic friction, or when the clutch is slipping. This is the same type of measured torque that Crane et al. presented. In contrast, the predicted torque uses static friction in its force and moment equilibrium equations. The coefficient of dynamic friction can be as much as 30-45% less than the coefficient of static friction for steel on steel.

Several issues were identified in the testing of these design iterations. The first had to do with the clutch's fatigue life. The first fabricated clutch did not contain fillets at the flexible segments, which caused the clutch to crack after a few engagement cycles. Such

TABLE 2.1 Preliminary test results for a 2 1/8 inch clutch.

	Original Connect Shoe Clutch	One-Piece FOA Clutch	Multiple Layered FOA Clutch
Predicted Engagement	N/A	3033	3009
Measured Engagement	3817	3681	3712
Percent Error	N/A	18%	19%
Predicted Torque	N/A	15.1	15.4
Measured Torque	9.8	9.3	9.8
Percent Error	N/A	62%	57%

fatigue failure is unacceptable for this application, where a minimum amount of 50,000 cycles is required. All future designs had fillets to relieve stress concentrations.

Another issue had to do with the continual under modeling of the engagement speed. The FOA engagement model predicts when contact will be made with the drum. Clutch engagement as described by clutch designers and outlined in the performance criteria as the moment when the clutch transmits a minimum amount of torque (i.e. 1.2 in-lb for the ground tiller). Because the model predicts contact engagement (zero transferred torque), the clutch must be designed to contact the drum at a lower speed than the engagement speed criterion. Care should be taken to make sure it is significantly different than the idle speed to alleviate idle engagement. Due to the different descriptions, future terminology will call the speed at which initial contact occurs as the *contact engagement speed* and the speed at which the minimum amount of torque is transferred as the *engagement speed*.

In addition to these two issues, significant differences in engagement speed (16% error [2]) were present when there was a gap between the hub and the clutch. This gap allows the clutch to float around the hub and other forces such as gravity can cause the clutch to contact the drum prematurely even at idle speed.

Another observation on all tested clutches was that of point burnishing or glazing. Each shoe only has a small surface area that engages with the drum. This small area slips on the drum and begins to look glazed. Such glazing decreases the coefficient of friction and significantly lowers the clutch's torque capacity.

Finally, it was observed that the clutch would have no contact at idle speeds until it was engaged for the first time. From that moment onward the clutch would stay lightly in contact with the drum. It was determined that the friction between the clutch and the clutch fixture (see Figure 2.14) was high enough to overcome the spring restitution forces of the flexible segments. To allow the clutch to return to normal size, the hub needed to be a little bit thicker than the clutch, which changed the friction from between clutch & clutch fixture to hub & clutch fixture.

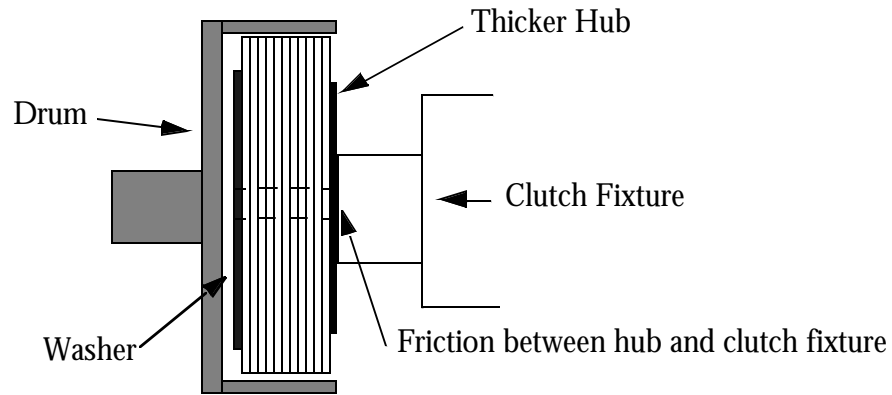


Figure 2.14 Friction between clutch and clutch fixture made the clutch not disengage from the drum.

2.5.2 Go-Kart Application

A one-piece FOA clutch was designed and produced to fit the criteria for a go-kart application. The manufacturer of the benchmark clutch states that the 4 inch clutch engages between 2000 and 2400 rpm with 30 in-lb and transfers 240 in-lb at 3600 rpm (dynamic COF), as well as 480 in-lb at 3600 rpm (static COF). In comparison, the predicted model stated that the new FOA clutch was only able to transfer 280 in-lb at 3600 rpm. In comparison testing performed by Hoffco-Comet, the FOA clutch performed significantly below that modeled value. It was unknown why the larger 4 inch FOA clutch was unable to perform relative to the benchmark clutch, while the smaller 2 1/8 inch FOA performed so well in comparison.

In addition to the one-piece FOA clutch, a multi-layered clutch (MFOA) was produced. This design contained 19 independent floating-layers stack together to act like one solid clutch. The measured contact speed was at 2000 rpm, while the measured torque capacity was 144 in-lb at 2500 rpm. Taking into account that the clutch was engaging prematurely, the torque capacity would be slightly less than 144 in-lb.

The major concern with the MFOA test was that of a catastrophic failure in 3 of 19 layers. These layers failed in multiple areas, but all failures were near the thin flexible segments. Such failure may be explained by clutch scoring and out-of-plane movement. As each layer began to exert greater pressure on the inside of the drum, the point contact

began to gouge or score the drum, which in turn caused the clutch to seize up momentarily. In addition to the scoring, each layer's thickness was less than the width of the flexible segment. As the clutch locked up, the layers would move (bend) out of plane. This out-of-plane movement caused the interior sharp corners to catch itself on other clutch layer's edges. With multiple layers locked together, the clutch failed.

2.5.3 Preliminary Test Problems

These preliminary tests for the 2 1/8 inch and the 4 inch clutch helped to uncover many problems with the FOA clutch design. Future research will help ensure that these problems are resolved in new designs. The following is a list of the preliminary problems encountered.

- Fatigue failure in the thin flexible segments.
- Under modeling the engagement speed by basing the design on the contact engagement speed.
- Premature engagement caused by the gap between hub and clutch.
- Point burnishing and glazing on the clutch, which significantly reduces the coefficient of friction.
- No disengagement because of the friction between clutch fixture and clutch.
- Insufficient torque capacity in comparison to benchmark.
- MFOA clutch layers scoring the drum.
- Out-of-plane movement of layers for the MFOA clutch.

The main objective of this thesis is to develop high-torque-capacity Floating Opposing Arm (FOA) centrifugal clutches that can be economically manufactured, while maintaining critical performance characteristics. This objective states three main characteristics of the desired clutch. First, it must maintain critical performance characteristics. This is why the clutch's sensitivity to both key design parameters and to manufacturing variations is explored. Analysis is presented that shows how the clutch's design can be adjusted in order to minimize performance sensitivity and create a robust design.

The second characteristic is that the clutch must be economically manufactured. The clutch must be fabricated in mass quantities at a reasonable cost. For this reason, research focuses solely on those processes that are deemed satisfactory in accomplishing high-volume manufacturing. It is believed that by manufacturing the compliant clutch in multiple layers, not only is it feasible to produce these clutches in high volumes, but the engagement and torque performance variations are tightened, therefore allowing the clutch to perform better.

Lastly, the clutch is designed for high-torque-capacity. Currently, the larger clutch prototypes significantly under-perform compared to the benchmark high-torque clutches. Research is presented that shows the FOA clutch performing comparable to the benchmark's torque capacity.

3.1 FOA Modeling

In order to achieve these three clutch characteristics, it is imperative that the research shows complete understanding of the FOA clutch design. Crane et al. created and tested a Pseudo-Rigid-Body-Model (PRBM) [1] that predicts the speed and torque performance of the FOA clutch. Unfortunately, this model was only verified with one steel clutch and several plastic clutches.

The FOA model was revisited and enhanced, as well as adequate PRBMs were formed in order to facilitate clutch design. This enhanced model explored the clutch's speed and torque characteristics and allowed the sensitivity analysis of key design parameters. In addition, this model was used to do Monte-Carlo simulations of the manufacturing variations. Such simulations show the behavior predictions of layered clutches.

3.2 Testing

Testing was performed in order to judge whether or not this FOA clutch's performance capabilities are comparable to the benchmark. The FOA model was evaluated for accuracy in predicting the torque-speed performance of high-torque-capacity applications. In addition, the test data showed the feasibility of the layered clutch approach.

3.2.1 Benchmarking

Benchmarking the FOA clutch with a traditional centrifugal clutch is essential to determine if the FOA clutch is able to operate efficiently and effectively in a specific application. The goal is to have the new FOA clutch be able to perform comparably to the benchmark clutch. It should be dependable on engagement, and it should transfer the necessary torque load. The benchmark clutch is a 4 inch Hoffco-Comet floating-shoe clutch that is used in snow-blowers, go-karts, and mini-bikes. By benchmarking the FOA clutch with this chosen representation of traditional clutches, it was possible to quantify a standard to measure performance. Table 3.1 shows the Comet clutch's performance specifications provided by the manufacture.



Figure 3.1 FOA clutch design to fit in the Comet (benchmark) clutch's drum.

3.2.2 Prototypes

Multiple FOA clutch prototypes were fabricated to show the feasibility of layer manufacturing and high-torque-capacity performance. In addition, the prototypes verified that the models are reliable and robust in order to design future clutches.

The ten clutch layers were cut from thin 1095 blue-tempered spring steel (0.062 inches) and then stacked to fit around a one-piece hub to form one clutch. The clutches were designed to fit on a retrofitted Comet clutch assembly. The hub and clutch were enclosed in same hub assembly as Comet's go-kart clutch.

TABLE 3.1 Description of the Hoffco-Comet's benchmark clutch.

	Hoffco-Comet 4 inch Clutch
Torque Capacity	20 ft-lb @ 3600 rpm (dynamic) 40 ft-lb @ 3600 rpm (static)
Engagement Speed	2000-2400 rpm
Idle Speed	1850 rpm
Type	Floating Shoe
Shoe Material	Steel
Hub Material	Steel
Direction	Reversible

3.2.3 Measured Test Data

The most important measured data is the clutch's torque vs. speed relationship. This data is imperative to ensure that the model adequately estimates the clutch's performance. The model's accuracy is viewed by having a real-time graph of the torque-speed characteristics (Figure 3.2).

3.3 Evaluation Criteria

The MFOA clutch design was evaluated based on the desired performance criteria that is described in the following sections. From this evaluation process, the FOA clutch was compared to the benchmark Comet clutch.

3.3.1 Torque Capacity

Torque-capacity is the maximum amount of torque that a clutch may transfer before it slips and is the most important criteria for compact clutches due to the size constraints. The torque is determined by the mass of the shoes, the coefficient of friction, the stiffness of springs, the driving speed, and the style of clutch (aggressive vs. non-aggressive). Figure 3.2 (a) shows the maximum amount of torque transfer by a clutch happens just before the clutch slips on the drum or the point when the output rpm decelerates from the input rpm.

3.3.2 Accuracy of Engagement

Variances in manufacturing may cause the clutch to engage prematurely, which is a performance hazard. In addition, the clutch may engage too late, which limits torque-capacity. The accuracy at which the clutch engages is a critical criterion. Premature engagement may cause wear. In addition, if equipment (e.g. chainsaw) engages at idle it may endanger the operator.

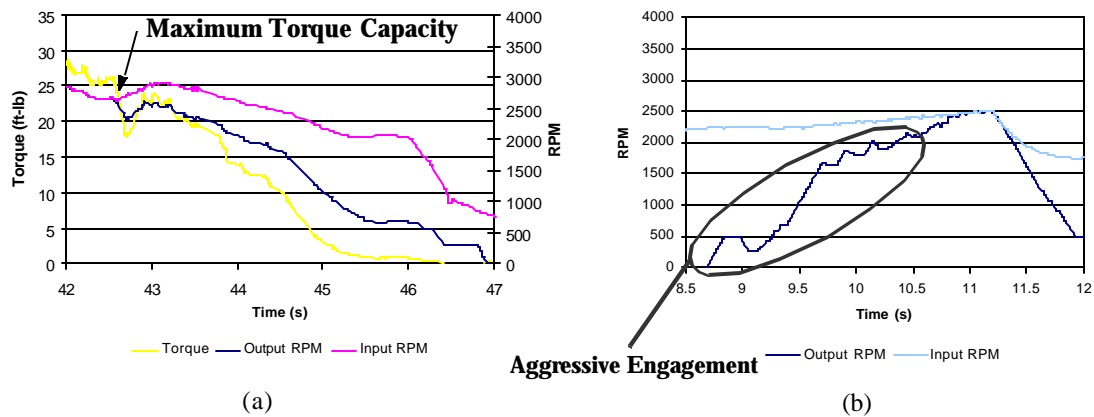


Figure 3.2 Sample data taken from the testing Comet's 2 1/8 clutch. a) Torque vs. rpm data when the clutch is slipping (b) Large spike represents an aggressive engagement.

3.3.3 Smoothness of Engagement

By using the real-time torque-speed data it was possible to see the rate at which the clutch engages with the drum. Large spikes indicate a faster rate of engagement, typically found in more aggressive style centrifugal clutches (Figure 3.2 (b)). There is normally a trade-off between torque-capacity and smoothness of engagement. The higher the torque the more the clutch is aggressive, which in turn causes a high-impact engagement or rough engagement. While smoothness is an important criterion, it is secondary to the torque capacity and accuracy of engagement for the applications targeted in this thesis.

3.3.4 Manufacturability of the Clutch

There are a few important factors such as the width of the inner and outer flexible segments, the thickness of the clutch, and the width of the inner and outer slots that affect the manufacturability of compliant clutches (Figure 3.3). The clutch's design constraints (size, engagement, etc.) limit the changeability of those critical features. Therefore, some designs are more easily manufactured than others. For example, any new design that maximizes the width of the flexible segment will be easier to manufacture.

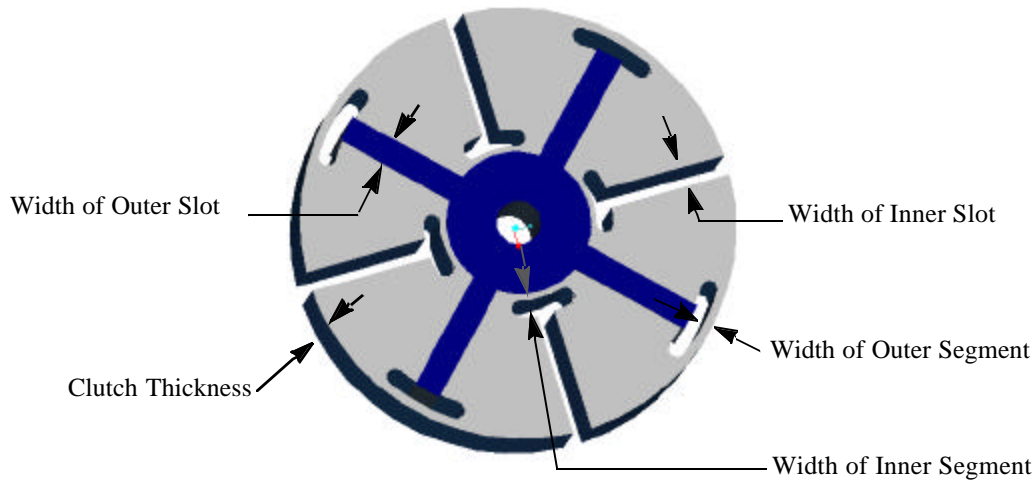


Figure 3.3 Main factors that affect the manufacturability of the FOA clutch.

3.3.5 Performance Sensitivity

Analysis was performed on the torque-speed performance sensitivity due to design parameters and manufacturing tolerances. Although it is hard to compare the sensitivity of the FOA clutch to that of the benchmark, the performance sensitivity is taken into account, especially in looking at how layers and riveted layers perform in comparison to a single layer clutch.

3.4 Clutch Testing

3.4.1 Test Setup

The test setup consisted of an engine with a large torque output (Figure 3.4). A Yamaha FJ 600 motorcycle was attached to a jack shaft in order to provide the necessary torque input. This engine drives the shaft (jack shaft) that is connected to the clutch's hub, which in turn drives the clutch. Upon acceleration, the clutch engages the drum and transfers torque to the output shaft. The output shaft is connected to a dynamometer, which uses a water break to load the clutch and measures the transferred torque with a torque transducer. The operator may vary the dynamometer load by turning the water break valve. There is one tachometer on the jack shaft and one on the output shaft to measure the

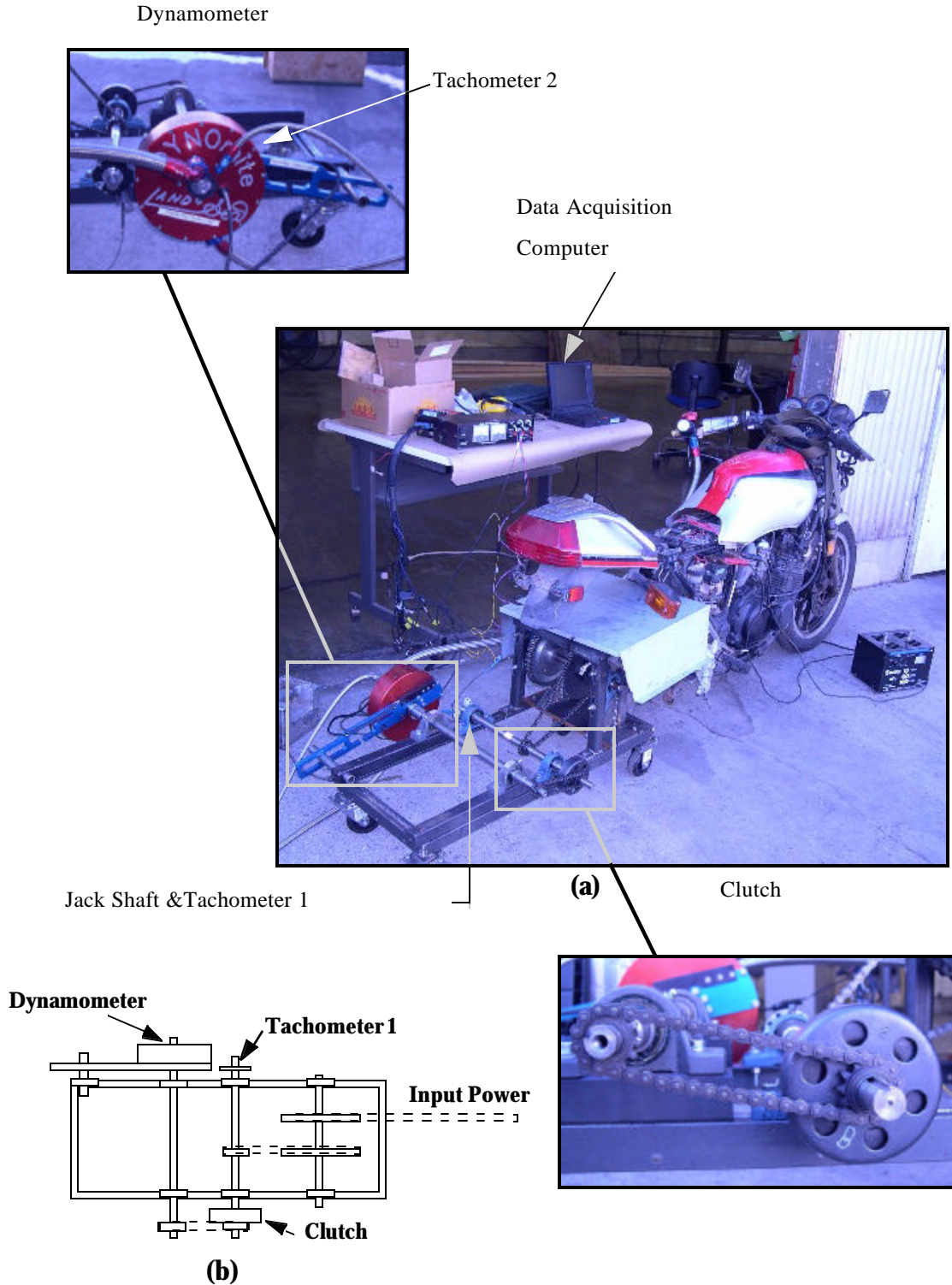


Figure 3.4 Set-up for testing the clutch's engagement accuracy and characteristics, as well as the clutch's torque capacity. (a) Actual pictures and (b) Top view schematic of testing apparatus

speed. The data acquisition computer synchronizes and records the transferred torque and both speed measurements. These three real-time measurements allow torque vs. time, rpm vs. time, and torque vs. rpm graphs to be used for analysis and comparisons.

3.4.2 Data Measurements

The two tachometers measure the speed of both input and output shafts with respect to time. In addition, the dynamometer records the amount of torque in comparison to time. These three real-time measurements allow torque vs. time, rpm vs. time, and torque vs. rpm graphs to be used for analysis and comparisons (Figure 3.2).

3.4.3 Test Procedures

Two types of tests are performed in order to obtain the necessary evaluation data. The first test is the *RPM Contact Test Procedure*. The objective of this test is to judge the accuracy and smoothness of contact. The second test is the *Torque Test Procedure*, which applies an increasing load to the output shaft in order to determine maximum torque capacity. The following outlines the sequential steps necessary for each procedure.

RPM Contact Test Procedure

1. Initiate computer aided data capture
2. Slowly increase engine (input) rpm until the output shaft rpm increases to match the engine's rpm
3. Slowly decrease engine rpm to idle
4. End data capture

Torque Test Procedure

5. Initiate computer aided data capture
6. Increase speed to 3600 rpm
7. Slowly increase the load while maintaining various speeds between 2500 to 3600 rpm

8. Continue to increase load until clutch slips. (The point where the two rpm values separate.)
9. End data capture

3.4.4 Error Sources

There are several possible sources of errors in the test setup used to find the rpm and torque characteristics of the clutches. These errors are listed below with a brief discussion of how they affect the performance of the clutches.

Friction in Bearings

There is some biasing in the data because of the friction within the bearings that center the output shaft (Figure 3.4). As the clutch engages, it must overcome the load that is caused by the friction in these two pillow blocks. The torque produced by this friction may be accounted for by adding the bearing torque to the measured torque.

Coefficient of Friction

The coefficient of friction (COF) directly affects the torque capacity of the clutches. Recalling that the amount of transferred torque is equal to $T = Nr\mu F_{normal}$, where μ is the COF. This equation shows the direct relationship between torque and COF. Even with tested values for the COF, there are still many unknowns that influence the true COF. Dirt and grease decrease the COF. In addition, South [24] shows that the COF varies with temperature and pressure, both of which are very prevalent in the FOA design.

In addition, the contact points begin to look burnished after initial testing. This burnished surface is natural and the COF is 20-30% less than initial values. Even though the COF initially decreases after burnishing, the COF remains constant until the clutch wears out. However, if excess heat and/or lubrication is present, glazing may occur. Glazed material appears glassy, and its COF becomes very low. Such low COF can render the clutch inoperable.

Tolerances of Machined Parts

Although the clutches are fabricated by using high precision techniques such as EDM, there may arise discrepancies between the modeled and actual parameters. This causes the measured torque-speed values to be slightly off of the modeled torque-speed values. In order to compensate, the modeled design is recalculated with the actual measured parameters and then compared to the measured torque-speed data.

Measuring Device Error

As with all measuring devices, there are certain limitations and inaccuracies. The dynamometer records rpm data on a cyclical basis and torque on a continuous basis. Both tachometers measure the rpm by an electric pulse that is triggered one time for every revolution. This cyclical recording creates some dynamics issues that affects measurement variations, but does not significantly affect the results.

Drum Scoring

Another error that arises in the multi-layered FOA clutch is that of scoring. Because of the multiple layers, there is a high force distributed over a very small surface area. This high pressure causes the contact point to dig into the drum. Such an occurrence creates a large spike in the transmitted torque. Scoring can be very dangerous to the equipment and operator and should be eliminated.

3.5 Comparing FOA Clutch to Benchmark Clutch

There are three reasons for testing the FOA and benchmark clutches. The first reason is to see the comparison between the torque capacity and engagement speeds of these two types of clutches. For comparison purposes, the FOA clutch was made so that it would fit in the same hub as the Comet clutch. In addition, the FOA's thickness was such that it would match that of the benchmark's. For comparison purposes it is not necessary to know the bearing friction and other test setup errors, because both clutches experience the same errors.

The second reason is to show the feasibility of using free floating layers in a compliant centrifugal clutch. Very little testing has been done on using stacked layers in a clutch. The few tests that have been done were inclusive, if not detrimental due to scoring.

Lastly, testing verifies the contact engagement speed and torque capacity models. Unlike the first reason for testing, verification of the models needs accurate data with no biasing of the data. On the other hand, the torque values are linear in comparison with the coefficient of friction. If there is some bias in the torque data, it would come out in the determination of the coefficient of friction.

The pseudo-rigid-body-model (PRBM) [1] was used to model the Floating-Opposing-Arm (FOA) and Floating 1 (F1) clutches. The PRBM allows for simple and accurate modeling of nonlinear deflections as found in the flexible segments of the FOA and F1 clutches. In order to design a compliant clutch for comparison with the benchmark clutch (Comet 4 inch), it was necessary to model the contact engagement speed and the torque capacity for each compliant clutch concept (FOA and F1). These new concept designs assume that the compliant clutches will be using the existing clutch drum and hub assembly of the Comet clutch. Crane et al. outlined a model for the FOA clutch, and this chapter will build on and improve that model.

These two concept models allow the accurate prediction of a clutch's performance for prototyping. Although only the MFOA clutch is prototyped, the F1 model was created to compare the sensitivity of key design parameters, as well as the performance tolerance zone of contact engagement speed and torque due to manufacturing tolerances.

4.1 Hoffco-Comet 4 inch Go-Kart Clutch

The Comet clutch is used in many high-torque applications. Its design consist of 6 shoes that are held together by a pre-loaded linear spring. Figure 4.1 shows a complete diagram of the various components of the Comet clutch. Modeling of the clutch may be

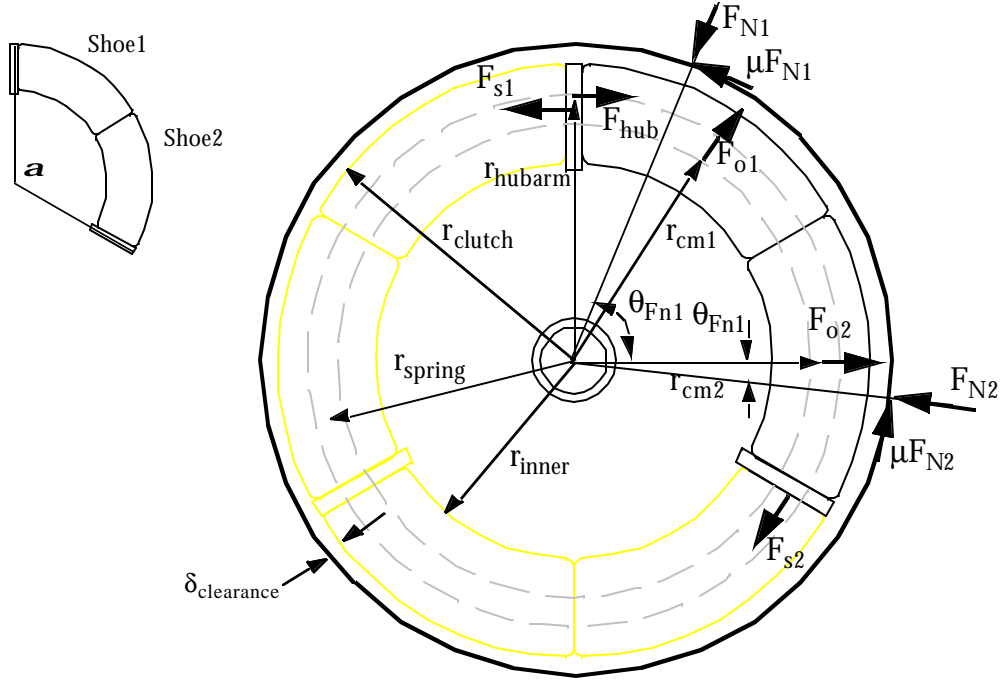


Figure 4.1 Model parameters of the Hoffco-Comet 4 inch clutch.

done by analyzing only one segment, because the geometry and loading of the clutch are symmetrical. Each segment consist of shoe 1, shoe 2, and the linear spring. The basic formula for this type of clutch is

$$F_{normal} = mr\omega^2 - k\lambda \quad (4.1)$$

where m is the mass per shoe, r is the radius to the shoe's center of mass, ω is the speed of the clutch, k is the linear spring constant, and λ is the displacement of the spring length.

4.1.1 Contact Engagement Speed Model

The contact engagement speed for the Comet clutch may be found by assuming that the F_{normal} is equal to zero. The summation of the forces for the two shoes is

$$0 = \vec{F}_{o1} + \vec{F}_{o2} + \vec{F}_{s1} + \vec{F}_{s2} \quad (4.2)$$

where

$$\vec{F}_o = mr\omega^2 \quad (4.3)$$

$$\vec{F}_s = k\lambda \quad (4.4)$$

$$\lambda = 2\pi r_{spring} - l_{spring} + 2\pi\delta_{clearance} \quad (4.5)$$

and l_{spring} is the original spring length, r_{spring} is the radius to the center of the spring, m is the shoe mass, r is the radius to the shoe's center of mass, and k is the spring constant. All variables are known besides ω . By making substitutions for \vec{F}_o and \vec{F}_s , the contact engagement speed ω may be found to be

$$\omega = \left[\frac{-k\lambda \left(\frac{\vec{F}_{s1}}{|\vec{F}_{s1}|} + \frac{\vec{F}_{s2}}{|\vec{F}_{s2}|} \right)}{m(r_{o1} + r_{o2})} \right]^{\frac{1}{2}} \quad (4.6)$$

4.1.2 Torque Model

Once the clutch is engaged, the shoes transmit torque to the drum. Normal forces may be solved for by using force equilibrium equations and a moment equilibrium equation for shoe 1 and shoe 2 (see Figure 4.1). The friction forces are a function of the normal forces. The hub force acts perpendicular to the point of contact on the face of the clutch. After these assumptions are taken into account there are only three unknowns: F_{hub} , F_{N1} , and F_{N2} .

The force equilibrium equation with their x and y components and the moment equilibrium equation are used to solve for the unknowns. These two equations give the following system of equations:

$$\begin{bmatrix} F_1 \\ F_2 \\ F_3 \end{bmatrix} = \begin{bmatrix} f_{11} & f_{12} & f_{13} \\ f_{21} & f_{22} & f_{23} \\ f_{31} & f_{32} & f_{33} \end{bmatrix} \begin{bmatrix} F_{hub} \\ F_{N1} \\ F_{N2} \end{bmatrix} \quad (4.7)$$

where the elements of the matrix are

$$f_{11} = 1 \quad (4.8)$$

$$f_{12} = \cos\left(-\frac{\pi}{2} - \theta_{Fn1}\right) + \mu \cos(\pi - \theta_{Fn1}) \quad (4.9)$$

$$f_{13} = \cos(\theta_{Fn2} + \pi) + \mu \cos\left(\theta_{Fn2} + \frac{\pi}{2}\right) \quad (4.10)$$

$$f_{21} = 0 \quad (4.11)$$

$$f_{22} = \sin(\theta_{Fn2} + \pi) + \mu \sin\left(\theta_{Fn2} + \frac{\pi}{2}\right) \quad (4.12)$$

$$f_{23} = -\mu \quad (4.13)$$

$$f_{31} = r_{hubarm} \quad (4.14)$$

$$f_{32} = -\mu r_{drum} \quad (4.15)$$

$$f_{33} = -\mu r_{drum} \quad (4.16)$$

$$F_1 = \cos\left(\frac{\pi}{2} - \frac{\alpha}{4}\right) m r_{cm1} \omega^2 + m r_{cm2} \omega^2 - F_{s1} + \cos(\alpha) F_{s2} \quad (4.17)$$

$$F_2 = \sin\left(\frac{\pi}{2} - \frac{\alpha}{4}\right) m r_{cm1} \omega^2 + \cos(\alpha) F_{s2} \quad (4.18)$$

$$F_3 = 0 \quad (0.1)$$

$$\alpha = \frac{2\pi}{3} \quad (0.2)$$

After the normal forces are determined, the basic torque equation (2.7) may be used to determine the transferred torque. The Comet clutch's torque transfer is given by

$$T = n \mu r_{drum} |F_{N1} + F_{N2}| \quad (4.19)$$

where n is the number of clutch arms, μ is the coefficient of friction, and r_{drum} is the inner radius of the drum.

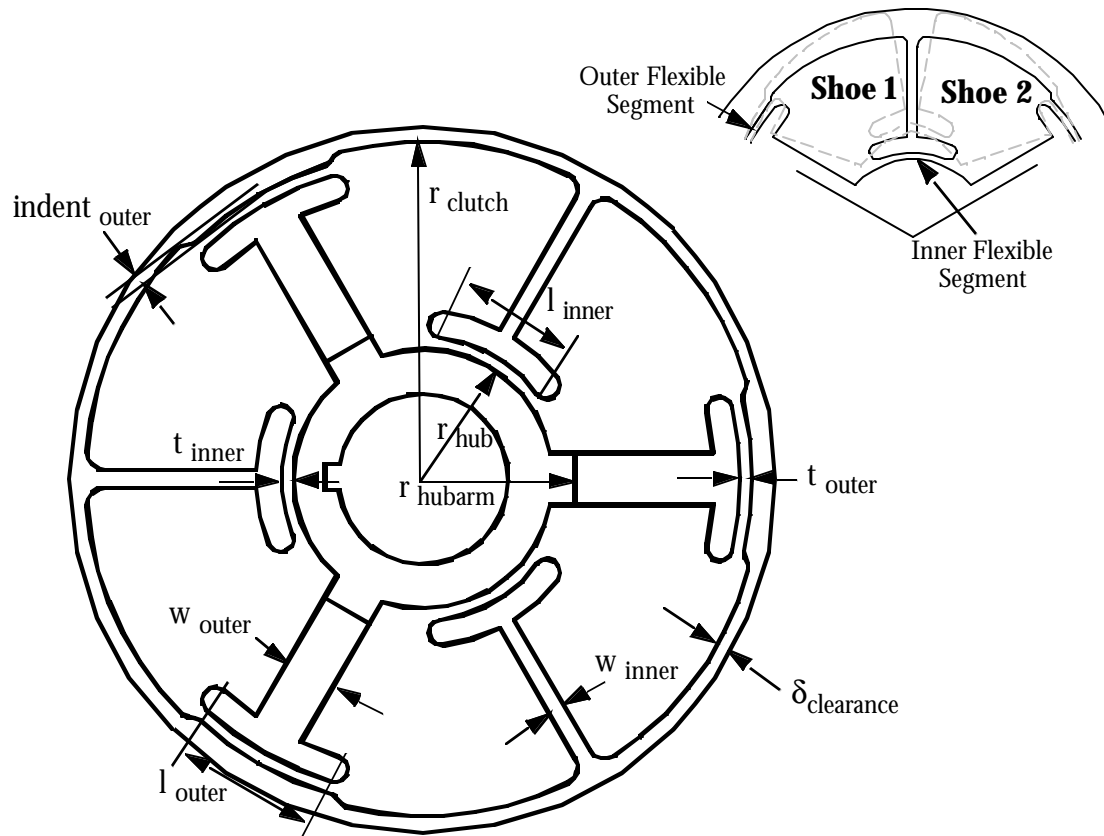


Figure 4.2 Floating-Opposing-Arm (FOA) clutch with key design parameters.

4.2 Floating-Opposing-Arm Clutch

The FOA clutch was the clutch concept that scored well in the evaluation criteria set forth by Crane et al. [5]. This clutch design combines a relatively high torque capacity with smooth engagement and direction reversibility. Similar to the F1 clutch, the hub carries all the torque load instead of the flexible segments. Figure 4.2 shows a complete diagram of the F1 clutch with its key parameters.

Modeling of the clutch may be done by analyzing only one segment, because the geometry and loading of the clutch are symmetrical. Each segment consist of shoe 1, shoe 2, the inner flexible segment, and each half of the outer flexible segment. In addition, each

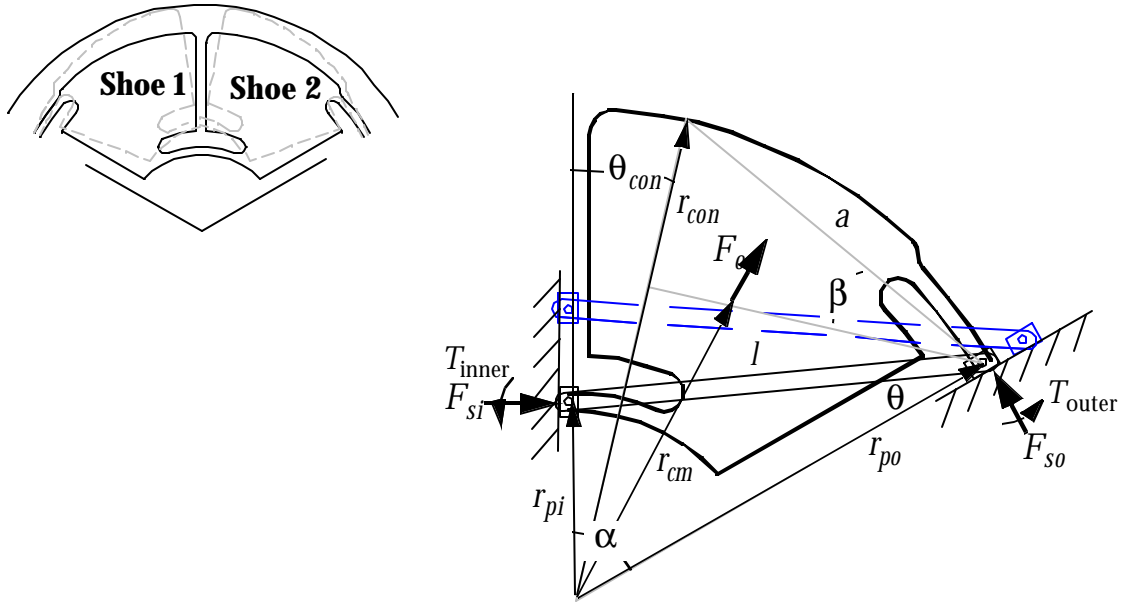


Figure 4.3 The design parameters of this section of a FOA segment is used to solve for the contact engagement speed.

segment may be modeled with sliders at the middle of the inner and outer flexible segments. Torque is transferred to the drum by both shoe 1 and shoe 2.

4.2.1 Contact Engagement Speed Model

The contact engagement speed is calculated by analyzing only half of a segment (see Figure 4.3). Initially, the link (l) must rotate so that the shoe contacts the drum. Unlike the model for the F1 clutch, an approximation was made for $\Delta\theta$ as

$$\Delta\theta = \theta - \theta_0 = \frac{\delta}{\left[l \left(\cos\theta \cot\frac{\pi}{n} - \sin\theta \right) \cos\left(\frac{\pi}{n} - \theta_{con}\right) + a(\cos\beta) \right]} \quad (4.20)$$

where the inclusive variables are defined as

$$l = \sqrt{r_{po}^2 + r_{pi}^2 - 2r_{po}r_{pi}\cos\alpha} \quad (4.21)$$

$$\theta = \arcsin\left(\frac{r_{pi}\sin\alpha}{l}\right) \quad (4.22)$$

$$\alpha = \frac{\pi}{n} \quad (4.23)$$

$$a = \sqrt{(r_{clutch} - \cos(\alpha - \theta_{con_0})r_{po_0})^2 + (\sin(\alpha - \theta_{con_0})r_{po_0})^2} \quad (4.24)$$

$$\beta = \text{asin}\left[\frac{r_{clutch} - r_{po_0}\cos(\alpha - \theta_{con_0})}{a}\right] \quad (4.25)$$

$$\delta = r_{drum} - r_{clutch} \quad (4.26)$$

where n is the number of segments, θ_{con} is the angle from the inner pin to point of shoe contact, and r_{po} , r_{pi_0} , r_{clutch} , and r_{hub} are given initially.

After $\Delta\theta$ is calculated, then the summation of the forces about the pseudo inner pin joint may be used to establish a relationship between the centrifugal force (F_o) and the rotation ($\Delta\theta$). The force equilibrium equation for Figure 4.3 is

$$[(\vec{r}_{cm} - \vec{r}_{si}) \times \vec{F}_o] + \hat{T}_{inner} + \hat{T}_{outer} + \left[l\angle\left(\frac{\pi}{2} + \frac{\pi}{n} - \theta\right) \times \vec{F}_{so}\right] = 0 \quad (4.27)$$

given that

$$\vec{F}_o = m\vec{r}_{cm}\omega^2 \quad (4.28)$$

$$\hat{T}_{inner} = k_{inner}\Delta\theta\hat{k} \quad (4.29)$$

$$\hat{T}_{outer} = k_{outer}\Delta\theta\hat{k} \quad (4.30)$$

$$r_{cm} = \left[\frac{2}{3} \frac{\sin(\alpha/2)}{\alpha/2}\right] \left[\frac{r_{clutch}^3 - r_{hub}^3}{r_{clutch}^2 - r_{hub}^2}\right] \quad (4.31)$$

$$\angle r_{cm} = \frac{\pi}{2} \pm \frac{\alpha}{2} \quad (4.32)$$

$$r_{pi} = \frac{l\sin\theta}{\sin\alpha} \quad (4.33)$$

$$|\vec{F}_{so}| = \frac{-F_o \sin\theta_{F_o}}{\sin(-\alpha)} \quad (4.34)$$

$$\angle F_{so} = -\alpha \quad (4.35)$$

where m is the mass and E is the modulus of elasticity. The variables k and I are defined

as $k_x = \frac{EI_{lx}}{l_x}$ and $I_x = \frac{t_{clutch} l_x^3}{12}$ where x is either the inner or outer flexible segment. The

initial values of t_{inner} , t_{outer} , l_{inner} , and l_{outer} are known. By dividing Equation (4.27) by

ω^2 and defining $\frac{F_o}{2} = m\vec{r}_{cm}$, the contact engagement speed (ω) may be solved for

explicitly where

$$\omega = \left[\frac{-(k_o + k_i)\Delta\theta\hat{k}}{\left[(\vec{r}_{cm} - \vec{r}_{pi_2}) \times \frac{\vec{F}_o}{\omega^2} \right] + \left[\vec{l} \times \frac{\vec{F}_{so}}{\omega^2} \right]} \right]^{1/2} \quad (4.36)$$

4.2.2 Torque Model

Once the clutch is engaged, the aggressive and non-aggressive shoes do not load the drum symmetrically, but the position is known. This allows the normal forces to be solved for by using force equilibrium equations for both shoes and the moment equilibrium equation for only one shoe (see Figure 4.4). The friction forces are a function of the normal forces. The reactions at the inner slider are assumed to be equal in magnitude and opposite in direction. The reactions at the outer sliders are equal in magnitude and perpendicular to \vec{r}_{so} . The hub force acts perpendicular to the point of contact on the face of the clutch. The geometry is constrained so that the inner and outer sliders must move radially outward from the center of the clutch. After these assumptions are taken into account there are only five unknowns: F_{so} , F_{si} , F_{hubarm} , F_{N1} , and F_{N2} .

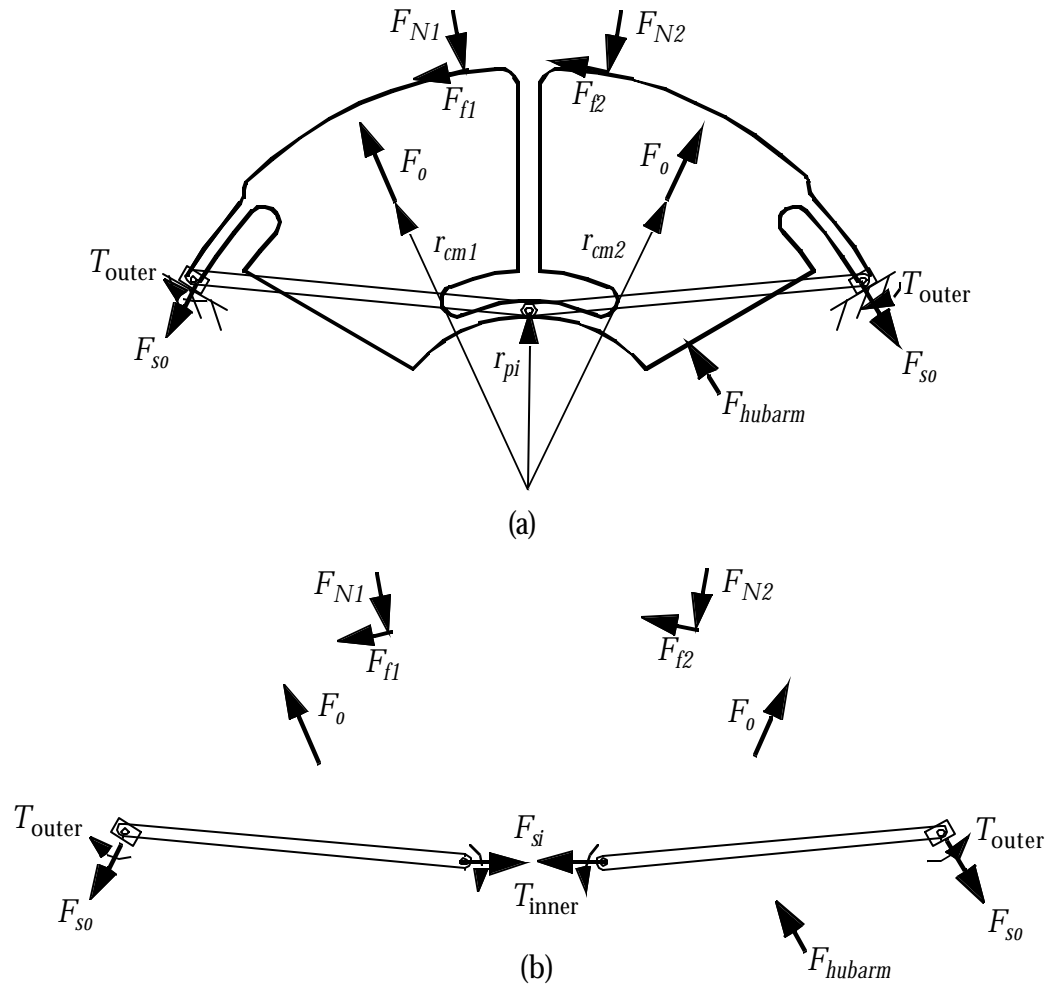


Figure 4.4 Force and moment equilibrium diagrams for the FOA clutch that are used to solve for torque capacity.

The two force equilibrium equations with their x and y components and the moment equilibrium equation are used to solve for the unknowns. These three equations give the following system of equations:

$$\begin{bmatrix}
 mr_{cm1x}\omega^2 \\
 -mr_{cm1y}\omega^2 \\
 \vec{T}_o + \vec{T}_i - [r_{cm1} - r_{pi}] \times [mr_{cm1}\omega^2] \\
 -mr_{cm2x}\omega^2 \\
 -mr_{cm2y}\omega^2
 \end{bmatrix} = \begin{bmatrix}
 f_{11} & 0 & f_{13} & f_{14} & 1 \\
 f_{21} & 0 & f_{23} & f_{24} & 0 \\
 f_{31} & 0 & f_{33} & f_{34} & 0 \\
 0 & f_{42} & 0 & f_{44} & -1 \\
 0 & f_{52} & 0 & f_{54} & 0
 \end{bmatrix} \begin{bmatrix}
 F_{N1} \\
 F_{N2} \\
 F_{hub} \\
 F_{so} \\
 F_{si}
 \end{bmatrix} \quad (4.37)$$

where the elements of the matrix are

$$f_{11} = \sin\theta_{con} - \mu\cos\theta_{con} \quad (4.38)$$

$$f_{13} = \sin(\alpha - \Delta\theta) \quad (4.39)$$

$$f_{14} = -\cos\alpha \quad (4.40)$$

$$f_{21} = -(\cos\theta_{con} + \mu\sin\theta_{con}) \quad (4.41)$$

$$f_{23} = \cos(\alpha - \Delta\theta) \quad (4.42)$$

$$f_{24} = -\sin\alpha \quad (4.43)$$

$$f_{42} = -(\sin\theta_{con} + \mu\cos\theta_{con}) \quad (4.44)$$

$$f_{44} = \cos\alpha \quad (4.45)$$

$$f_{52} = -\cos\theta_{con} + \mu\sin\theta_{con} \quad (4.46)$$

$$f_{54} = -\sin\alpha \quad (4.47)$$

After the normal forces are determined, the basic torque equation (2.7) may be used to determine the transferred torque. The FOA clutch's torque transfer is given by

$$T = n\mu r_{drum} |F_{N1} + F_{N2}| \quad (4.48)$$

where n is the number of clutch arms, μ is the coefficient of friction, and r_{drum} is the inner radius of the drum.

4.3 Floating 1 (F1) Clutch

The F1 clutch was one of the original clutch concepts developed by Crane et al. [5]. This F1 clutch concept is modeled after traditional aggressive floating shoe clutches. Unlike the compliant s-clutch, this clutch's hub bears the torque load instead of the flexible segments. The F1 design presented in this thesis has a stiffer shoe 1 for better accuracy in modeling, whereas before the shoe 1 deflected similar to the other flexible segments. Figure 4.5 shows a complete diagram of the F1 clutch with its key parameters.

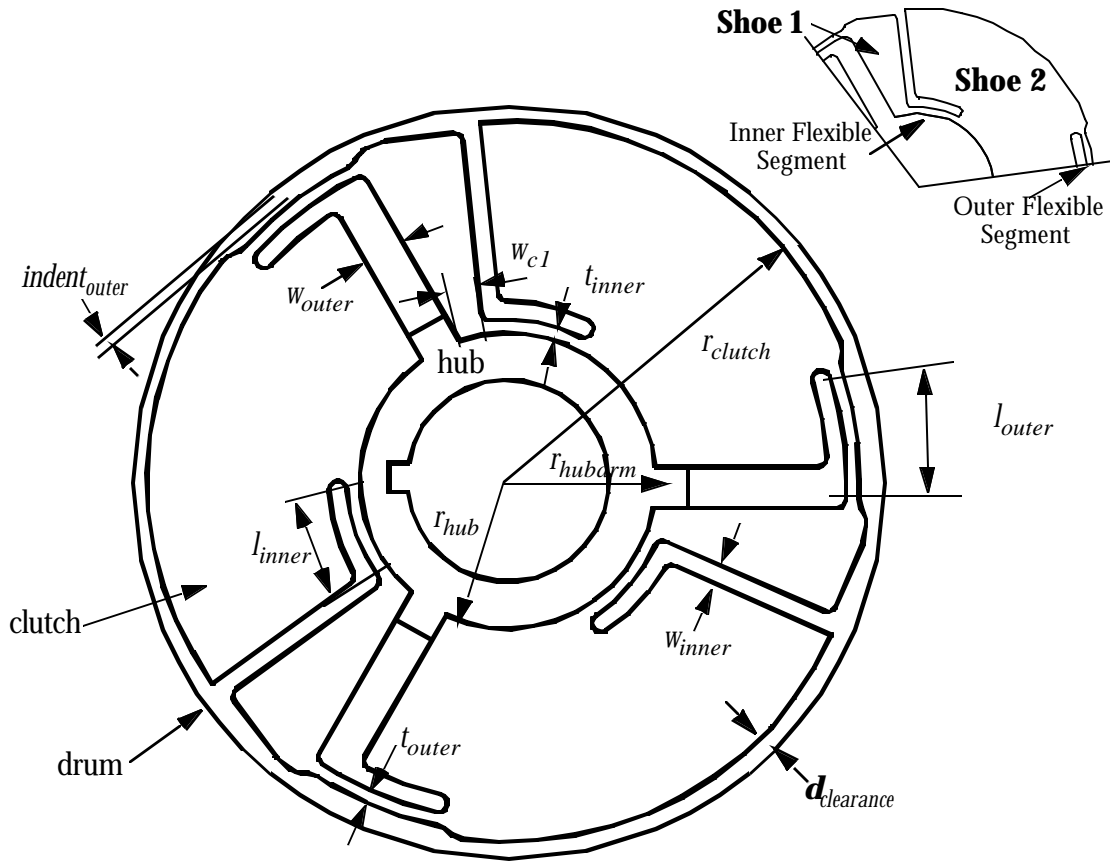


Figure 4.5 The Floating 1 (F1) clutch with key design parameters.

Modeling of the clutch may be done by analyzing only one segment, because the geometry and loading of the clutch are symmetrical. Each segment consists of a shoe 1, shoe 2, the inner flexible segment, and each half of the outer flexible segment. In addition, each segment may be modeled with pseudo sliders at the middle of the inner and outer flexible segments. Torque is transferred by shoe 2, which comes into contact with the drum.

4.3.1 Engagement Model

The F1 clutch's contact engagement speed is calculated by finding the outer rotation ($\Delta\theta_2$) and outward translation (Δr_{po}) necessary to make contact with the drum. There is no explicit way of finding these values, and therefore an optimization routine was used, where $\Delta\theta_2$ and Δr_{po} converge to the optimal values such that

$r_{clutch} - (r_{pinouter} + a)$ is equal to zero. An additional constraint was that the value of the new l_2 must equal the value of the old l_2 .

The contact engagement speed (ω) is calculated by taking the summation of the forces about the center of the clutch. The force equilibrium equation for Figure 4.6 is

$$(\vec{r}_{cm1} \times \vec{F}_{o1}) + \vec{T}_2 + \vec{T}_3 + (\vec{r}_{cm2} \times \vec{F}_{o2}) + (\vec{r}_{po2} \times \vec{F}_{so2}) + (\vec{r}_{pi} \times \vec{F}_{si}) = 0 \quad (4.49)$$

Given that

$$\vec{T}_2 = k_{outer} \cdot \Delta\theta \hat{k} \quad (4.50)$$

$$\vec{T}_3 = k_{inner} \cdot \frac{\Delta\phi}{2} \hat{k} \quad (4.51)$$

$$\vec{F}_{o2} = m \vec{r}_{cm2} \omega^2 \quad (4.52)$$

$$|\vec{r}_{cm2}| = \left[\frac{2}{3} \frac{\sin\left(\frac{\theta_{innerslot}}{2}\right)}{\frac{\theta_{innerslot}}{2}} \right] \left[\frac{r_{clutch}^3 - r_{hub}^3}{r_{clutch}^2 - r_{hub}^2} \right] \quad (4.53)$$

$$\angle \vec{r}_{cm2} = \theta_{innerslot} / 2 \quad (4.54)$$

$$|\vec{r}_{po}| = r_{po_0} + \Delta r_{po} \quad (4.55)$$

$$|\vec{r}_{pi}| = \frac{l_2}{\sin\theta_{pi}} \sin\theta \quad (4.56)$$

$$\angle \vec{r}_{po2} = \theta_{po2} = \frac{l_{outer}}{2} r_{po} - \frac{w_{outer}}{2} r_{po} \quad (4.57)$$

$$\angle \vec{r}_{pi} = \theta_{pi} = \theta_{innerslot} + \frac{l_{inner}}{2} r_{pi} \quad (4.58)$$

$$|\vec{F}_{so}| = \frac{-F_{o2} \sin(\theta_{cm2}) - F_{si} \cos(\theta_{Fsi2})}{\cos(\theta_{Fso2})} \quad (4.59)$$

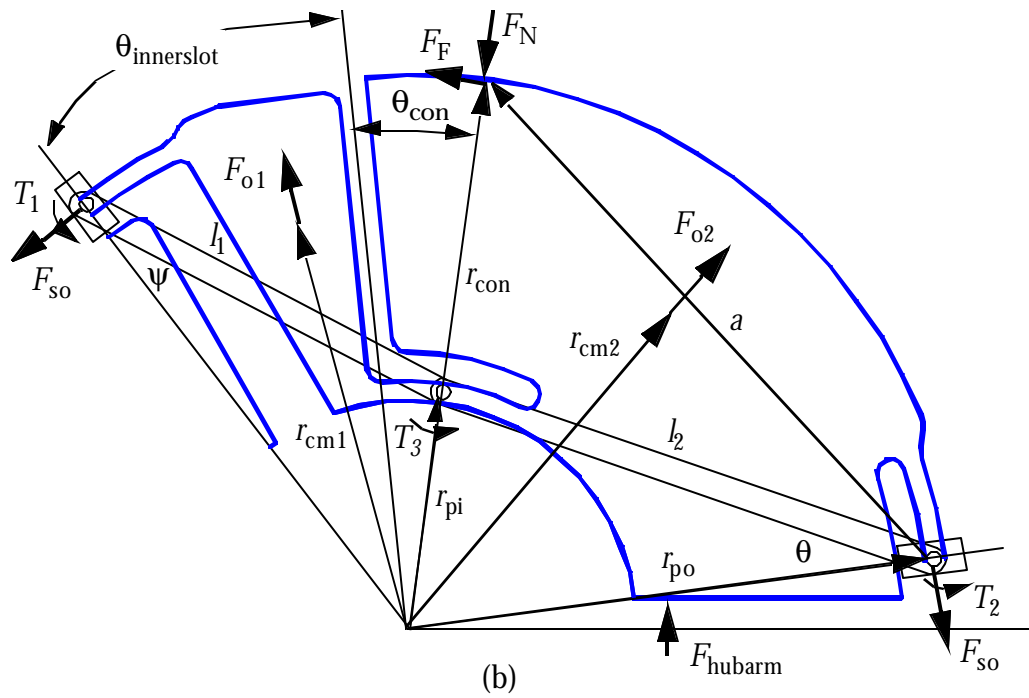
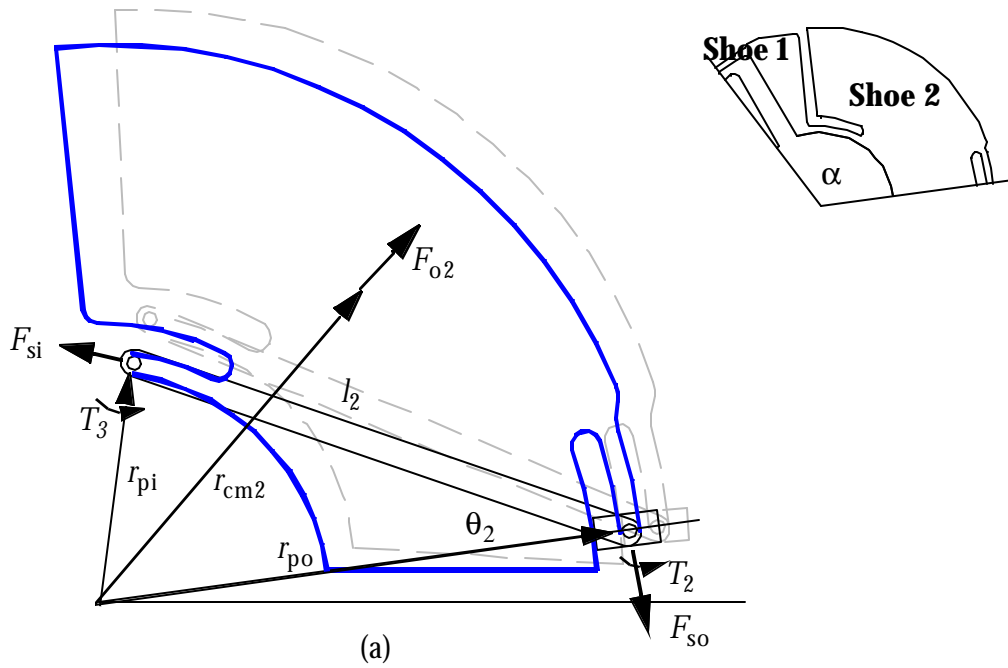


Figure 4.6 Force and moment diagrams for (a) half a segment and (b) one segment of the F1 clutch.

$$|\vec{F}_{si}| = \frac{-F_{o2} \sin(\theta_{cm2}) + \frac{F_{o2} \cos(\theta_{cm2}) \sin(\theta_{Fso2})}{\cos(\theta_{Fso2})}}{\sin(\theta_{Fsi}) - \frac{\cos(\theta_{Fsi2}) \sin(\theta_{Fso2})}{\cos(\theta_{Fso2})}} \quad (4.60)$$

$$\angle F_{so2} = \theta_{po2} - \pi/2 \quad (4.61)$$

$$\angle F_{si2} = \theta_{pi} + \pi/2 \quad (4.62)$$

$$\theta_{innerslot} = \alpha - \left(\frac{w_{c1} + \frac{w_{innerslot}}{2} + \frac{w_{outerslot}}{2}}{r_{pi}} \right) \quad (4.63)$$

$$\alpha = \frac{2\pi}{n} \quad (4.64)$$

$$\theta = \text{asin} \left[\frac{\sin(\alpha - \theta_{pi} + \theta_{po2})}{l_2} r_{pi} \right] \quad (4.65)$$

$$\phi = \psi + \alpha - \theta \quad (4.66)$$

$$\psi = \text{asin} \left[\frac{\sin(\alpha - \theta_{pi} + \theta_{po2})}{l_1} r_{pi} \right] \quad (4.67)$$

$$l_2 = [r_{po}^2 + r_{pi}^2 - 2r_{po}r_{pi} \cos(\theta_{pi} - \theta_{po2})]^{1/2} \quad (4.68)$$

$$l_1 = [r_{po}^2 + r_{pi}^2 - 2r_{po}r_{pi} \cos(\alpha - \theta_{si} + \theta_{po2})]^{1/2} \quad (4.69)$$

where n is the number of segments, m is the mass, and E is the modulus of elasticity. k

and I are defined as $k_x = \frac{EI_{lx}}{l_x}$ and $I_x = \frac{t_{clutch} t_x^3}{12}$ where x is either the inner or outer flex-

ible segment. The initial values of r_{clutch} , r_{hub} , t_{clutch} , t_{inner} , t_{outer} , l_{inner} , l_{outer} ,

$w_{innerslot}$, $w_{outerslot}$, w_{c1} , r_{pi_0} , r_{po_0} are known. $\Delta\theta$ and Δr_{po} are solved for with an opti-

mization routine. By dividing Equation (4.27) by ω^2 and defining $\frac{F_o}{\omega^2} = m\vec{r}_{cm}$, the contact engagement speed (ω) may be solved for explicitly where

$$\omega = \left| \frac{-(\hat{T}_2 + \hat{T}_3)}{\left(\vec{r}_{cm2} \times \frac{\vec{F}_{o2}}{\omega^2} \right) + \left(\vec{r}_{po2} \times \frac{\vec{F}_{so2}}{\omega^2} \right) + \left(\vec{r}_{pi} \times \frac{\vec{F}_{si}}{\omega^2} \right)} \right|^{1/2} \quad (4.70)$$

4.3.2 Torque Model

Once the clutch makes contact engagement, only shoe 2 has a normal force association. This normal force may be solved for by using force and moment equilibrium equations for both shoes (see Figure 4.6). The friction force is a function of the normal force (μF_N). The reaction forces at the inner slider are assumed to be equal in magnitude and opposite in direction. Similarly, the reaction forces at the outer sliders are related by $F_{sox2} = -F_{soy1}$ and $F_{soy2} = F_{sox1}$. The hub force acts perpendicular to the point of contact on the face of the clutch. The geometry is assumed to be constrained so that the outer sliders must move radially outward from the center of the clutch. After these assumptions are taken into account there are only six unknowns: F_{six} , F_{siy} , F_{sox1} , F_{soy1} , F_N , and F_{hubarm} .

The two force equilibrium equations with their x and y components, as well as the moment equilibrium equations are used to solve for the unknowns. These four equations give this system of equations.

$$\begin{bmatrix} -mr_{cm2x}\omega^2 \\ -mr_{cm2y}\omega^2 \\ -mr_{cm1x}\omega^2 \\ -mr_{cm1y}\omega^2 \\ -(T_1 - T_3) \\ -(T_2 + T_3) \end{bmatrix} = \begin{bmatrix} -1 & 0 & 0 & -1 & f_{15} & 0 \\ 0 & 1 & -1 & 0 & f_{25} & 1 \\ 1 & 0 & -1 & 0 & 0 & 0 \\ 0 & -1 & 0 & 1 & 0 & 0 \\ f_{51} & f_{52} & f_{53} & f_{54} & 0 & 0 \\ f_{61} & f_{62} & f_{63} & f_{64} & f_{65} & f_{66} \end{bmatrix} \begin{bmatrix} F_{six} \\ F_{siy} \\ F_{sox1} \\ F_{soy1} \\ F_N \\ F_{hubarm} \end{bmatrix} \quad (4.71)$$

where the elements of the matrix are

$$f_{15} = \cos(\theta_{con} + \pi) + \mu \cos(\theta_{con} + \pi/2) \quad (4.72)$$

$$f_{25} = \sin(\theta_{con} + \pi) + \mu \sin(\theta_{con} + \pi/2) \quad (4.73)$$

$$f_{51} = -r_{piy} \quad (4.74)$$

$$f_{52} = -r_{pix} \quad (4.75)$$

$$f_{53} = r_{poy1} \quad (4.76)$$

$$f_{54} = r_{pox1} \quad (4.77)$$

$$f_{61} = r_{piy} \quad (4.78)$$

$$f_{62} = r_{pix} \quad (4.79)$$

$$f_{63} = -r_{pox2} \quad (4.80)$$

$$f_{64} = r_{poy2} \quad (4.81)$$

$$f_{65} = \hat{r}_{con} \times (\vec{F}_N + \mu \vec{F}_N) \quad (4.82)$$

$$f_{66} = \hat{r}_{hubarm} \quad (4.83)$$

In addition, the following relationships are also identified within the matrix: $f_{11} = -f_{31}$, $f_{22} = -f_{42}$, $f_{14} = f_{33}$, and $f_{23} = -f_{44}$.

After the normal force is solved for by standard methods, the basic torque equation (2.7) may be used to determine the transferred torque. The F1 clutch's torque transfer is given by

$$T = n\mu r_{drum} |F_N| \quad (4.84)$$

where n is the number of clutch arms, μ is the coefficient of friction, and r_{drum} is the radius of the drum.

This chapter discusses engagement speed and torque performance sensitivity to variations in manufacturing and design tolerances. In addition, robust designs and multiple layers are discussed for minimizing the FOA clutch's performance tolerances. While manufacturing issues and possible manufacturing processes for compliant mechanisms will be discussed, this thesis will not specify clutch manufacturing cost. The thesis will focus on standard economical manufacturing processes that are maintained within their normal tolerance capabilities.

5.1 Manufacturing Issues for Compliant Mechanisms

Herring et al. [28] were able to create various manufacturing process tables and charts that represent process capabilities appropriate for compliant mechanisms with long thin beams. Table 5.1 shows process capabilities in relation to the key design parameters of the FOA clutch. The table has been adapted for short thin beams (small-length flexural pivots).

Unfortunately, none of the high production processes listed by Herring et al. are capable of producing the configuration of the FOA clutch in one piece. Laser cutting and axial powder compaction are two of the closest processes, but neither is able to achieve a width of 0.015 to 0.020 inches for the smaller (2") clutch. The laser cutting constrains the

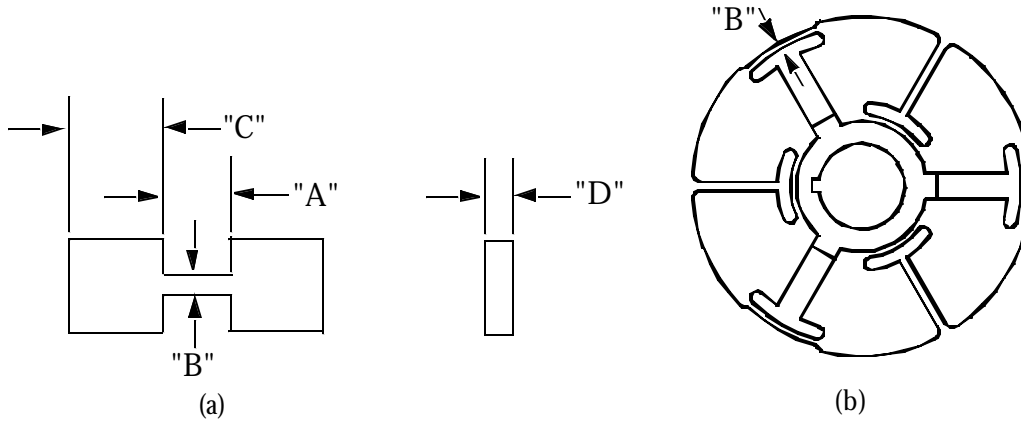


Figure 5.1 Key parameters for manufacturing process capabilities of compliant mechanisms. (a) shows the thickness, length and depth of the flexible segment and (b) shows how the thickness of the flexible segment relates to the FOA clutch.

TABLE 5.1 Process capabilities for compliant mechanisms as they relate to the small-length flexural pivots found on the FOA clutch.

Process	Process Capabilities			
	Minimum Beam Dimension "B"	Ratio D:B or Longest Dimension "D"	Ratio C:B or Longest Dimension "C"	Tolerance of "B"
Extrusion	0.05"	N/A	1.8:1	±8 -10% thickness
Laser Cutting	0.0625" - 0.25"	1:1 -4:1	N/A	±0.001 *
Water-Jet	0.05" - 0.08"	4"	N/A	±0.020 *
Axial Powder Compaction	0.06" - 0.1"	1/2"	N/A	±0.002 **
Die Casting	0.08" - 0.09"	N/A	2:1-4:1	±0.015
Metal Injection Molding	0.05" - 0.08"	1/2"	2:1-4:1	±0.003
Needed Capabilities for Small (2") clutch	< 0.020"	12:1 - 38:1 or $D \geq 1/2$ "	1:1 - 2:1	<±0.001
Needed Capabilities for Large (4") Clutch	< 0.060"	12:1 - 38:1 or $D \geq 1$ "	1:1 - 2:1	<±0.001

* ±0.005 inches due to undercutting

** 200 gram weight limit

TABLE 5.2 Two new process capabilities for compliant mechanisms

Fine Blanking	N/A	1:1 - 1.5:1	N/A	±0.0005
Stamping (Conventional Blanking)	N/A	1:1 - 1.5:1	N/A	±0.002

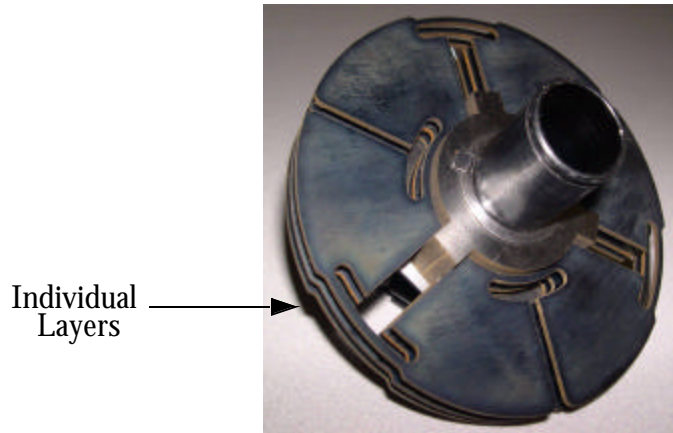


Figure 5.2 FOA clutch shown with multiple layers that float on hub.

clutch to be made in layers because of the 1:1 ratio of "D" to "B", where "D" is the clutch's thickness "B" is the flexible segment's thickness. In addition, the laser beam expansion causes a ± 0.005 inches tolerance because of undercutting. This characteristic is undesirable considering the clutch's performance sensitivity to those tolerances. Axial powder compaction is limited to a width of 1/2 inch and a maximum weight of 200 grams. Both of these stipulations would be violated by the larger (4") clutch design. In addition, the tolerance of ± 0.002 inches is still less than the desired ± 0.001 inches. The impact of these differences in tolerances on clutch performance will be discussed in "Sensitivity of Key Parameters" on page 66.

Since Herring et al. focused solely on long thin beams, the original process capability table included no information on such processes as fine blanking and stamping. These are two process that are infeasible with long thin beams, but would work ideally with the short beams found on the clutch. Table 5.1 includes both of these processes and their corresponding capabilities.

As suggested by Herring et al. the best solution for the clutch would be to create a hybrid process. This process would consist of cutting/forming the clutch out of thin sheets of metal and then joining the multiple layers together with a mechanical, thermal or chemical process. The joining of the layers may not be necessary in the case of the clutch, where each layer may float freely around the hub (Figure 5.2). More research will be presented on this topic in the following sections.

When the hybrid process is used with fine-blanking, all needed capabilities are achieved. Fine-blanking is ideal because it produces a clean, smooth edge on the part, unlike the burrs, roll-over, burnish, or fractures that are typical attributes of die-cut edges [29]. In addition, fine-blanking can produce between 240 and 480 layers per minute (enough for 20-40 four inch clutches per minute). Such high tolerances and small die-part clearances (1% of thickness) are attributed to the use of a v-shaped impingement ring that immobilizes the material before the part is sheared out.

In comparison to fine-blanking, when the hybrid process is used with stamping all needed capabilities are not achieved. Stamping would eliminate the impression marks left by the fine-blanking impingement ring. In addition, stamping is less expensive than fine-blanking. One disadvantage of stamping is that a die-cut edge normally has four distinctive attributes: roll-over, burnish, fracture, and burrs. These edge attributes would significantly change the torque-speed characteristic of the clutch. They could also lead to early fatigue failure by causing stress raisers. In addition to the edge attributes, stamping typically has a ± 0.010 inch tolerance. In order to achieve the ± 0.002 inch tolerance as stated in Table 5.1, it would be significantly more expensive. One last disadvantage is that the clearance between punch and part is typically 8 to 10% of stock's thickness. Such high clearance accounts for all of the negative edge attributes.

5.1.1 Advantages of the Hybrid Process

The hybrid process has several advantages. By using a high production process, such as fine-blanking, it would be easy to produce high volumes of layers a short period of time (240-480 layers per minute). These layers could then be automatically grouped together in sets for assembly with the clutch's hub. The increased part count due to the layers may be offset by the high production rates and automatic assembly.

If the layers were not joined together, then the layers would give the advantage of conforming to the drum profile. The drum's profile varies in diameter due to the manufac-

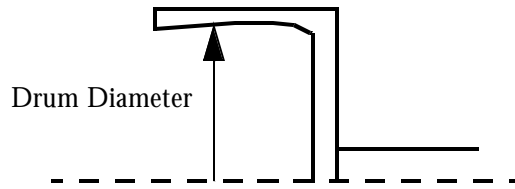


Figure 5.3 Drum profile due to manufacturing process.

turing process. Figure 5.3 shows how the drum may vary in diameter. Multiple layers would ensure that there were multiple points of contact within the drum.

In addition, the advantage of multiple layers is a lower clutch torque-speed variance. Each layer will have a certain variance due to the manufacturing process, yet when the sum of each layer's variance is taken to achieve the total variance of the clutch, it is predicted that the total variance will be lower. This lower variance is significant, because the clutch will perform much more accurately. This is discussed in more detail in “Performance of Layers” on page 79.

5.1.2 Disadvantages of the Hybrid Process

If the clutch's layers were not joined together, then one problem is that if the flexible segment is not thicker than it is wide, then each layer will have the tendency to bend out of plane. This was seen in the preliminary tests of “Results of Preliminary Testing” on page 26. Herring says that "this problem (bending out of plane) can be avoided by making the beam thicker in each layer than it is wide, thereby giving the beam a tendency to bend in the desired plane" [28].

Another unknown is whether or not it will be possible to keep the necessary tolerances on the flexible segments. The sensitivity of the clutch's performance to these key design parameters makes this issue very significant.

The last disadvantage of using layers is that of scoring. Scoring is caused by the high pressures of the thin layers exerted on the drum. These high pressures may cause the thin layers to cut grooves on the drum and cause catastrophic failure of the clutch.

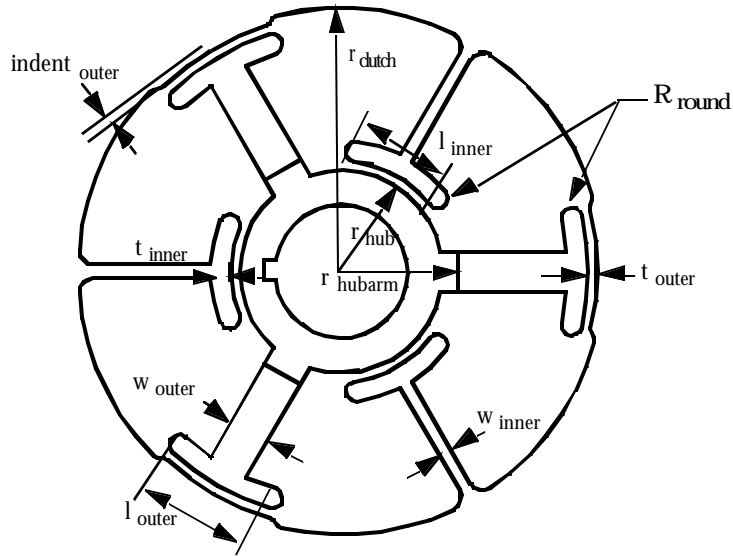


Figure 5.4 FOA clutch's design parameters.

5.2 Sensitivity of Key Parameters

Preliminary testing showed that the FOA clutch's torque-speed performance is sensitive to several design parameters. Figure 5.4 shows all design parameters used in the FOA model. The most sensitivity parameters were determined by performing model sensitivity analyses. This sensitivity analysis evaluates numerical derivatives of design parameters in order to create a robust design, as well as basic cause-effect relationships between these parameters and the clutch's engagement speed & torque-capacity for verification.

5.2.1 Numerical Derivatives

If an equation for some model is known, then the sensitivity of any parameter may be calculated by solving for the partial derivative of that parameter with respect to the desired output (i.e. torque). Unfortunately, the F1 and FOA models do not result in a single equation for engagement speed and torque. Instead, a numerical derivative is calculated by using the forward difference method or the central difference method (Equation

(5.2) and Equation (5.3) respectively). These methods are derived from a Taylors Series Expansion.

$$f(x + \Delta x) = f(x) + \frac{\partial f}{\partial x}(\Delta x) + \frac{1}{2} \frac{\partial^2 f}{\partial x^2}(\Delta x) + \dots \quad (5.1)$$

where the series is truncated and for which $\frac{\partial f}{\partial x}$ is solved as

$$\frac{\partial f}{\partial x} = \frac{f(x + \Delta x) - f(x)}{\Delta x} \quad (5.2)$$

$$\frac{\partial f}{\partial x} = \frac{f(x + \Delta x) - f(x - \Delta x)}{2\Delta x} \quad (5.3)$$

Multiple steps (Δx) were used to calculate the numerical derivatives in order to determine the effects of truncation and round-off errors from the previous equations. After the derivatives or sensitivities were found with respect to engagement speed and torque, they were ranked (1 being most sensitive). Table 5.3 shows the results for *Sensitivity* for engagement and torque for the FOA clutch using the central difference method¹. (See Figure 5.4 for the each term definition.) The table lists each individual model parameter, along with their original value, their associated manufacturing tolerance, and the step (Δx) used in the central difference method. Similar results for the F1 clutch are found in Appendix A.2.

Figure 5.5 shows that the FOA clutch parameters that affect the contact engagement speed and torque-capacity the most are r_{clutch} , t_{inner} , t_{outer} , and r_{drum} . The variables r_{clutch} and r_{drum} essentially combine to create $\delta_{clearance}$. These results were expected from previous tests and is supported by the “Basic Parameter-Performance Relationships” on page 78. All other engagement sensitivities are significantly lower. The next two closest engagement parameter sensitivities are $indent_{outer}$ and r_{hub} , which are lower by a factor of 10. On the other hand, the remaining parameters for the torque model

1. See Appendix A.1 for all original values of input design parameters, as well as outputs.

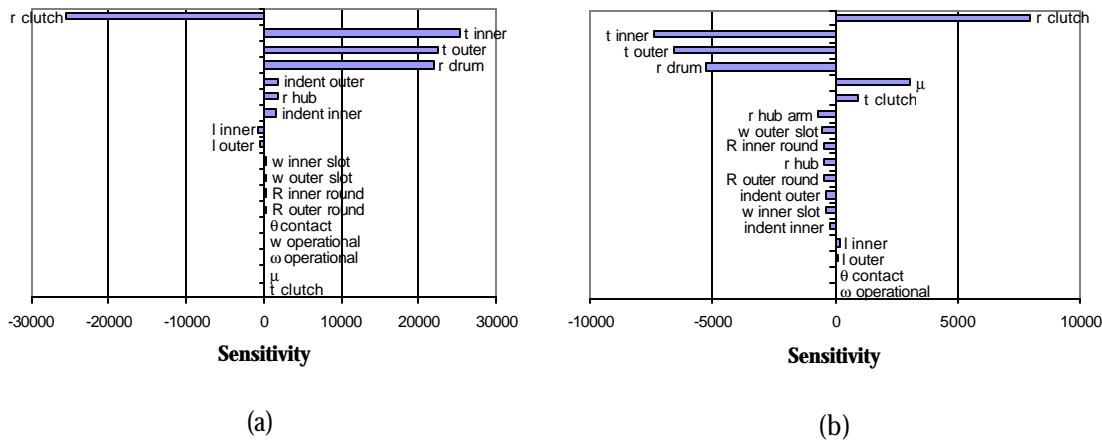


Figure 5.5 The FOA clutch's most sensitive clutch parameters for (a) Contact Engagement Speed and (b) Torque Capacity. Sensitivities are the same as those found in Table 5.3

TABLE 5.3 Parameter sensitivities for the FOA clutch using central difference method to calculate numerical derivatives.

INPUTS	Mft & Design		Contact Engagement					Torque				
	Original	Tolerance	Adjusted Sensitivity			New		Adjusted Sensitivity			New	
			Step	Sensitivity	Rank	by Tol	Rank	Step	Sensitivity	Rank	by Tol	Rank
t clutch	0.626	0.005	0.0001	0.0	15	0.00	14	0.0001	933.9	6	4.67	6
r hub	0.750	0.003	0.0001	1825.4	6	5.48	7	0.0001	-444.0	10	-1.33	10
r drum	2.000	0.005	0.0001	21816.5	4	109.08	1	0.0001	-5293.6	4	-26.47	1
r clutch	1.950	0.003	0.0001	-25568.1	1	-76.70	2	0.0001	7988.3	1	23.97	2
t outer	0.070	0.003	0.0001	22376.0	3	67.13	4	0.0001	-6591.1	3	-19.77	4
t inner	0.070	0.003	0.0001	25189.2	2	75.57	3	0.0001	-7398.2	2	-22.19	3
l outer	0.800	0.003	0.0001	-546.9	9	-1.64	9	0.0001	130.6	16	0.39	15
l inner	0.700	0.003	0.0001	-725.7	8	-2.18	8	0.0001	184.0	15	0.55	14
w outer slot	0.300	0.003	0.0001	416.7	10	1.25	10	0.0001	-519.3	8	-1.56	8
w inner slot	0.100	0.003	0.0001	416.7	10	1.25	10	0.0001	-352.1	13	-1.06	13
r hub arm	0.950	0.005	0.0001	0.0	15	0.00	14	0.0001	-677.6	7	-3.39	7
θ contact (high)	10.00	2	1	13.2	14	26.45	5	1	9.5	17	18.99	5
R outer round	0.075	0.003	0.0001	381.7	13	1.15	13	0.0001	-433.0	11	-1.30	11
R inner round	0.075	0.003	0.0001	401.5	12	1.20	12	0.0001	-482.3	9	-1.45	9
μ	0.420	0	0.0001	0.0	15	0.00	14	0.0001	3088.5	5	0.00	16
ω operational	3600	0	100	0.0	15	0.00	14	100	0.5	18	0.00	16
indent outer	0.050	0.003	0.0001	1868.0	5	5.60	6	0.0001	-386.9	12	-1.16	12
indent inner	0.000	0	0.0001	1579.3	7	0.00	14	0.0001	-236.1	14	0.00	16

ω contact eng	2139.3	rpm	Tolerance (Eng) = ±	169.6	rpm	Tolerance (T) = ±	50.6	in-lb
T operating	584.6	in-lb	Std Dev (Eng) = ±	56.54	rpm	Std Dev (T) = ±	16.88	in-lb

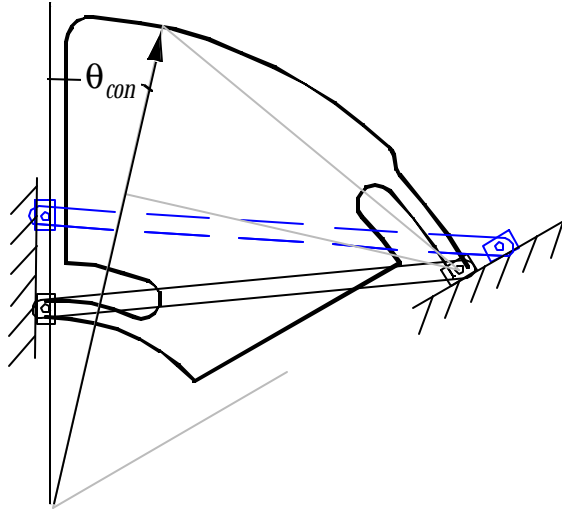


Figure 5.6 θ_{con} is the angle that determines how much of the clutch's surface engages with the drum.

are much closer to the top four parameters. The variable r_{hub} is only lower by a factor of 2. This means that the torque is more sensitive to more of the design parameters.

In addition, by changing the mean value of these parameters it is possible to increase or decrease their sensitivity. Unfortunately, most of the parameters are limited by their design space. The only significant parameter that may be changed dramatically is θ_{con} . Figure 5.6 shows that θ_{con} is the angle that determines how much of the clutch's surface engages with the drum. By increasing its value to 20 degrees, it becomes the most sensitive parameter.¹

5.2.2 Manufacturing and Design Tolerances

In addition to finding the numerical derivatives (sensitivities) for each parameter, there was an additional weight assigned to each parameter. For a certain manufacturing

1. See Appendix A.4 for sensitivity chart for $\theta_{con} = 20$.

process, each variable will have a specific tolerance. This manufacturing tolerance (ψ_i) may be used as a weight in order to adjust the sensitivities as

$$\frac{\partial f_a}{\partial x_i} = \frac{\partial f}{\partial x_i} \cdot \psi_i \quad (5.4)$$

where $\frac{\partial f_a}{\partial x_i}$ is the adjusted sensitivity of the contact engagement speed or torque capacity due to some parameter (x). This assignment of weights is important because it alters the order of the most significant parameters, as well as makes previously insensitive variables sensitive (e.g. $\theta_{contact}$). The adjusted sensitivities due to manufacturing or design tolerances, along with new ranks are found in Table 5.3.

5.2.3 Performance Tolerances

Contact engagement speed and torque capacity are the two critical performance criteria for designing centrifugal clutches. If the specifications for a clutch state that the clutch must engage between two values (e.g. 2000 to 2400 rpm for Comet 4 inch clutch), and have a minimum torque, then the worst case scenario should behave within those constraints. By using traditional error analysis methods, it is possible to determine the tolerance range for both contact engagement speed and torque capacity. Tolerance range is defined as the minimum to maximum value of a performance criteria. These tolerance ranges for contact engagement speed and torque capacity will be referred to as performance tolerances (ψ_f). This method accurately predicts how manufacturing tolerances will affect the performance tolerances. The performance tolerance is calculated by taking the square root of the sum of the squares of the adjusted sensitivities, or

$$\psi_f = \left[\sum_i \left(\frac{\partial f}{\partial x_i} \cdot \psi_i \right)^2 \right]^{\frac{1}{2}} \quad (5.5)$$

where i is i^{th} parameter in the model, f denotes either contact engagement speed or torque capacity, and ψ_i is the manufacturing tolerance of the i^{th} parameter.

Table 5.4 shows values for the contact engagement speed and torque capacity performance tolerances for different scenarios. Scenario A assumes a coefficient of friction (COF) tolerance and operating speed tolerance (ω) of zero. The results are given for a 4 inch clutch design with two different contact angles (θ_{con}) and a 2 inch clutch design with only one contact angle. As expected, the torque performance tolerance increases by nearly 50% with an increase in the COF tolerance. In addition, the torque performance tolerance is decreased by the increase in contact angle.

While it is not the focus of this thesis to present all design iterations, it is worthy to note that the F1 clutch and a smaller FOA clutch (2 1/8 inch) have the same highly sensitive parameters (see Appendix A.3). While the torque capacity sensitivity stays the same between different size clutches, the contact engagement speed is much more sensitive to these parameters in smaller size clutches. This leads to a much higher performance toler-

TABLE 5.4 Performance tolerances for several scenarios with the 4 inch and 2 inch FOA clutch.

Scenario	Performance Tolerance	
	Contact Engagement Speed (rpm)	Torque Capacity (in-lb)
A. μ tolerance = ± 0 , ω tolerance = ± 0		
4 inch clutch		
$\theta_{con} = 10$ deg *	± 176.1	± 52.4
$\theta_{con} = 20$ deg **	± 165.0	± 39.7
2 inch clutch		
$\theta_{con} = 3$ deg ***	± 601.8	± 6.5
B. μ tolerance = ± 0.03 , ω tolerance = ± 0		
4 inch clutch		
$\theta_{con} = 10$ deg	± 176.1	± 105.6
$\theta_{con} = 20$ deg	± 165.0	± 91.1
2 inch clutch		
$\theta_{con} = 3$ deg	± 601.8	± 7.1

* The parameter values and manufacturing & design tolerances used are found in Appendix A.1.

** The parameter values and manufacturing & design tolerances used are found in Appendix A.4.

*** The parameter values and manufacturing & design tolerances used are found in Appendix A.3.

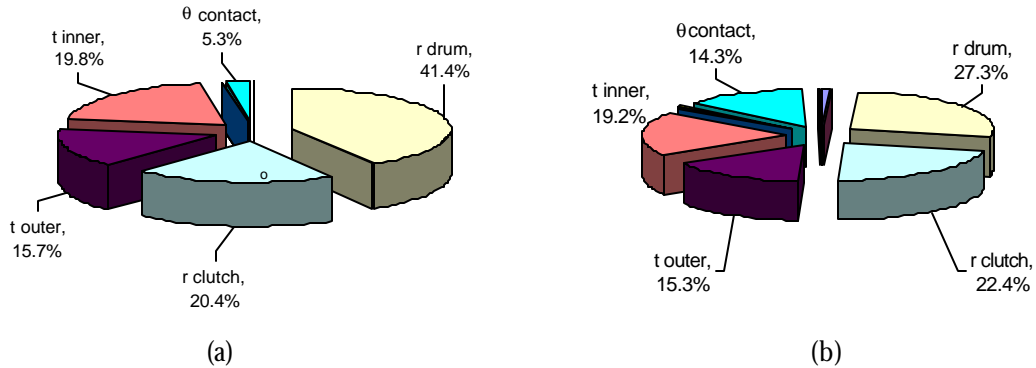


Figure 5.7 Percent contribution of design parameters to the (a) contact engagement speed and (b) torque capacity for the FOA clutch.

ance. For example the 4 inch FOA clutch may have a contact engagement speed tolerance of ± 150 rpm, whereas the 2 inch FOA clutch would have ± 600 rpm tolerance.

Once the performance tolerance is known, it is possible to determine the percent contribution that each parameter adds to the overall performance tolerance. This is done by dividing the square of each individual adjusted sensitivities by the performance tolerance.

$$\% \text{ Contribution} = \frac{\left(\frac{\partial f}{\partial x_i} \cdot \psi_i\right)^2}{\sum_i \left(\frac{\partial f}{\partial x_i} \cdot \psi_i\right)^2} \quad (5.6)$$

The percent contribution shows which parameters affect the performance tolerance and by what degree. Figure 5.7 shows the division of the performance tolerance by its design parameters.

In order to verify the accuracy of the performance tolerances found in the previous sections, Monte-Carlo simulations were used with varying manufacturing tolerances. Each Monte-Carlo simulation consisted of 30,000 trials¹. The design parameters were assigned

1. The minimum number of trials where the changes in the nominal values ceased to occur.

a 3σ tolerance based on a normally distributed manufacturing process. The percent difference between the predicted performance tolerance and that of the simulation is shown in Table 5.5¹. There is minimal difference between the predicted performance tolerance and that of a simulated manufactured batch of 30,000 clutches. This accuracy of the predicted performance tolerance allows for much simpler methods in optimizing the FOA clutch design.

5.2.4 Accuracy of Performance Tolerance Modeling

In addition to verifying the accuracy of the predicted performance tolerance, the Monte-Carlo simulation allows for the determination of the necessary manufacturing tolerance constraints. It was assumed in Table 5.1 that the necessary tolerance on the flexible segments needed to be ± 0.001 inches. This constraint may be relaxed by insuring that the given performance tolerance and failure safety factors² are within their corresponding constraints.

Table 5.6 shows the contact engagement speed and torque results for multiple Monte Carlo simulations with different assumed manufacturing processes. The table con-

TABLE 5.5 Percent difference between the estimated performance tolerance and that of the Monte-Carlo simulation.

Operation - Tolerance -	Water jet 0.020	Laser 0.005	Metal Injection 0.003	Stamping 0.002	Accurate Stamping * 0.001	Fine Blanking 0.0005
Engagement						
Estimated Std Dev	317.1	80.3	49.3	34.3	20.6	15.4
Monte-Carlo Std Dev	321.8	80.2	49.4	34.2	20.6	15.5
% Difference	1.5%	-0.1%	0.2%	-0.3%	0.0%	0.6%
Torque						
Estimated Std Dev	39.7	10.3	6.6	4.87	3.4	2.9
Monte-Carlo Std Dev	41.4	10.3	6.6	4.9	3.4	3.0
% Difference	4.1%	0.0%	0.0%	0.6%	0.0%	3.3%

* Either a stamping processes that is held in tight controls or a fine blanking process that relaxes controls.

1. Appendix A.5 contains the entire simulation data of design parameter values, manufacturing or design tolerances, and results.
2. A stress failure safety factor of 2 is set on each of the flexible segments.

tains the average, standard deviation, minimum and maximum values of contact engagement speed or torque that was found after 30,000 trials. The percent of rejects due to poor performance tolerance (under the minimum values highlighted in Table 5.6) and stress failure was found by the simulations performed for each assumed manufacturing process. Table 5.6 shows that the percent rejects due to contact engagement speed and stress failure for such processes as waterjet are unacceptable at 32.6% and 30.1% respectively. Nevertheless, a process such as stamping (0.002 inch tolerance) would be acceptable. It would also be feasible to relax the tolerance of fine-blanking to 0.002 inches, which would add the value of fewer edge adnormalities that cause early fatigue failure.

TABLE 5.6 Performance tolerance results and percent rejects for various manufacturing processes.

Operation -		Water jet	Laser	Metal Injection	Stamping	Accurate Stamping *	Fine Blanking
Tolerance -		0.020	0.005	0.003	0.002	0.001	0.0005
Contact Engagement Speed							
Average	2132.5 rpm	2144.7	2132.8	2132.8	2132.8	2132.8	2132.8
Std Dev	N/A rpm	321.8	80.2	49.4	34.2	20.6	15.5
Min	2000 rpm	960.5	1818.3	1933.8	1995.2	2049.4	2074.0
Max	N/A rpm	3536.6	2461.8	2330.2	2281.6	2222.9	2195.9
% Rejects		32.648%	4.888%	0.359%	0.005%	0.000%	0.000%
Torque Capacity							
Average	241.3 in-lb	237.2	241.2	241.3	241.4	241.4	241.4
Std Dev	N/A in-lb	41.4	10.3	6.6	4.9	3.4	3.0
Min	200 in-lb	12.3	198.5	213.4	221.5	228.9	229.8
Max	N/A in-lb	354.1	279.2	267.8	262	255.9	255.7
% Rejects		18.445%	0.003%	0.000%	0.000%	0.000%	0.000%
Minimum Safety Factors							
SF outer		1.49	2.34	2.55	2.62	2.72	2.75
% Rejects (below 2)		2.51%	0%	0%	0%	0%	0%
SF inner		1.3	2.08	2.25	2.3	2.37	2.41
% Rejects (below 2)		10.64%	0%	0%	0%	0%	0%
SF hubarm		1.37	1.86	1.95	2	2.05	2.05
% Rejects (below 2)		30.120%	0.069%	0.006%	0.000%	0.000%	0.000%

* Either a stamping processes that is held in tight controls or a fine blanking process that relaxes controls.

5.2.5 Robust Clutch Design

Because there is minimal difference between the predicted performance tolerance and that of the simulated performance tolerance (see Table 5.5), the predicted tolerance may be used to solve for a robust design. A robust design is one that meets key performance characteristics regardless of the variation in the design parameters.

In the case of the FOA clutch, it is necessary to decrease the performance tolerance, which is the square of the sum of the squares of the adjusted sensitivities (Equation (5.5)). This minimization cannot be done intuitively by examination of design parameters and corresponding sensitivities. An optimization routine was set-up that minimized both the contact engagement speed and torque capacity performance tolerance. The following constraints were set up to insure a feasible solution¹:

- Minimum and maximum bounds on design parameters
- Minimum and maximum bounds on contact engagement speed accounting for its performance tolerance
- Minimum bound on the torque capacity
- Several design space constraints
- Stress failure constraints on inner and outer beam thickness, as well as hub arm

After multiple iterations within the design space, it appears that there are various local optimums. The design parameters of the best local optimum that was found are in Table 5.7. From the various optimization iterations performed there were a few observations that came to light. First, the optimization routine increases clearance between the radius of the clutch and the inner radius of the drum. By increasing the clearance the sensitivities of r_{clutch} and r_{drum} decrease. Comparison of Table 5.3 with Table 5.8 shows this decrease. In contrast, the sensitivities of t_{outer} and t_{inner} increase, yet the net is a decrease in overall performance tolerance. As stated previously these two design parameters are

1. See Appendix A.6 for actual design parameter values and bounds.

equal to the $\delta_{clearance}$ of the clutch. While unexpected, this increase in $\delta_{clearance}$ is an added advantage because it helps to alleviate premature engagements at idle speeds.

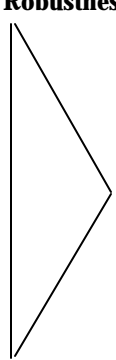
Another observation is that due to the constraints on torque capacity, safety factors, l parameters and the t parameters, no engagement speed tolerance below ± 145 rpm were seen in the design space.

In addition, once the contact engagement speed tolerance is minimized to about 150 rpm, it is still possible to increase the torque capacity dramatically. For example, by increasing or decreasing r_{hubarm} the average torque changes with no change in engagement speed (Table 5.9). While Table 5.9 shows that there is an increase in torque performance tolerance, this is offset by the large increase in average torque. The value that

TABLE 5.7 Design parameters and corresponding sensitivity values for the optimal solution in minimizing torque capacity performance tolerance.

Key Parameters	Tolerance	Starting Design	Robust Design
t_{clutch}	0.005	0.626	0.626
r_{hub}	0.003	0.75	0.734
r_{drum}	0.005	2	2.000
r_{clutch}	0.003	1.95	1.919
t_{outer}	0.003	0.07	0.063
t_{inner}	0.003	0.07	0.060
l_{outer}	0.003	0.8	1.000
l_{inner}	0.003	0.7	0.767
$w_{outer\ slot}$	0.003	0.3	0.294
$w_{inner\ slot}$	0.003	0.1	0.075
$r_{hub\ arm}$	0.005	0.95	1.200
$\theta_{contact\ (high)}$	2	10	10
$R_{outer\ round}$	0.003	0.075	0.075
$R_{inner\ round}$	0.003	0.075	0.075
μ	0	0.42	0.42
$\omega_{operational}$	0	3600	3600
$indent_{outer}$	0.003	0.05	0.050

Optimizing Design



Robustness

Performance (rpm)		(in-lb)	
Average Eng Speed	2133.5		2147.5
Contact Eng Speed Tol	± 169.2	±	147.5
Average Torque Capacity	590.4		434.1
Torque Capacity Tol	± 50.7	±	34.1

r_{hubarm} should be set at depends on the minimum amount of torque needed for the application. The torque capacity may also be increased by changing θ_{con} . Unlike r_{hubarm} , changes in θ_{con} will increase the contact engagement speed and its corresponding performance tolerance.

TABLE 5.8 Parameter sensitivity values for the FOA clutch after minimizing performance tolerances.

Variable	Value	Tol	Engagement Sensitivity	Torque Sensitivity
n segments	3	N/A	N/A	N/A
t clutch	0.626 in	N/A	N/A	N/A
r hub	0.734 in	0.003	5.75	-1.49
r drum	2.000 in	0.005	68.92	-12.36
r clutch	1.919 in	0.003	-52.93	13.78
δ clearance	0.081 in	N/A	N/A	N/A
t outer	0.063 in	0.003	75.34	-16.85
t inner	0.060 in	0.003	87.85	-19.57
l outer	1.000 in	0.003	-1.29	0.21
l inner	0.767 in	0.003	-1.97	0.36
W outer slot	0.294 in	0.003	1.28	-1.08
W inner slot	0.075 in	0.003	1.28	-0.80
r hub arm	1.200 in	N/A	N/A	N/A
θ contact (high)	10 deg	2	27.20	12.25
μ	0.42	N/A	N/A	N/A
ω operational	3600 rpm	N/A	N/A	N/A
indent outer	0.050 in	0.003	5.84	-1.33
indent inner	0.000 in	0	N/A	N/A

Mean =	2147.5	434.1
Tolerance = \pm	147.5	34.1
Std Dev = \pm	49.2	11.4

TABLE 5.9 Change in torque performance tolerance with changes in r_{hubarm} and θ_{con} .

r_{hubarm}	Torque	Tolerance	θ_{con}	Torque	Tolerance
0.85"	654.0	\pm 53.2 in-lb	10 deg	434.1	\pm 34.1 in-lb
1.2"	434.1	\pm 34.1 in-lb	20 deg	519.7	\pm 53.2 in-lb
1.7"	293.3	\pm 23.2 in-lb			

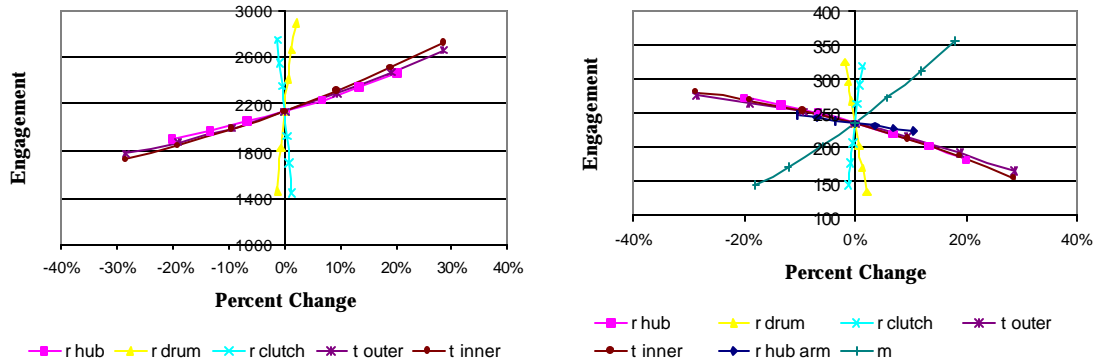


Figure 5.8 Cause-effect relationship between design parameters and engagement & torque performance.

5.2.6 Basic Parameter-Performance Relationships

In order to verify the results of the sensitivity analysis and the optimization, it is necessary to have a basic understanding of how a slight change in a design parameter value affects the engagement and torque performance of the clutch. Several visual graphs were made that show how the torque and speed vary with small percent changes in design parameter values. This process assumes that only one parameter is changed at a time. Figure 5.8 shows how the more sensitive parameters affect the torque and engagement speed. The parameters with a steeper slope are the more sensitive parameters. The visual sensitivity check confirms the numerical derivative solutions. As seen in the numerical derivatives the variables with the steepest slope or highest sensitivities are r_{clutch} , t_{inner} , t_{outer} , and r_{drum} .

The less sensitive parameters may be used to increase torque and fine tune engagement speed without adding much variance to the contact engagement speed and the torque capacity of the clutch. For example, the values of l_{outer} and l_{inner} may be increased so that t_{outer} and t_{inner} may be increased. The increase in sensitivity for the l 's is significantly less the decrease in t 's sensitivities, which results in a net decrease of overall performance tolerance. In addition, w_{outer} , w_{inner} , R_{outer} , and R_{inner} may be decreased,

which would add mass to the clutch and increase the torque capacity. R_{hubarm} may be decreased to increase the torque capacity without affecting the contact engagement speed. θ_{con} may be increased in order to increase the torque output, but this also increases the necessary angle of rotation in order to contact the drum.

In order to maximize torque capacity of a clutch, there are a few simple guidelines to follow. First, maximize the mass by decreasing r_{hub} and decreasing w_{outer} (limited by stress constraint) and w_{inner} . Secondly, minimize r_{hubarm} as much as possible. Thirdly, maximize θ_{con} , which will increase the torque by changing the mechanical advantage. Lastly, minimize $indent_{outer}$. All other parameters should be adjusted in order to achieve the targeted contact engagement speed.

5.3 Performance of Layers

The hybrid process discussed previously is a feasible process for manufacturing compliant mechanisms. This process would consist of making the FOA clutch in multiple layers and then joining the layers together. This section explores the benefits of making the clutch in multiple layers and the difference between joining those layers together or letting them float independently around the clutch's hub (see Figure 5.9). Joining of these layers may be performed in a variety of different methods by mechanical, thermal, or chemical processes. Riveting the layers together is one such method and will be referred to throughout this thesis to represent joining clutch layers.

5.3.1 Benefits of Multiple Layers

Manufacturing the compliant clutch in multiple layers allows the use of manufacturing processes such as stamping and fine-blanking. These are two standard, economical manufacturing processes that would allow for high rates of production.

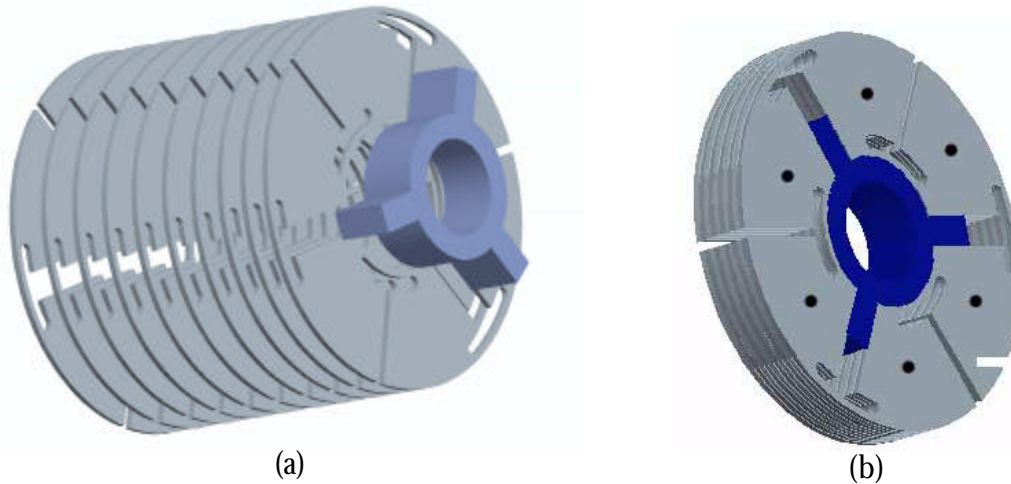


Figure 5.9 Different layered clutches: a) Free-floating and b) Riveted.

In addition, free floating layers provide the advantage of the clutch conforming to the drum profile. When the drum is fabricated, it varies in diameter. Multiple layers would insure that there were multiple points of contact with the drum.

Another advantage of multiple layers is lower clutch torque-speed variance. Each layer will have a certain variance due to the manufacturing process, yet when the sum of each layer's variance is taken it creates a lower total performance tolerance. Further evaluation will be given in the next section.

5.3.2 Monte-Carlo Simulations for Multiple Layers

Monte-Carlo simulations were performed in order to predict the behavior of a clutch made of multiple layers. Three different simulations were performed: a single layer clutch, a free-floating layered clutch, and a riveted layered clutch. Each simulation consisted of 35,000 trials. Each of the FOA clutch model's parameters has a manufacturing or design tolerance associated with it. This may be transformed into a normal standard deviation by the assumption that the tolerance is equal to three standard deviations (3σ). By using a random number generator, the parameters were randomly assigned a value within its normal distribution. After each parameter in the model is assigned a new number within its normal distribution, the contact engagement speed and torque capacity are calculated from the FOA model. This random parameter assignment, based on their toler-

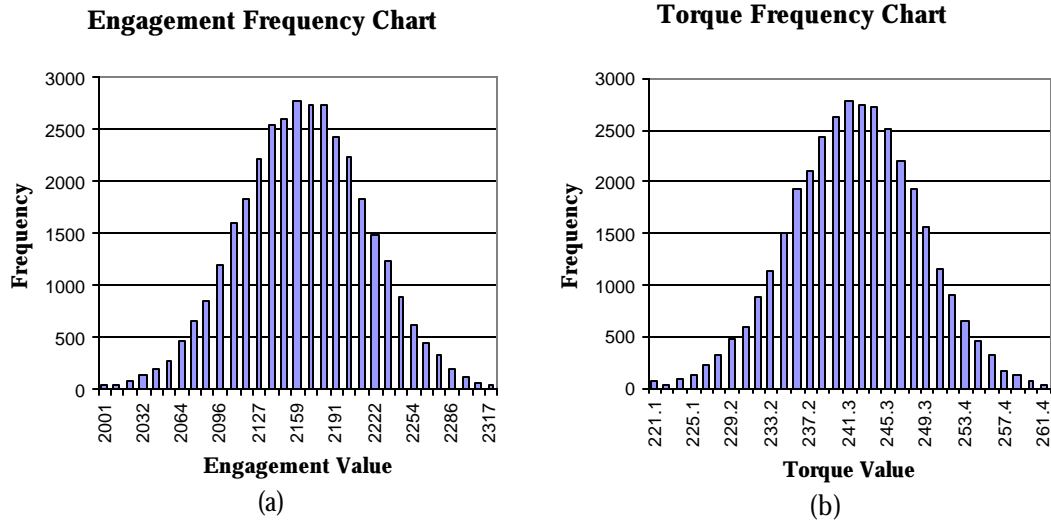


Figure 5.10 Frequency chart for the single layer clutch: (a) contact engagement speed and (b) torque capacity.

ances, provides a different performance each time it is calculated. After 35,000 trials, a mean and standard deviation is calculated for the contact engagement speed and torque capacity. In the case of the single layer clutch, the simulation is performed exactly as explained. Figure 5.10 shows a frequency chart for both contact engagement speed and torque capacity¹.

Unlike the single layer clutch, the free floating layer clutch contained 11 layers within one clutch. As the clutch is rotated, one layer engages with the drum first based on clearance, flexible segment stiffness, and mass. This layer determines the contact engagement speed, and explains why the average speed is lower than the one-piece clutch. In contrast, all layers contribute to the clutch's torque capacity. In order to create a real-life simulation it was necessary to determine whether each individual parameter changes by the layer or by the clutch. In other words does the simulation use the same r_{hubarm} value for all layers within the clutch or does it vary r_{hubarm} for each layer. Since the clutch's hub is one solid piece, r_{hubarm} varies by the clutch and not by the layer. Appendix A.8 contains data on if the parameters are associated with the clutch or with the layer.

1. Appendix A.7 contains the performance frequency for the free floating layer clutch and riveted layer clutch

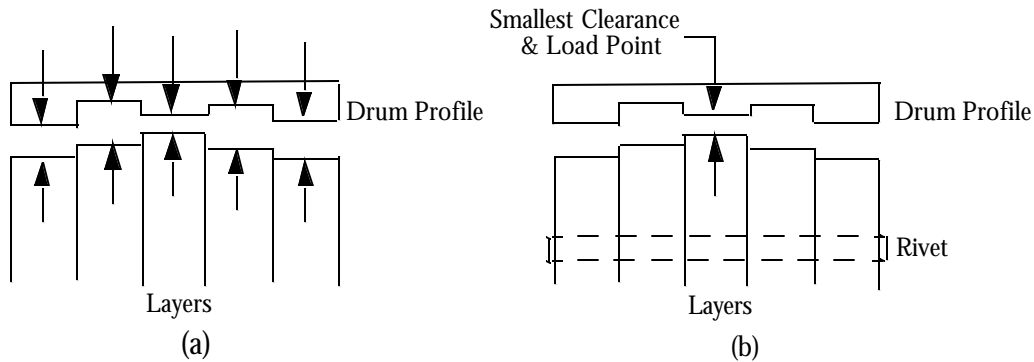


Figure 5.11 The (a) free floating layer clutch's engagement and torque are based on individual layer parameters, while the (b) riveted layer clutch's engagement and torque are based on the average parameter values for all layers and the smallest clearance.

Similar to the free floating layer clutch, the riveted layer clutch's simulation is performed in the same manner. The difference is that once the clutch is riveted together it engages and transmits the load at the layer with the smallest clearance (see Figure 5.11). The contact engagement speed and torque capacity are found by adding up the inner and outer stiffness (K 's) for each layer and then solving for t_{inner} and t_{outer} , which do not vary linearly. Total clutch mass is also added up on a layer basis. The values for r_{drum} , r_{clutch} , and $\theta_{contact}$ are set at the same values of the layer where clearance was the smallest. All other parameters have a linear relationship with engagement speed and torque, and are therefore averaged between layers.

The simulation results for the three clutch types are found in Table 5.10¹. The free floating layer clutch and riveted layer clutch were simulated twice: once with a drum that varies due to a manufacturing tolerance and once when the drum does not vary. As hypothesized, the free floating layer clutch and the riveted layer clutch tightens the performance tolerance of the FOA clutch. The contact engagement speed performance tolerance is reduced by 44%, while the torque capacity performance tolerance is reduced by 69%

1. Appendix A.8 contains the parameter mean values and assigned manufacturing or design tolerances.

when free floating layers are used. The riveted clutch is even more promising, because it reduces engagement speed and torque tolerances by 83%. This type of reduction is excellent because it insures that the compliant clutch will operate within the performance constraints (e.g. engage between 2000 and 2400 rpm) set forth by the application. In addition, the mean torque increases by 3% due to the riveted clutch's single load point. The performance tolerance reduction even permits those performance constraints to be tightened.

5.4 Summary

This chapter discussed engagement speed and torque performance sensitivity to variations in manufacturing and design tolerances. The FOA clutch parameters that affect the contact engagement speed and torque-capacity the most are the r_{clutch} , t_{inner} , t_{outer} , θ_{con} , and r_{drum} . Through other design iterations, these are the same highly sensitive parameters found in similar clutch designs (e.g. Floating 1), and in other scaled versions of the FOA clutch. While the torque capacity sensitivity stays the same between different size clutches, the contact engagement speed is much more sensitive to these parameters in smaller size clutches.

It was also determined that a robust compliant FOA clutch may be designed by minimizing the performance tolerance for both contact engagement speed and torque capacity. This performance tolerance takes into account the manufacturing and design tolerance of individual model parameters. The robust design insures that the clutch will oper-

TABLE 5.10 Torque performance tolerance for the three types of FOA layered clutches.

Layer Type	Contact Eng.		Torque (in-lb)	
	Speed (rpm)	± Tolerance		± Tolerance
One-piece clutch	2159.0	± 158.2	241.3	± 20.1
Free Floating Layers				
Drum varies	2075.8	± 89.7	241.2	± 6.2
Drum does not vary	2091.8	± 116.7	241.3	± 11.7
Riveted Layers				
Drum varies	2099.7	± 26.3	248.2	± 3.5
Drum does not vary	2125.8	± 36.3	245.6	± 4.4

ate within the prescribed application constraints. Such optimizing leads to a design with a larger clearance between clutch and drum, which helps to alleviate premature engagements at idle speeds. In addition, once the contact engagement speed tolerance is minimized, it is still possible to increase the torque capacity dramatically without affecting contact engagement speed by decreasing r_{hubarm} or increasing θ_{con} .

In addition, the analysis and modeling performed in this chapter show that using a layered clutch is feasible and beneficial. Not only was it determined that such economical manufacturing processes as stamping and fine-blanking would work ideally for the fabricating the FOA clutch in layers, but that multiple clutch layers would significantly tighten the contact engagement speed and torque performance tolerances. The contact engagement speed performance tolerance is reduced by 44%, while the torque capacity performance tolerance is reduced by 69% when free floating layers are used. The riveted clutch is even more promising, because it reduces engagement and torque tolerances by 83%.

Testing was performed in order to compare the performance of the MFOA clutch with the benchmark clutch. As discussed in Chapter 3, the main criteria for comparison are torque capacity, accuracy of engagement, and smoothness of engagement. One Comet clutch and two MFOA clutches were tested in multiple runs to collect the necessary data for comparison. In addition to the benchmark, testing performed on the 4 inch MFOA clutch helps to validate the engagement and torque models, the feasibility of using free floating layers to act as one clutch, and the feasibility of using compliant centrifugal clutches in high torque applications.

6.1 Test Setup

The test setup consisted of an engine with a large torque output (Figure 6.1). A Yamaha FJ 600 motorcycle was attached to a jack shaft in order to provide the necessary input. This engine drives the shaft (jack shaft) that is connected to the clutch's hub, which in turn drives the clutch. Upon acceleration, the clutch engages the drum and transfers torque to the output shaft. The output shaft is connected to a dynamometer, which uses a water break to load the clutch and measures the transferred torque with a torque transducer. The operator may vary the dynamometer load by turning the water break valve. There is one tachometer on the jack shaft and one on the output shaft to measure the speed.

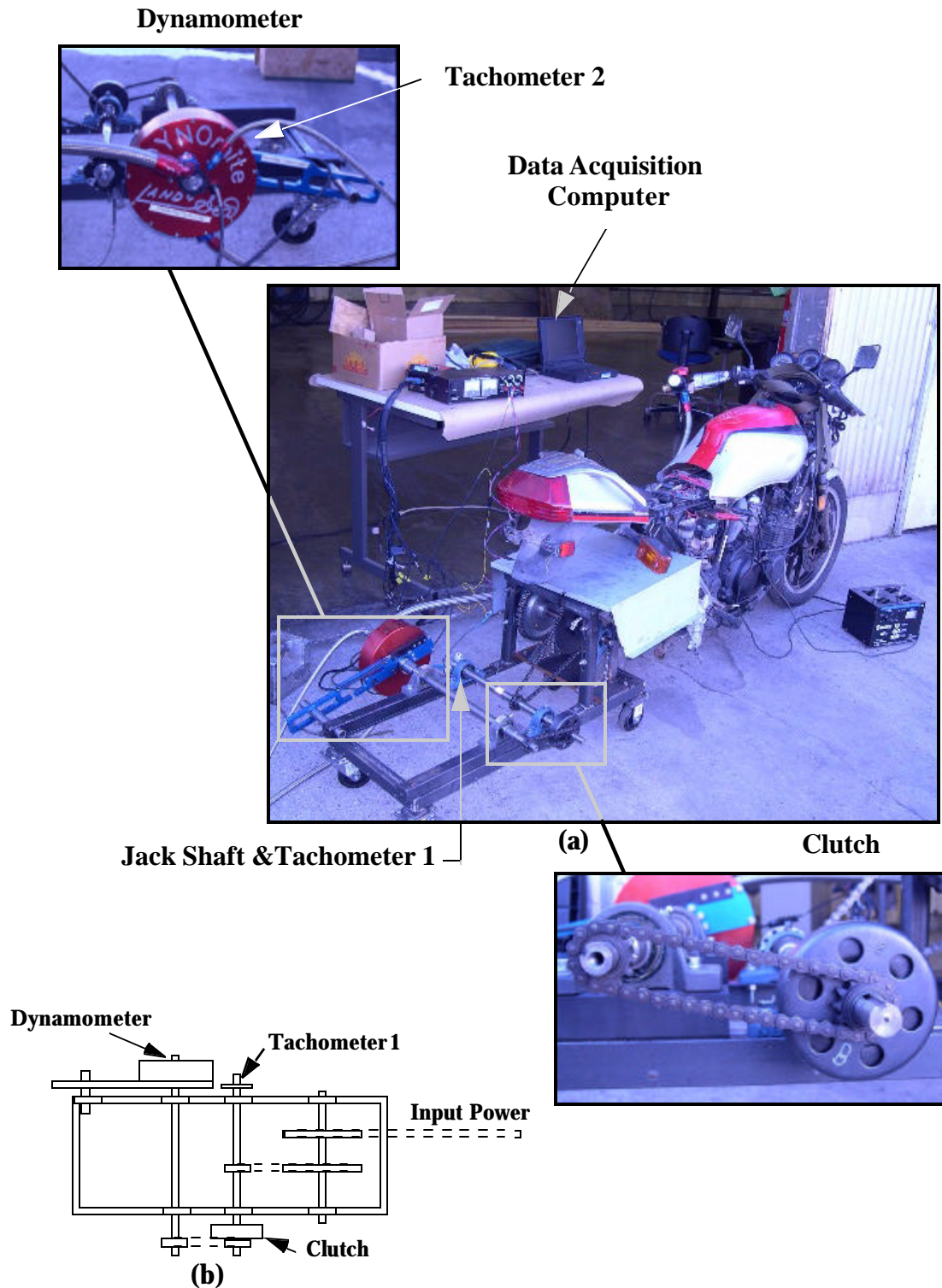


Figure 6.1 Set-up for testing the clutch's engagement accuracy and characteristics, as well as the clutch's torque capacity. (a) Actual pictures and (b) Top view schematic of testing apparatus

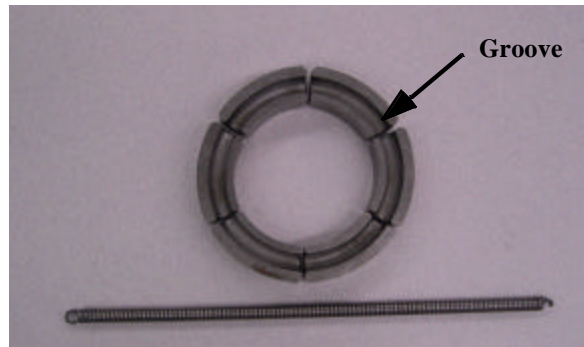


Figure 6.2 Hoffco-Comet 4 inch go-kart clutch. Consist of 6 shoes held together by a spring wrapped around the groove.

The data acquisition computer synchronizes and records the transferred torque and both speed measurements. These three real-time measurements allow torque vs. time, rpm vs. time, and torque vs. rpm graphs to be used for analysis and comparisons.

As discussed in Chapter 3, there were two types of tests performed in order to obtain the necessary evaluation data. The first test was the *RPM Contact Test Procedure*. The objective of this test was to judge the accuracy and smoothness of contact. The second test was the *Torque Test Procedure*, which applied an increasing load to the output shaft in order to determine maximum torque capacity.

6.2 Benchmarking (Hoffco-Comet) Testing

The first clutch tested was the Hoffco-Comet 4 inch go-kart clutch. This clutch consisted of 6 metal shoes held in a circle by a pre-loaded linear spring. The shoes are then rotated by the hub. As the speed increases, the weight of the shoes overcome the restitution force of the spring and move radially outward, thereby engaging with the drum and transmitting torque.

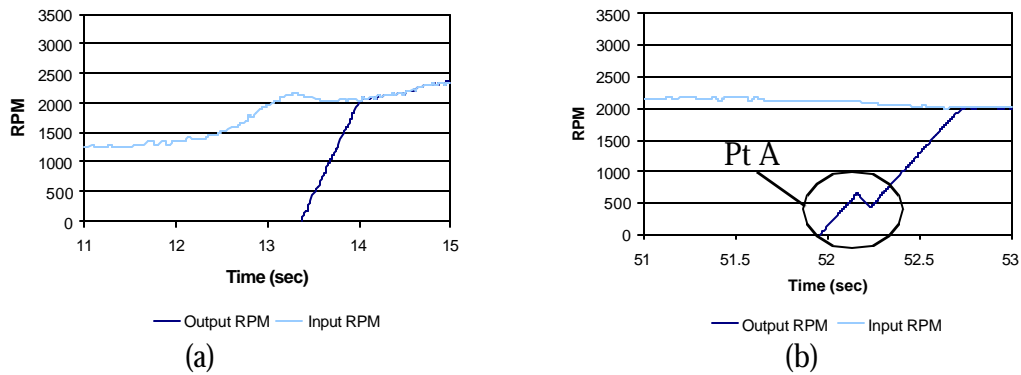


Figure 6.3 Contact engagement speed (2055 rpm) and smoothness of engagement for the Comet 4 inch go-kart clutch: (a) smooth engagement and (b) mild rough engagement.

6.2.1 Contact Engagement Speed (Comet)

The Comet clutch performed very well in reliable contact engagement speed. Multiple *RPM Contact Tests* were conducted. Figure 6.3 shows the smoothness of engagement. Figure 6.3 (a) shows the initial contact speed as 2055 rpm. Other tests ranged from 1966 to 2165 rpm¹. This engagement speed almost fits the benchmark’s performance criteria of engaging between 2000 and 2400 rpm for typical go-karts.

The smoothness of the engagement may also be seen from Figure 6.3. There are two characteristics that show how the clutch engages. First, the sharp peaks and valleys present on the output shaft’s rpm line as it increases in speed to match the input shaft’s rpm (see Pt A in Figure 6.3 (b)) signify a sudden increase and then slippage of the clutch. The roughness of such an engagement is mild and is not felt by the operator. The second characteristic is when the output shaft’s rpm line meets the input shaft rpm line. This is the point where the clutch ceases to slip on the drum. In some cases, there is a distinct saw tooth pattern between the two rpm lines. The Comet clutch exhibited none of this characteristic, but it will be seen in the FOA clutch with short hub arms in the next section.

1. See Appendix B.2.1 for complete Comet clutch contact engagement graphs for multiple tests.

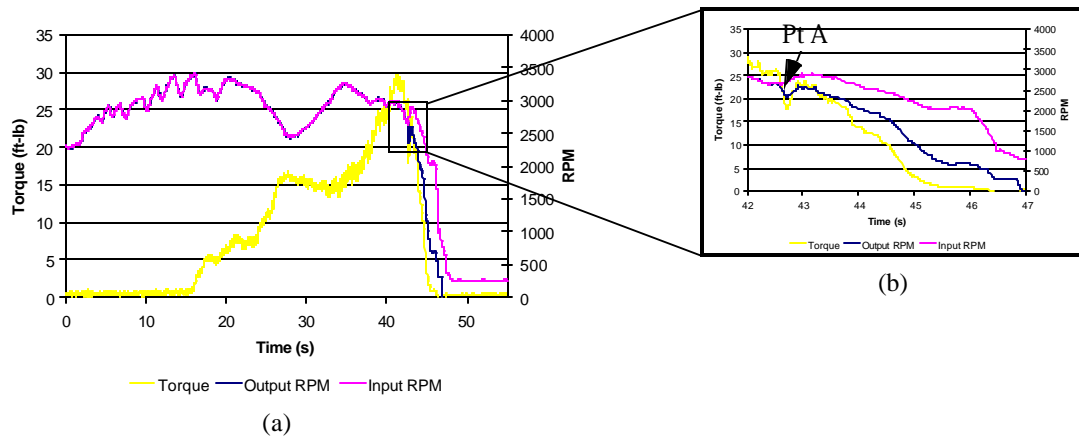


Figure 6.4 Maximum torque capacity of Comet clutch. Max torque capacity occurs when the clutch slips on the hub (Pt A).

6.2.2 Torque Capacity (Comet)

The specifications of the Comet clutch stated that the clutch transmitted 40 ft-lb @ 3600 rpm with static friction, and 20 ft-lb @ 3600 with dynamic friction (slipping). The torque capacity testing was to verify those specifications and then make a comparison to the FOA clutch. The torque value at which the Comet clutch slipped between the hub and the drum is seen in Figure 6.4¹. The slip points occur when the clutch slips because too high of a load is applied, and it is essentially a single point on the clutch torque capacity curve. By recording enough torque slip points over a wide range of speed, it is possible to graph the clutch torque curve. Due to the constraints of the test engine, it was infeasible to get the necessary torques at higher rpm values. Table 6.1 contains the multiple slip points measured between 2400 and 2800 rpm, along with the predicted torque values when the coefficient of friction is assumed to be 0.42. Figure 6.5 shows both sets of data points plotted. The Comet clutch model predicts that the torque will be 58 ft-lb at 3600 rpm, which is about 50% above the clutch's specifications. Further discussion of this superb performance will be discussed later in the chapter.

1. See Appendix B.2.3 for all Comet clutch torque capacity test data.

TABLE 6.1 (a) Torque slippage points where clutch slips and (b) torque values that are under torque curve.

Torque Slippage Points		
RPM	Torque (ft-lb)	Predicted* Torque (ft-lb)
2474	14.4	18.1
2494	18.7	18.7
2563	21.3	20.9
2660	26.1	24.0
2422	16.5	16.5
2779	28.3	28.0

* When $\mu = 0.42$

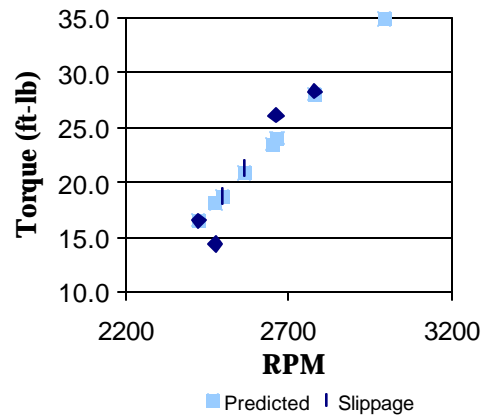


Figure 6.5 Plotted torque values where Comet clutch slipped and other torque values along with predicted values from model.

6.2.3 Observations of Benchmark Testing

Testing of Comet's 4 inch go-kart clutch showed that the clutch has a very smooth engagement. There were no sudden impact loads due to excessive aggressiveness. In addition, the clutch repeatedly engaged between 2000 and 2400 rpm.

After testing, the clutch was taken apart to see the wear on the clutch shoes, as well as on the drum. Figure 6.6 shows the minimal wear on each. The drum and shoes were evenly worn with no apparent scoring. One interesting point is that because of the Comet design of wrapping a spring around the inner part of the shoes is not symmetric, the shoes rotate slightly, which causes the shoe to only engage and wear on half of its side.

6.3 Multi-layer Floating Opposing Arm (MFOA) Testing

Two MFOA clutches were fabricated out of 0.062" spring steel (1095). These clutches each consisted of 10 layers assembled with a single piece hub in the Comet clutch drum (see Figure 6.6). A Comet clutch was retrofitted to show that a MFOA clutch would fit in the existing space, as well as to maintain consistencies in drum profiles.



Figure 6.5 The (a) shoe and (b) drum wear of the Comet clutch. Only half of the shoe engages with the drum because the spring wraps around the shoe a little off center.



Figure 6.6 MFOA clutch assembled into a Comet drum. The clutch consist of 10 layers of spring steel: each 0.062" thick.

The first MFOA clutch (vA) was designed to engage at 2155 and transmit 48 ft-lb of torque at 3600 rpm when $\mu = 0.42$. The second MFOA clutch (vB) was designed to engage at 2028 and transmit 70 ft-lb of torque at 3600 rpm when $\mu = 0.42$. In addition to these two design iterations of the MFOA clutch, two different hubs were made. The short hub arm (SHA) had a hub arm length of 0.95 inches, and the long hub arm (LHA) had a

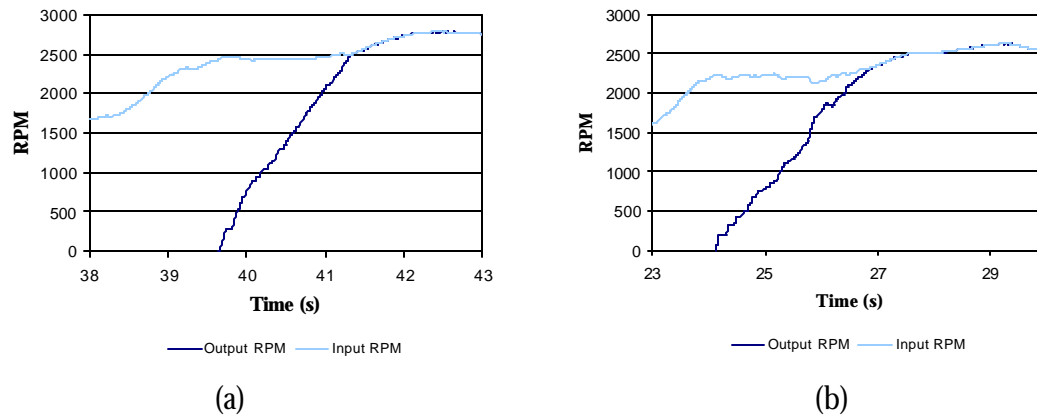


Figure 6.7 Contact engagement speed (2436 & 2224) and smooth engagement for the (a) MFOA vA LHA clutch and (b) MFOA vB LHA clutch.

length of 1.25 inches. Both of the above mentioned torque predictions are based on the short hub arm. All design parameters of these clutches are found in Appendix B.3.1.

6.3.1 Contact Engagement Speed (MFOA)

Similar to the Comet clutch, the MFOA clutch performed well with reliable contact engagement. Figure 6.7 shows two of those engagements for the MFOA vA and vB LHA. Figure 6.7 (b) shows that the initial contact speed for vB was 2224 rpm. In addition, it only varied from 2142 to 2251 rpm¹. This engagement speed fits the application criteria of engaging between 2000 and 2400 rpm for typical go-karts.

When the small hub arm is used with the MFOA clutch, the contact engagement is much rougher than for the Comet clutch (see Figure 6.8). Initial testing of the MFOA SHA clutch showed a high level of vibration when the output rpm approached the input rpm. This distinct saw tooth pattern caused the test stand apparatus to shake noticeable. The rough engagement stops when the hub is switched to the longer hub arm (LHA), which decreases the amount of transferred torque. This decrease in torque is not due to mass, but

1. See Appendix B.3 for complete MFOA contact engagement graphs for multiple tests.

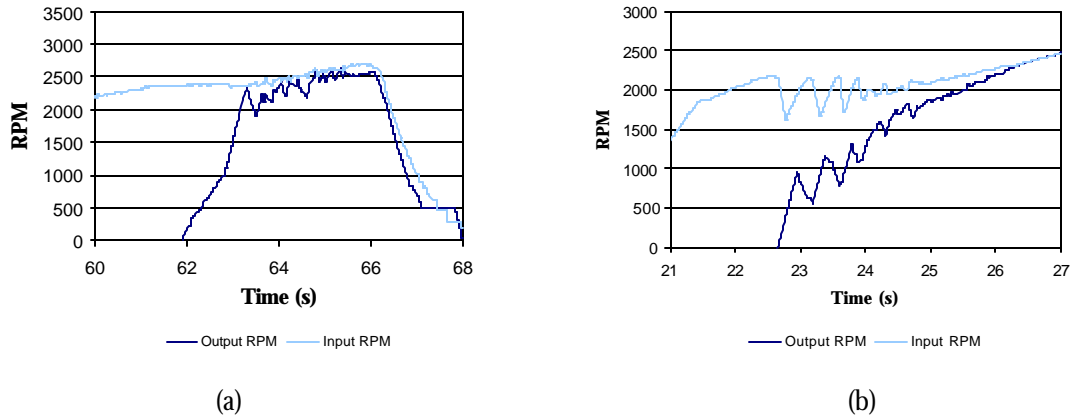


Figure 6.8 Contact engagement speed (2364 & 2102) and rough engagement for the (a) MFOA vA SHA clutch and (b) MFOA vB SHA clutch.

to the mechanical advantage and aggressiveness of the shoes. It is also possible that the high normal force on a thin walled drum excites the natural frequency of the system.

The other important result from the contact engagement experimental data is how well the FOA model predicted the engagement speed. The individual parameters for each layer in the clutch were recorded after they were made. These new values were used in the contact engagement & torque models. Table 6.2 shows that the MFOA vA clutch's predicted contact engagement speed was off by 17%, while the MFOA vB clutch predicted contact engagement speed was off by 1%. It is unknown why the MFOA vA deviated by such a significant amount, but some possible sources of error are the miscalculations of one of the following:

TABLE 6.2 MFOA's measured contact engagement speeds. In addition, the predicted and adjusted predicted values are compared to the experimental values.

Clutch	Average Measured Speed (rpm)	Range of Measured Speeds (rpm)	Predicted Speed (rpm)	Adjusted Predicted Speed (rpm)	Percent Error
MFOA vA					
Short Hub Arm	2344	2171-2517	2155	2009	-16.7%
Long Hub Arm	2379	2333-2436	2155	2009	-18.4%
MFOA vB					
Short Hub Arm	2187	2066-2262	2028	2178	-0.4%
Long Hub Arm	2206	2142-2251	2028	2178	-1.3%

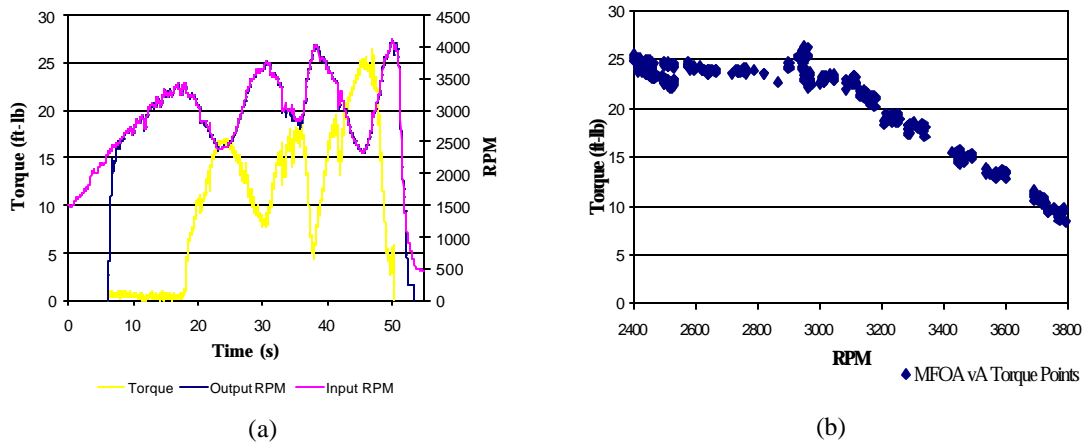


Figure 6.9 (a) Loading of the MFOA vA SHA clutch. (b) Torque points for the MFOA vA SHA clutch that are limited by the engine's output torque.

- Mass
- Center of mass
- Angle of rotation

6.3.2 Torque Capacity (MFOA)

The test setup was not able to produce enough torque to get the MFOA clutch to slip. Figure 6.9 (a) shows one of the torque loading tests. As the water brake was applied and transferred torque increased, the rpm values decreased due to the maximum engine output. Figure 6.9 (b) shows the engine's torque output limitation by the amount of torque transferred by the MFOA vA SHA¹. In other words, with the engine running at 3600 rpm the clutch is loaded with the water brake. Even with increasing the throttle to maintain constant velocity, the loading causes the engine to decelerate. This deceleration in Figure 6.9 (b) is the engine torque curve and not the clutch's torque curve. Theoretically, a centrifugal clutch's torque increases quadratically with speed. Since no slip points were achieved with this test setup and the results are limited by the engine torque curve, all of these torque points are below the clutch's torque capacity curve.

1. See Appendix B.3.6 for all MFOA torque capacity test data.

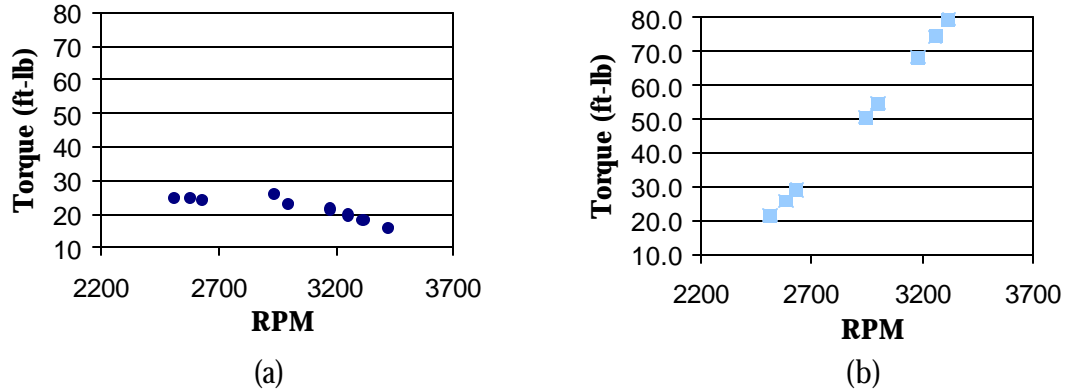


Figure 6.10 (a) Measured torque values that are below the torque curve because of the engine output limitation. No clutch slippage occurred at these points (b) FOA model's estimated torque values when the COF is 0.55

Figure 6.11(a) shows the measured torque values when no clutch slippage occurred. This means that the test data was limited by the engine output torque and not by the clutch's torque capacity. In addition, Figure 6.10(b) shows the predicted torque points when the COF is 0.55. At this large value for the COF, the MFOA model predicts that MFOA vA SHA would have a torque capacity of 104 ft-lb at 3600 rpm, which is about 44% more than the predicted Comet clutch with the same COF.

6.3.3 Observations of MFOA Testing

Testing of MFOA clutch showed that the clutch has smooth engagement and very high torque capacity. The vibrational roughness that was seen in testing the MFOA with short hub arms, was eliminated by reducing the amount of transferred torque with longer hub arms. There were no sudden impact loads do to excessive aggressiveness for the MFOA LHA clutches. In addition, the clutch repeatedly engaged between 2333 and 2436 rpm for vA and between 2142 and 2256 for vB.

After testing, the clutch was taken apart to inspect the wear on the clutch shoes, as well as the drum. Figure 6.11 shows minimal wear on each. The drum and shoes were evenly worn with only a little sign of scoring for one layer with the MFOA vA clutch. The

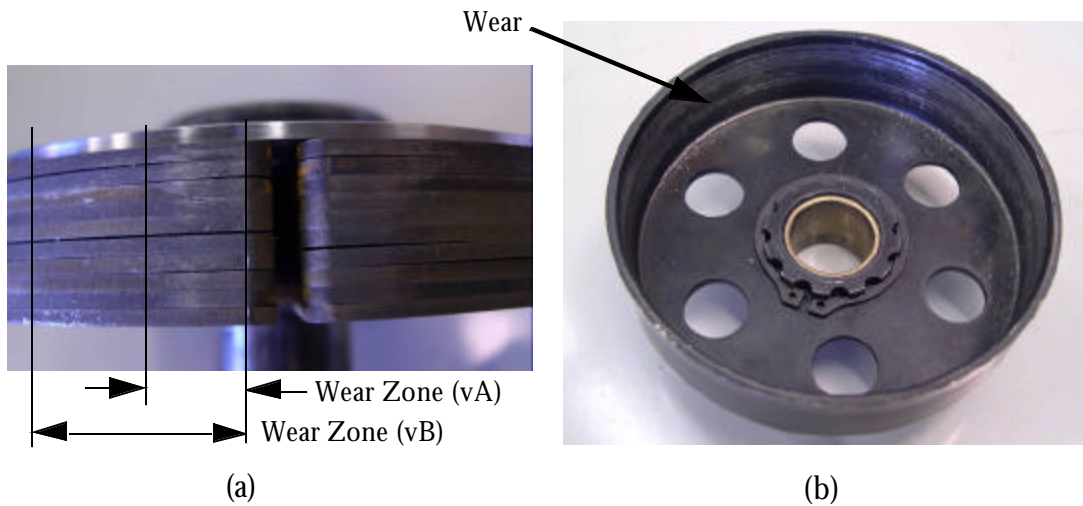


Figure 6.11 The (a) shoe and (b) drum wear of the MFOA vA clutch.

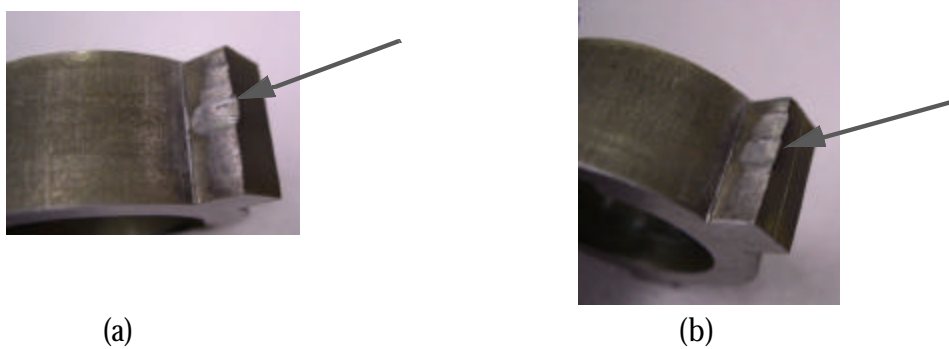


Figure 6.12 Impression marks left by the clutch on the short hub arms.

MFOA vB design increased θ_{con} from 10 to 20 degrees and the outer fillet from 0.1 to 0.2 inches. These two changes increased the contact area and alleviated all signs of drum scoring.

Another interesting observation is the deformation of the small hub arms. The hub is made out of a softer steel than the clutch layers and the hub arms partially deformed at the points of contact. Figure 6.12 shows the impression marks left by individual layers.

6.4 Comparison of Comet Clutch to the MFOA Clutch

6.4.1 Contact Engagement

Both clutches engaged the clutch at repeatable and accurate RPM values. The Comet clutch had a range of about 200 rpm over which it engaged. The MFOA likewise had a range of about 200 rpm in which the clutch consistently engaged. Table 6.3 shows the values and ranges of the Comet and MFOA clutches.

The Comet clutch had a smoother engagement than the MFOA. Initially the MFOA had vibration chatter upon contact. This rough engagement was eliminated by increasing the length of the hub arm, which also decreased the torque capacity. The reason that the Comet clutch has a smoother engagement is because the design is non-aggressive, while that of the FOA is half aggressive and half-non-aggressive. While such a dual design gives more torque than a totally non-aggressive design, it also causes or contributes to such vibrations.

6.4.2 Torque Capacity

The first torque test that yielded both Comet slip torque points and the MFOA torque points was performed at the same time and under the same conditions. Each drum

TABLE 6.3 Comet and MFOA clutch's measured contact engagement speeds.

Clutch	Average Measured Engagement (rpm)	Range of Measured Engagement (rpm)
Comet 4 inch	2076	1966-2165
MFOA vA		
Short Hub Arm	2344	2171-2517
Long Hub Arm	2379	2333-2436
MFOA vB		
Short Hub Arm	2187	2066-2262
Long Hub Arm	2206	2142-2251

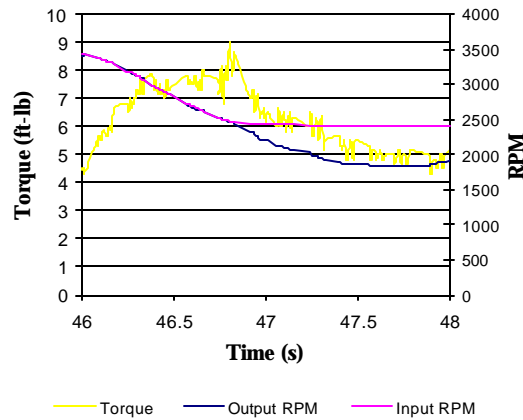


Figure 6.13 The MFOA vB LHA slipping at 2500 rpm and 8 ft-lbs

and clutch had no wear or burnished points. The Comet clutch exceeded the manufacturer's specification, while the MFOA was 44% more than the Comet clutch.

In order to match the two clutch models with the experimental data, it was necessary to use high coefficients of friction (0.42 and 0.55). While these COF are not infeasible, they are rather high for the given material and in comparison to preliminary testing. After analyzing the experimental data, it is believed that the first torque test had high coefficients of friction because the clutches and drums were not worn. It also may have been that the MFOA's friction was extremely high at 0.55 in comparison to the Comet's friction at 0.42. After initial wear, these coefficients of friction decreased and therefore the torque capacities also decreased. It was seen in later tests that the clutch would slip around 2500 rpm when transferring only 7-10 ft-lbs. Figure 6.13 shows the MFOA vB LHA slipping at 8 ft-lbs. This low torque transfer would represent a COF of 0.32.

Figure 6.14 shows the experimental data in relation to the model data for all three different designs (Comet, MFOA vA, & MFOA vB) with various coefficients of friction. The upper line shows the FOA vA SHA model with a COF of 0.55, which would give 104 ft-lbs at 3600 rpm. The Comet (COF=0.42) lines gives 59 ft-lbs at 3600 rpm. The MFOA vB LHA (COF=0.32) line is also shown matching well with the recorded data.

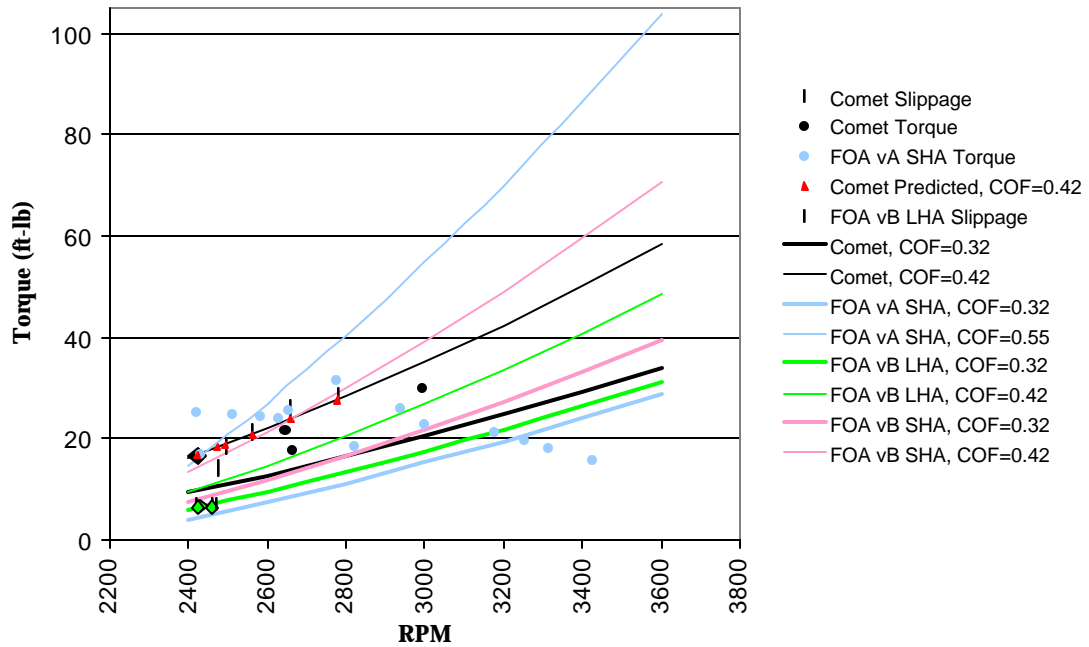


Figure 6.14 Experimental data in relation to the model data for all three different designs (Comet, MFOA vA, & MFOA vB) with various coefficients of friction

It is believed that both the Comet and the MFOA clutch's torque capacities are closer to those torque lines where the COF is 0.32. This would give the Comet clutch 34 ft-lbs at 3600 rpm, which is much closer to the manufacturer's specifications. In addition, it would match the MFOA clutch up well with the cluster of slip points around 8 ft-lbs and 2500 rpm. These lower torque curves would also match the general observations of the clutches' performance in the first test in comparison to later test. Re-testing of the Comet clutch never showed slip points, but the maximum torque seen was around 10 ft-lbs at 2500 rpm. Table 6.4 shows the comparison of the five clutch's with the torque capacity at 2400 and 3600 rpm when the COF is 0.32 and 0.42.

6.5 Results of Layered Approach

In order to benefit from the advantages of the hybrid process and also alleviate the problems associated with it, layered clutches were prototyped out of 0.062" thick spring steel (11 layers) and then combined together into one unit. The layers of both MFOA clutches free floated around the hub, or in other words they were not joined together by fasteners. In addition, the outer profile of the clutches were cut in such a manner as to increase the surface area contact of the clutch, thereby decreasing the pressure points and scoring.

These layers appeared to operate in the same manner as a single clutch. There was no scoring of the drum as seen in preliminary test. The layer thickness was sufficiently thick at 0.062 inches to stop the layers from bending out of plane. In addition, the wear of the clutch and the drum was very similar to that of the Comet clutch.

6.6 Summary

The MFOA clutch compares very well to the benchmark Comet clutch. The MFOA repeatedly engages in the same rpm range span as the Comet clutch. In addition, the MFOA is comparable to the Comet clutch in smoothness of engagement. Testing showed that the MFOA clutch transfers similar torque loads ($\pm 10\%$). The Comet clutch would transfer 34 ft lbs at 3600 rpm and with a COF of 0.32, while the FOA vB LHA would transfer 31 ft-lbs.

TABLE 6.4 Torque capacity of the five clutches at 2400 and 3600 rpm.

Clutch	Torque @ 2400 rpm		Clutch	Torque @ 3600 rpm	
	m=0.32	m=0.42		m=0.32	m=0.42
Comet	9.3	16.2	Comet	34.1	58.3
MFOA vA SHA	4.1	6.9	MFOA vA SHA	28.9	48.7
MFOA vA LHA	3.4	5.1	MFOA vA LHA	23.9	36.1
MFOA vB SHA	7.6	13.6	MFOA vB SHA	39.4	70.6
MFOA vB LHA	6.0	9.3	MFOA vB LHA	31.4	48.4

In addition, the FOA model predicted the contact engagement speed for version B to within 1%, while it predicted version A to within 17%. The discrepancy may have been model based, or it may have been some irregularity of the layers (e.g. l was not the value stated in the design) in comparison to the base design. The torque model accuracy was not validated experimentally, because torque heavily depends on the coefficient of friction, and this value varies significantly in the given application.

CONCLUSIONS AND RECOMMENDATIONS

The objective of this thesis was to develop high-torque-capacity floating opposing arm clutches that are manufacturable by using standard economical manufacturing, while maintaining critical performance characteristics. It was believed that by manufacturing the compliant clutch in multiple layers, not only was it feasible to produce these clutches in high volumes, but the engagement and torque performance variations are tightened, therefore allowing the clutch to perform more consistently. In addition, the high-torque FOA design accounted for performance sensitivity to variations in both design parameters and manufacturing processes and minimizes such variations.

7.1 Contributions

7.1.1 Modeling of Comet, FOA, and F1 Clutches

Contact engagement speed and torque capacity models were created that allowed the prediction of torque-speed relationships. The models also allowed the determination of the most sensitive design variables, the minimization of performance tolerances, and the predictive behavior of stacked layers.

The FOA model predicted the contact engagement speed for version B to within 1%, while it predicted version A to within 17%. The discrepancy between these two is unknown. It may have been model based, or it may have been some irregularity of the lay-

ers (e.g. l was not the value stated in the design) in comparison to the base design. The torque model accuracy is unknown because torque heavily depends on the coefficient of friction, and this value varies significantly in the given application.

7.1.2 Parameter Sensitivity Analysis

The most sensitive design parameters were identified and coupled with their associated manufacturing processes. This allows the designer to minimize torque-speed performance variation and insure that those manufacturing tolerances are upheld.

The FOA clutch parameters that affect the contact engagement speed and torque-capacity the most are the r_{clutch} , t_{inner} , t_{outer} , θ_{con} , and r_{drum} . Through other design iterations, these are the same highly sensitive parameters found in similar clutch designs (e.g. Floating 1), and in other scaled versions of the FOA clutch. While the torque capacity sensitivity stays the same between different size clutches, the contact engagement speed is much more sensitive to these parameters in smaller size clutches.

7.1.3 Minimizing Engagement & Torque Performance Tolerances

A robust design was created that minimizes the total torque-speed performance tolerances. It was also determined that a robust compliant FOA clutch may be designed by minimizing the performance tolerance for both contact engagement speed and torque capacity. This performance tolerance takes into account the manufacturing and design tolerance of individual model parameters. The robust design insures that the clutch will operate within the prescribed application constraints. Such optimizing leads to a design with a larger clearance between clutch and drum, which helps to alleviate premature engagements at idle speeds. In addition, once the contact engagement speed tolerance is minimized, it is still possible to increase the torque capacity dramatically without affecting contact engagement speed by decreasing r_{hubarm} or increasing θ_{con} .

7.1.4 Simulation of Free Floating and Riveted Layer Clutches

Models were used to simulate the production of clutches with multiple layers around a single hub. One simulation allowed the layers to float independently and the other riveted all layers together.

The analysis and modeling performed showed that using a layered clutch is feasible and beneficial. Not only was it determined that such economical manufacturing processes as stamping and fine-blanking would work ideally for fabricating the FOA clutch in layers, but that multiple clutch layers would significantly tighten the contact engagement speed and torque performance tolerances. The contact engagement speed performance tolerance is reduced by 44%, while the torque capacity performance tolerance is reduced by 69% when free floating layers are used. The riveted clutch is even more promising, because it reduces engagement and torque tolerances by 86%.

7.1.5 Testing of two Multi-layer Floating Opposing Arm Clutches

Two MFOA clutches were fabricated and tested for torque-speed characteristics. Each clutch consisted of 10 layers and assembled into the drum of the benchmark clutch. Testing was performed to compare performance between benchmark and FOA clutches, to validate the torque-speed models, and to assess the feasibility of using layers.

The MFOA clutch compares well to the benchmark Comet clutch. The MFOA repeatedly engages in the same rpm range as the Comet clutch. In addition, the MFOA is comparable to the Comet clutch in smoothness of engagement. Testing showed that the MFOA clutch transfers similar torque loads ($\pm 10\%$). The Comet clutch would transfer 34 ft-lbs at 3600 rpm and with a COF of 0.32, while the FOA vB LHA would transfer 31 ft-lbs.

In addition, the testing showed that it is feasible to use layered compliant centrifugal clutches. These layers did not excessively wear the drum. No drum scoring was prevalent, nor was there out of plane movement. The torque-speed characteristics performed comparable to that of a single piece clutch.

7.2 Summary of Keys to Future FOA Clutches Design

As a result of this thesis, there are a few keys to consider in the future designing and testing of FOA clutches. Below is a summation of those keys:

- Use layers when manufacturing the clutch in mass quantities. Modeling showed that both the free-floating and riveted layers have a much smaller torque-speed performance variation, than that of a single-piece clutch.
- Take into account performance tolerances when setting the contact engagement speed and the torque capacity. This helps to ensure that the worst and best cases are within the application constraints.
- Ensure that there is sufficient contact surface with the drum to achieve a more reliable coefficient of friction and to stop burnishing and scoring. To increase the contact surface, increase θ_{con} and contour the shoe to match the drum upon clutch rotation.
- Use thick layers to alleviate scoring and out of plane movement. The thicker the layers are the better. This is dependent on manufacturing process capabilities, but it is recommended to maximize the thickness for the process used.
- Create a recess between the outer flexible segment and the clutch outer diameter. This alleviates wear on the flexible segment, which is a very sensitive parameter. This is done by increasing $indent_{outer}$.
- Optimize the FOA design by minimizing the contact engagement and torque performance tolerances. This will increase the clearance between the clutch and drum and allow the clutch to operate much more robustly.
- Alleviate self-tightening of the clutch. This happens in some applications when the clutch's hub screws onto a shaft. If the clutch can not

float freely, then the friction forces between layers is too great for the clutch to disengage.

- Maximize torque by minimizing the hub arm and maximizing θ_{con} .
- Set contact engagement speed at an earlier part of application specifications because loaded engagement happens 150 to 250 rpm later.
- The length of the hub arms may be varied to fine tune the clutch's torque capacity. In the 4 inch clutch case, a difference of 200% may be seen between a very short hub arm and that of a very long hub arm.

7.3 Recommendations

7.3.1 Fatigue Testing

While some fatigue testing has been performed in preliminary testing, there has been no extensive research in this area. Fatigue testing is a critical part of the design process, and it would ensure that the FOA clutch would have a long enough life cycle to be produced in mass quantities. The models show that all flexible segments had a safety factor of at least 2 for yielding.

7.3.2 Accurately Determine the Coefficient of Friction

As discussed in Chapter 6, the torque model is hard to verify because of the coefficient of friction is unknown and hard to accurately determine due to the system dynamics. Some method should be devised in order to predict the COF with better accuracy. This would allow for the correct determination of the accuracy of the torque capacity model.

7.3.3 Benchmark Costs of Manufacturing

This thesis made the assumption that producing the FOA clutch with standard economical manufacturing processes would save cost in comparison to benchmark clutches. No data was gathered on actual manufacturing cost of the benchmark clutches, nor cost

quotes for the production ramp up of the FOA clutch (both fixed and variable). It's recommended that this data be gathered in order to show whether or not the production of compliant centrifugal clutches will be less expensive than that of the benchmark clutch.

7.3.4 Dynamics of the Clutch System

Testing revealed vibration at engagement when the short hub arm was used. More research should be done on the clutch system to determine the correlation between drum geometry, shoe aggressiveness, and torque output.

7.3.5 Create a Multi-Engagement Speed Clutch

By the use of layers within the clutch, it would be possible to have each layer engage at different speeds. This multi-step engagement would allow the clutch to engage smoother, or with no sudden impact loading. It's recommended that such a clutch be prototyped and tested.

7.4 Conclusions

Clutch modeling showed the most sensitive parameters, while taking into account manufacturing tolerances. Knowing the sensitivities allowed a robust clutch to be designed that minimized the torque-speed performance tolerances. The modeling also showed the relationship between different parameters and how to change torque or contact engagement speed without increasing performance tolerances. In addition, modeling showed that free floating and riveted layers tighten the performance tolerance of the FOA clutch, while testing showed that layers are feasible.

Clutch testing showed that the MFOA clutch is comparable to the benchmark Comet clutch. The MFOA engages smoothly and repeatedly at set speeds. While there are discrepancies between actual and predicted engagement speeds, both the contact engagement speed and torque capacity models are adequate for the design of such clutches.

REFERENCES

- [1] Howell, Larry L., 2001. *Compliant Mechanisms*, John Wiley & Sons, Inc., New York.
- [2] Crane, Nathan B., 1999, "Compliant Centrifugal Clutches: Design, Analysis, and Testing," M.S. Thesis, Brigham Young University, Provo, Utah.
- [3] Roach, G.M. and Howell, L.L., 1999, "Evaluation and Comparison of Alternative Compliant Over-running Clutch Designs," *1999 ASME Design Engineering Technical Conferences*, DETC99/DAC-8619.
- [4] Berglund, M. D., 1998, "A Methodology for the Evaluation and Seletion of Acceptable Design Concept Alternatives for Compliant Mechanisms," M.S. Thesis, Brigham Young University, Provo, Utah.
- [5] Crane, Nathan B., Howell, Larry L., and Weight, Brent L., 2000, "Design and Testing of a Compliant Floating-Opposing-Arm (FOA) Centrifugal Clutch," *Proceedings of the 2000 ASME Design Engineering Technical Conferences*, DETC2000/PTG-14451.
- [6] Crane, Nathan B., Weight, Brent L. and Howell, Larry L., 2001, "Investigation of Compliant Centrifugal Clutch Designs," *Proceedings from the 2001 ASME Design Engineering Technical Conferences*, DETC2001/DAC-21071.
- [7] Goodling, E. C., 1974, "Fighting High Energy Costs with Centrifugal Clutches," *Machine Design*, Vol. 46 No. 23, pp. 119-124.
- [8] St. John, R. C., 1979 "Centrifugal Clutch Basics," *Power Transmission Design*, Vol. 21, No. 3, pp.52-55.

- [9] St. John, R. C., 1975 "Centrifugal Clutch Has Gentle Touch," *Power Transmission Design*, Vol. 17, No. 3, pp.40-42.
- [10] St. John, Richard C., 1980, "Centrifugal Clutch Construction," United States Patent No. 4226320.
- [11] Nagashima et al., 1988, "Centrifugal Clutch," United States Patent No. 4756396.
- [12] Luerken, Adolf, 1981, "Automatic two-way centrifugal clutch for motor driven apparatus," United States Patent No. 4296852.
- [13] Weiss, H., 1984, "Centrifugal Clutch for Power Saws," United States Patent No. 4446954.
- [14] Shimizu, Y. and Ogura, M., 1987, "Centrifugal Clutch Instantly Engageable and Disengageable" United States Patent No. 4687085.
- [15] Shultz, W.L., 1996, "Bi-directional centrifugal clutch," United States Patent NO. 5503261.
- [16] Kellerman, R. and Fischer, J.L., 1976, "Centrifugal Clutch with One Piece Rotor," United States Patent No. 3945478.
- [17] Roddy, Joseph T. and Page, Wayne L., 1973, "Centrifugal Friction Clutch," United States Patent No. 3712438.
- [18] Sageshima et al., 1990, "Centrifugal clutch," United States Patent No. 4960194.
- [19] Suchdev, L. S., and Campbell, J. E., 1989, "Self Adjusting Rotor for Centrifugal Clutch," United States Patent No. 4821859
- [20] Dietzsh, G., Frers, G., Henning, K., and Lux, H., 1977, "Rotor for Centrifugal Clutch," United States Patent No. 4016964.
- [21] Norton, Robert L., 2000, *Machine Design*, Second Edition, Prentice-Hall Inc., Upper Saddle River, New Jersey.
- [22] Orthwein, W.C., 1986, *Clutches and Brakes Design and Selection*, Marcel Dekker, Inc., New York, New York.
- [23] Shigley, J.R. and Mischke, C.R., 2001, *Mechanical Engineering Design*, Sixth Edition, McGraw-Hill, New York, New York.
- [24] South, D.W. and Mancuso, J.R., 1994, *Mechanical Power Transmission Components*, Marcel Dekker, Inc., New York, New York.

- [25] Goodling, E. C., 1977, "Trailing Shoe Type Centrifugal Clutch-Design Principles and Characteristics," *ASME Papers*, DET-126.
- [26] Dekhanov, V.I. and Makhtinger, V.L., 1987, "Variable Drive of Centrifugal Separator," *Chemical and Petroleum Engineering*, Vol. 23, No. 1-2, pp. 3-5.
- [27] Scott, Thomas E., 2000, *Power Transmission*, Prentice Hall, Upper Saddle River, New Jersey.
- [28] Herring, Aaron L., 2001, "High Production Manufacturing Considerations for Metallic Compliant Mechanisms with Long Thin Beams," M.S. Thesis, Brigham Young University, Provo, Utah.
- [29] Todd, Robert H. and et. al., 1994. *Manufacturing Process Reference Guide*, Industrial Press Inc., New York.
- [30] Achi, P.B.U., 1986, "Design and Testing of an Automatic Clutch," *Sadhana*, Vol. 9, No. 3, pp. 23-238.
- [31] Mamiti, G. I., 1994, "Friction Clutches Designed for Slipping," *Journal of Friction and Wear*, Vol. 150, No. 2, pp. 109.

SENSITIVITY OF KEY DESIGN PARAMETERS

A.1 Design Parameters for 4 inch FOA Clutch

This chart contains the baseline FOA clutch's parameter values used in many of the analyses and simulations.

INPUTS			OUTPUTS		
Parameter	Value	Units	Value	Units	
n_{segments}	3	segs	$\omega_{\text{contact eng}}$	2139.3	rpm
t_{clutch}	0.626	in	$T_{\text{operating}}$	584.6	in-lb
r_{hub}	0.750	in	$\Delta\theta$	0.033	rad
r_{drum}	2.000	in	σ_{outer}	41372	psi
r_{clutch}	1.950	in	σ_{inner}	47078	psi
$\delta_{\text{clearance}}$	0.050	in	$\sigma_{\text{hub arm}}$	62261	psi
t_{outer}	0.070	in			
t_{inner}	0.070	in			
l_{outer}	0.800	in			
l_{inner}	0.700	in			
$W_{\text{outer slot}}$	0.300	in			
$W_{\text{inner slot}}$	0.100	in			
$r_{\text{hub arm}}$	0.950	in			
$\theta_{\text{contact (high)}}$	10.0	deg			
$R_{\text{outer round}}$	0.075	in			
$R_{\text{inner round}}$	0.075	in			
μ	0.420	unitless			
$\omega_{\text{operational}}$	3600	rpm			
$\text{indent}_{\text{outer}}$	0.050	in			
$\text{indent}_{\text{inner}}$	0.000	in			
S_y	120000	psi			
E	3.0E+07	lb/in ²			
Density	0.283	lb/in ³			
S_y_{hub}	55000	psi			

A.2 Floating 1 (F1) Clutch's Sensitivity

The following table contains the parameter sensitivity values for the F1 clutch. The same parameters, r_{clutch} , t_{inner} , t_{outer} , and r_{drum} , are the most sensitive.

INPUTS	Original	Tol
	t clutch	0.636
r hub	0.750	0.003
r drum	2.000	0.005
r clutch	1.950	0.003
t outer	0.080	0.003
t inner	0.080	0.003
l outer	0.800	0.003
l inner	0.700	0.003
W outer slot	0.300	0.003
W inner slot	0.100	0.003
W c1	0.150	0.000
r hub arm	0.950	0.005
θ contact (low)	3.000	0.000
θ contact (high)	20.000	0.000
R outer round	0.150	0.003
R inner round	0.100	0.003
μ	0.25	0.000
ω operational	3600	0.000
indent outer	0.050	0.003
indent inner	0.000	0.000
ω contact eng	2207.6	
T operating	220.6	

Contact Engagement						
Step	Sensitivity	Rk	Adjusted by Tol	NRk	% Cont	
0.0001	-2.3E-09	16	0.0	13	0.0%	
0.0001	1304	6	3.9	6	0.1%	
0.0001	21032	3	105.2	1	44.5%	
0.0001	-24739	1	-74.2	2	22.2%	
0.0001	19871	4	59.6	4	14.3%	
0.0001	22701	2	68.1	3	18.7%	
0.0001	-511	14	-1.5	12	0.0%	
0.0001	-928	9	-2.8	8	0.0%	
0.0001	601	13	1.8	11	0.0%	
0.0001	684	11	2.1	10	0.0%	
0.0001	626	12	0.0	14	0.0%	
0.0001	0E+00	17	0.0	14	0.0%	
0.0001	0E+00	17	0.0	14	0.0%	
3	7E+00	15	0.0	14	0.0%	
0.0001	721	10	2.2	9	0.0%	
0.0001	1124	7	3.4	7	0.0%	
0.0001	0E+00	17	0.0	14	0.0%	
100	0E+00	17	0.0	14	0.0%	
0.0001	1632	5	4.9	5	0.1%	
0.0001	1024	8	0.0	14	0.0%	

Tolerance (Eng) = ± 157.6 rpm
Std Dev (Eng) = ± 52.5

Torque						
Step	Sensitivity	Rk	Adjusted by Tol	NRk	% Cont	
0.00001	346.8	11	1.7	5	0.3%	
0.00001	-366.1	7	-1.1	8	0.1%	
0.00001	-3852.7	4	-19.3	1	38.4%	
0.00001	5362.8	1	16.1	2	26.8%	
0.00001	-3965.6	3	-11.9	4	14.7%	
0.00001	-4499.2	2	-13.5	3	18.9%	
0.00001	108.6	16	0.3	13	0.0%	
0.00001	-28.4	17	-0.1	14	0.0%	
0.00001	-332.5	12	-1.0	11	0.1%	
0.00001	-354.9	9	-1.1	10	0.1%	
0.00001	-347.3	10	0.0	15	0.0%	
0.00001	-271.1	14	-1.4	6	0.2%	
0.00001	0.0	20	0.0	15	0.0%	
3	-3.5	18	0.0	15	0.0%	
0.00001	-306.4	13	-0.9	12	0.1%	
0.00001	-357.7	8	-1.1	9	0.1%	
0.00001	1834.9	5	0.0	15	0.0%	
100	0.2	19	0.0	15	0.0%	
0.00001	-441.4	6	-1.3	7	0.2%	
0.00001	-259.7	15	0.0	15	0.0%	

Tolerance (T) = ± 31.1 rpm
Std Dev (T) = ± 10.4 rpm

A.3 Sensitivity of the 2 1/8 inch FOA Clutch

This table contains the FOA clutch's parameter sensitivity values for the 2 1/8 inch clutch. It shows that the same parameters are the most sensitive, and that the engagement speed sensitivities are about 4 times as much for the 4 inch FOA clutch.

INPUTS	Tol	
	Original	
t clutch	0.500	0.005
r hub	0.300	0.003
r drum	1.060	0.005
r clutch	1.040	0.003
t outer	0.035	0.003
t inner	0.040	0.003
l outer	0.400	0.003
l inner	0.221	0.003
W outer slot	0.149	0.003
W inner slot	0.112	0.003
r hub arm	0.750	0.005
θ contact (high)	3.00	1
R outer round	0.050	0.003
R inner round	0.050	0.003
μ	0.250	0.03
ω operational	5000	0
indent outer	0.000	0.003
indent inner	0.000	0
ω contact eng	3429.7	
T operating	20.8	

Contact Engagement

Step	Sensitivity	Rk	Adjusted by Tol	NRk	% Cont
0.0001	0.0	15	0	14	0.0%
0.0001	4228.8	7	12.69	7	0.0%
0.0001	85097.7	3	425.49	1	50.0%
0.0001	-95622.8	1	-286.87	2	22.7%
0.0001	42988.9	4	128.97	4	4.6%
0.0001	95127.5	2	285.38	3	22.5%
0.0001	-816.9	12	-2.45	12	0.0%
0.0001	-4899.5	5	-14.70	5	0.1%
0.0001	2054.2	10	6.16	10	0.0%
0.0001	2054.2	10	6.16	10	0.0%
0.0001	0.0	15	0	14	0.0%
1	10.2	14	10.15	8	0.0%
0.0001	2240.3	9	6.72	9	0.0%
0.0001	-28.9	13	-0.09	13	0.0%
0.0001	0.0	15	0	14	0.0%
100	0.0	15	0	14	0.0%
0.0001	4701.3	6	14.10	6	0.1%
0.0001	4145.4	8	0	14	0.0%

Tolerance (Eng) = ± **601.8** rpm
 Std Dev (Eng) = ± **200.61** rpm

Torque

Step	Sensitivity	Rk	Adjusted by Tol	NRk	% Cont
0.0001	41.5	13	0.21	6	0.1%
0.0001	-54.6	8	-0.16	9	0.1%
0.0001	-880.7	3	-4.40	1	38.2%
0.0001	1097.7	1	3.29	2	21.4%
0.0001	-465.8	4	-1.40	5	3.8%
0.0001	-1027.6	2	-3.08	3	18.7%
0.0001	4.9	16	0.01	16	0.0%
0.0001	48.8	10	0.15	10	0.0%
0.0001	-46.7	12	-0.14	12	0.0%
0.0001	-47.0	11	-0.14	11	0.0%
0.0001	-14.8	15	-0.07	13	0.0%
3	0.0	17	0.05	15	0.0%
0.0001	-55.8	7	-0.17	8	0.1%
0.0001	-20.4	14	-0.06	14	0.0%
0.0001	99.4	5	2.98	4	17.5%
100	0.0	18	0.00	17	0.0%
0.0001	-57.1	6	-0.17	7	0.1%
0.0001	-52.7	9	0.00	17	0.0%

Tolerance (T) = ± **7.1** in-lb
 Std Dev (T) = ± **2.38** in-lb

A.4 FOA Sensitivity Chart when $\theta_{con} = 20$ degrees

This table contains the FOA clutch's parameter sensitivity values when θ_{con} was set to 20 degrees. θ_{con} became the most sensitive parameter in the torque model.

INPUTS		
	Original	Tol
t clutch	0.626	0.005
r hub	0.750	0.003
r drum	2.000	0.005
r clutch	1.950	0.003
t outer	0.067	0.003
t inner	0.066	0.003
l outer	0.900	0.003
l inner	0.800	0.003
W outer slot	0.300	0.003
W inner slot	0.100	0.003
r hub arm	0.950	0.005
θ contact (high)	20.00	2
R outer round	0.075	0.003
R inner round	0.075	0.003
μ	0.420	0
ω operational	3600	0
indent outer	0.050	0.003
indent inner	0.000	0
ω contact eng	2011.6	
T operating	847.1	

Contact Engagement						
Step	Sensitivity	Rk	Adjusted by Tol	NRk	% Cont	
0.0001	0.0	15	0.00	14	0.0%	
0.0001	1918.4	5	5.76	6	0.1%	
0.0001	20587.7	4	102.94	1	38.9%	
0.0001	-24212.6	2	-72.64	3	19.4%	
0.0001	22660.1	3	67.98	4	17.0%	
0.0001	24490.8	1	73.47	2	19.8%	
0.0001	-468.2	10	-1.40	10	0.0%	
0.0001	-574.1	8	-1.72	8	0.0%	
0.0001	396.2	12	1.19	12	0.0%	
0.0001	396.2	12	1.19	12	0.0%	
0.0001	0.0	15	0.00	14	0.0%	
1	17.8	14	35.56	5	4.6%	
0.0001	455.7	11	1.37	11	0.0%	
0.0001	495.9	9	1.49	9	0.0%	
0.0001	0.0	15	0.00	14	0.0%	
100	0.0	15	0.00	14	0.0%	
0.0001	1843.5	6	5.53	7	0.1%	
0.0001	1679.4	7	0.00	14	0.0%	

Tolerance (Eng) = ± 165.0 rpm
Std Dev (Eng) = ± 55.01 rpm

Torque						
Step	Sensitivity	Rk	Adjusted by Tol	NRk	% Cont	
0.0001	1353.2	6	6.77	6	0.7%	
0.0001	133.5	14	0.40	13	0.0%	
0.0001	-4817.9	5	-24.09	5	9.0%	
0.0001	8323.4	3	24.97	4	9.7%	
0.0001	-8361.6	2	-25.08	3	9.8%	
0.0001	-8830.4	1	-26.49	2	10.9%	
0.0001	131.4	15	0.39	14	0.0%	
0.0001	171.8	13	0.52	12	0.0%	
0.0001	-796.7	8	-2.39	8	0.1%	
0.0001	-485.2	11	-1.46	11	0.0%	
0.0001	-1294.6	7	-6.47	7	0.7%	
1	30.8	17	61.54	1	58.9%	←
0.0001	-705.4	10	-2.12	10	0.1%	
0.0001	-784.3	9	-2.35	9	0.1%	
0.0001	5140.5	4	0.00	16	0.0%	
100	0.7	18	0.00	16	0.0%	
0.0001	-99.0	16	-0.30	15	0.0%	
0.0001	426.2	12	0.00	16	0.0%	

Tolerance (T) = ± 80.2 in-lb
Std Dev (T) = ± 26.72 in-lb

A.5 FOA Performance Tolerance Verification

This two tables contain the entire manufacturing process' simulation data of (a) design parameter values, (a) manufacturing or design tolerances, and (b) results.

Parameters	Value	Units	Manufacturing or Design Tolerances					
			Metal			Accurate	Fine	
			Water jet	Laser	Injection	Stamping	Stamping *	Blanking
n _{segments}	3	in	0	0	0	0	0	0
t _{clutch}	0.636	in	0.020	0.005	0.003	0.002	0.001	0.0005
r _{hub}	0.750	in	0.020	0.005	0.003	0.002	0.001	0.0005
r _{drum}	2.000	in	0.020	0.005	0.003	0.002	0.001	0.0005
r _{clutch}	1.950	in	0.020	0.005	0.003	0.002	0.001	0.0005
t _{outer}	0.070	in	0.020	0.005	0.003	0.002	0.001	0.0005
t _{inner}	0.070	in	0.020	0.005	0.003	0.002	0.001	0.0005
l _{outer}	0.800	in	0.020	0.005	0.003	0.002	0.001	0.0005
l _{inner}	0.700	in	0.020	0.005	0.003	0.002	0.001	0.0005
w _{outer slot}	0.300	in	0.020	0.005	0.003	0.002	0.001	0.0005
w _{inner slot}	0.100	in	0.020	0.005	0.003	0.002	0.001	0.0005
r _{hub arm}	0.950	in	0.020	0.005	0.003	0.002	0.001	0.0005
θ _{contact (high)}	10.00	deg	3.0	3.0	3.0	3.0	3.0	3.0
R _{outer round}	0.075	in	0.020	0.005	0.003	0.002	0.001	0.0005
R _{inner round}	0.075	in	0.020	0.005	0.003	0.002	0.001	0.0005
μ	0.25		0	0	0	0	0	0
ω _{operational}	3600	rpm	0	0	0	0	0	0
indent _{outer}	0.05		0.020	0.005	0.003	0.002	0.001	0.0005
indent _{inner}	0		0	0	0	0	0	0

(a)

Operation - Tolerance -	Water jet 0.020	Laser 0.005	Metal Injection 0.003	Stamping 0.002	Accurate Stamping * 0.001	Fine Blanking 0.0005
----------------------------	--------------------	----------------	-----------------------------	-------------------	---------------------------------	----------------------------

Contact Engagement Speed

Average	2132.5 rpm	2144.7	2132.8	2132.8	2132.8	2132.8	2132.8
Std Dev	N/A rpm	321.8	80.2	49.4	34.2	20.6	15.5
Min	2000 rpm	960.5	1818.3	1933.8	1995.2	2049.4	2074.0
Max	N/A rpm	3536.6	2461.8	2330.2	2281.6	2222.9	2195.9
% Rejects		32.648%	4.888%	0.359%	0.005%	0.000%	0.000%

Torque Capacity

Average	241.3 in-lb	237.2	241.2	241.3	241.4	241.4	241.4
Std Dev	N/A in-lb	41.4	10.3	6.6	4.9	3.4	3.0
Min	200 in-lb	12.3	198.5	213.4	221.5	228.9	229.8
Max	N/A in-lb	354.1	279.2	267.8	262	255.9	255.7
% Rejects		18.445%	0.003%	0.000%	0.000%	0.000%	0.000%

Minimum Safety Factors

SF outer		1.49	2.34	2.55	2.62	2.72	2.75
% Rejects (below 2)		2.51%	0%	0%	0%	0%	0%
SF inner		1.3	2.08	2.25	2.3	2.37	2.41
% Rejects (below 2)		10.64%	0%	0%	0%	0%	0%
SF hubarm		1.37	1.86	1.95	2	2.05	2.05
% Rejects (below 2)		30.120%	0.069%	0.006%	0.000%	0.000%	0.000%

* Either a stamping processes that is held in tight controls or a fine blanking process that relaxes controls.

(b)

A.6 FOA Robust Design Parameter

The following table contains the FOA clutch's parameter values when the contact engagement speed and torque performance tolerances were minimized. It also contains the ending performance tolerance values and the minimum and maximum constraints set on both input and output parameters.

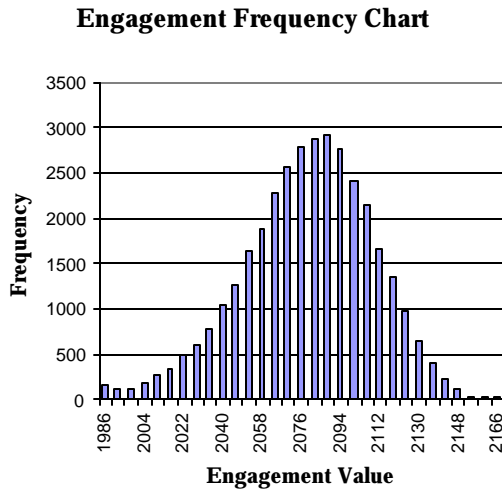
INPUTS	Constraints			
	Initial	Units	Min	Max
n segments	3	segs	N/A	N/A
t_{clutch}	0.626	in	N/A	N/A
r_{hub}	0.734	in	0.650	1.500
r_{drum}	2.000	in	N/A	N/A
r_{clutch}	1.919	in	1.850	1.990
$\delta_{clearance}$	0.081	in	0.030	N/A
t_{outer}	0.063	in	0.060	0.120
t_{inner}	0.060	in	0.060	0.120
l_{outer}	1.000	in	0.600	1.000
l_{inner}	0.767	in	0.600	0.850
$W_{outer\ slot}$	0.294	in	0.200	0.350
$W_{inner\ slot}$	0.075	in	0.075	0.150
$r_{hub\ arm}$	1.200	in	N/A	N/A
$\theta_{contact\ (high)}$	10.00	deg	10.00	30.00
$R_{outer\ round}$	0.075	in	N/A	N/A
$R_{inner\ round}$	0.075	in	N/A	N/A
μ	0.42	unitless	N/A	N/A
$\omega_{operational}$	3600	rpm	N/A	N/A
indent _{outer}	0.050	in	0.05	0.1
indent _{inner}	0	in	N/A	N/A
S_y	120000	psi	N/A	N/A
E	3.0E+07	lb/in ²	N/A	N/A
Density	0.283	lb/in ³	N/A	N/A

OUTPUTS		
Contact Engagement	Constraint	
Tolerance (Eng) = \pm	147.52 rpm	
Std Dev (Eng) = \pm	49.17 rpm	57.0
Min	2000.0 rpm	2000
Max	2295.0 rpm	2300

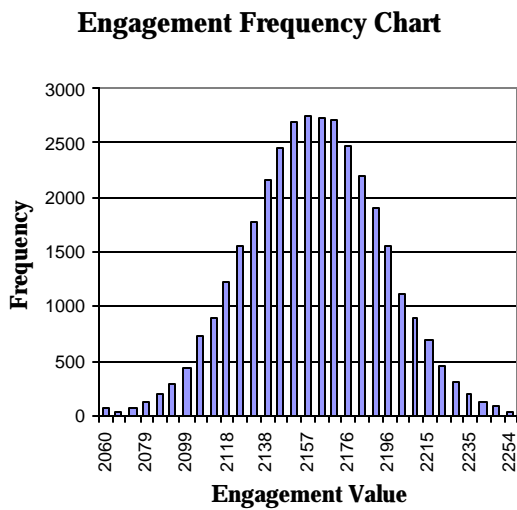
Torque		
Tolerance (T) = \pm	34.14 in-lb	49.5
Std Dev (T) = \pm	11.38 in-lb	16.5
Min	400.00 in-lb	400
Max	468.28 in-lb	

A.7 FOA Performance Frequency Chart

These frequency charts contain the FOA clutch's contact engagement speed and torque capacity performance data for the (a) free floating layer and (b) riveted layer simulations performed. Each simulation consisted of 35,000 trials.



(a)



(b)

A.8 Monte Carlo Layer Simulation

This table contains the Monte Carlo simulation data for the values of the FOA clutch's parameters, their associated tolerances, and if the parameter changes by the layer or by the clutch.

INPUTS					
	Average	Tol	Std Dev	Units	Changes by:
n_{segments}	3	0	0	segs	Clutch
t_{clutch}	0.6360	0.005	0.00167	in	Clutch
r_{hub}	0.7282	0.003	0.001	in	Layer
r_{drum}	2.0000	0.005	0.00167	in	Layer
r_{clutch}	1.9408	0.003	0.001	in	Layer
$\delta_{\text{clearance}}$	0.0592	0	0	in	Layer
t_{outer}	0.0694	0.003	0.001	in	Layer
t_{inner}	0.0647	0.003	0.001	in	Layer
l_{outer}	0.7989	0.003	0.001	in	Layer
l_{inner}	0.6991	0.003	0.001	in	Layer
$W_{\text{outer slot}}$	0.2874	0.003	0.001	in	Layer
$W_{\text{inner slot}}$	0.0902	0.003	0.001	in	Layer
$r_{\text{hub arm}}$	0.9282	0.005	0.00167	in	Clutch
$\theta_{\text{contact (high)}}$	10.00	2	0.66667	deg	Layer
$R_{\text{outer round}}$	0.0750	0.003	0.001	in	Layer
$R_{\text{inner round}}$	0.0750	0.003	0.001	in	Layer
μ	0.25	0	0	unitless	Clutch
$\omega_{\text{operational}}$	3600	0	0	rpm	Clutch
$\text{indent}_{\text{outer}}$	0.0500	0.003	0.001	in	Layer
$\text{indent}_{\text{inner}}$	0	0	0	in	Layer

Engagement and Torque Values		
$\omega_{\text{contact eng}}$	2158.5	rpm
$T_{\text{operating}}$	241.3	in-lb

TEST SET-UP AND TEST RESULTS

B.1 Dynamometer



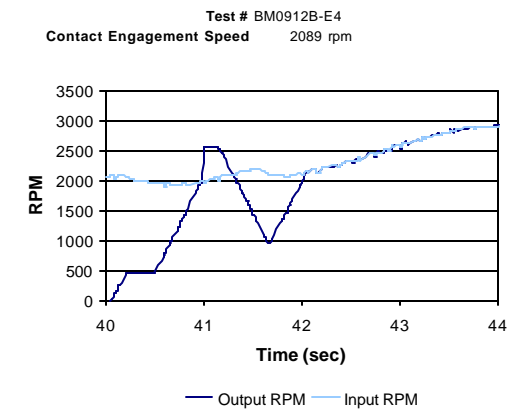
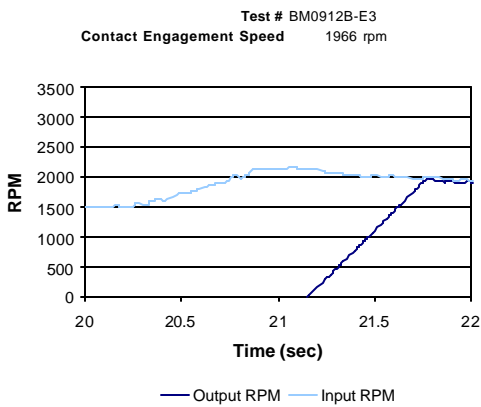
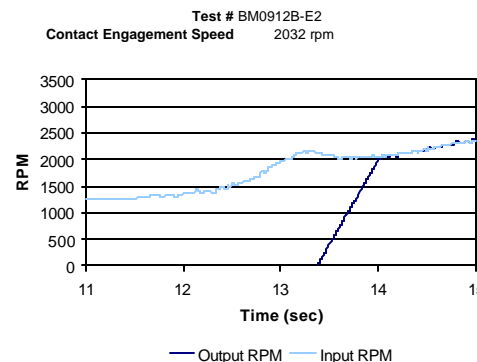
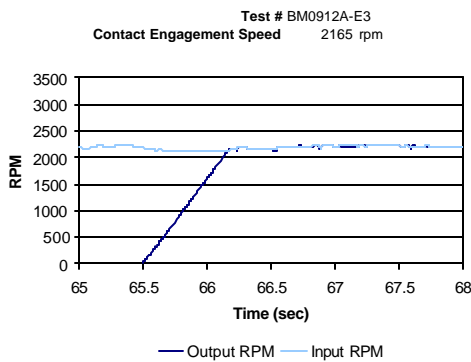
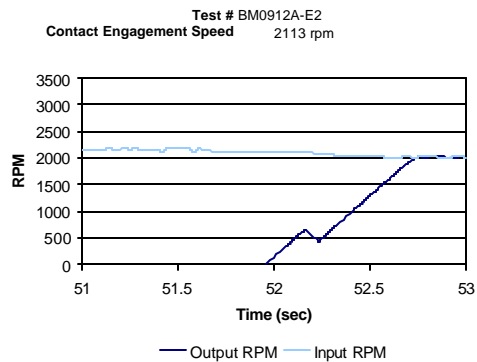
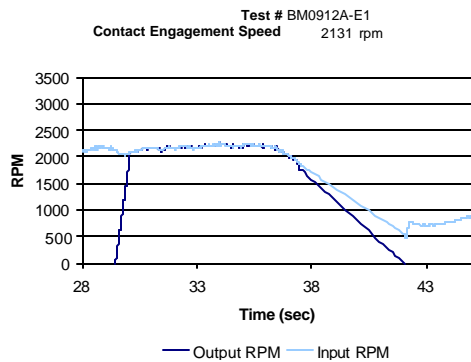
The DYNomite Land and Seas dynamometer was used to gather all clutch test data. The Dynomite consist of a 9" toroid water break absorber, electronic torque arm transducer, data wiring harness, and data acquisition computer. The dynamometer uses a manual water brake load valve to apply a torque load to the output shaft, while the torque arm transducer records the transmitted torque from the engine.

The data acquisition computer records 200 recordings per second. The torque transducer is an environment sealed strain gauge with ½% of full scale typical accuracy and semi-automatic zero offset calibration. The torque capacity of the Dynomite ranges from 5 to 200 ft.-lbs. Its RPM capacity ranges from 1,000 to 12,000. The engine tachometer measures from 0 to 32,000 RPM.

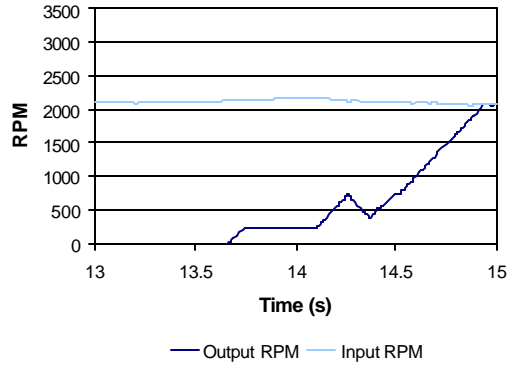
B.2 Benchmark Clutch

B.2.1 Benchmark Contact Engagement Speed Data

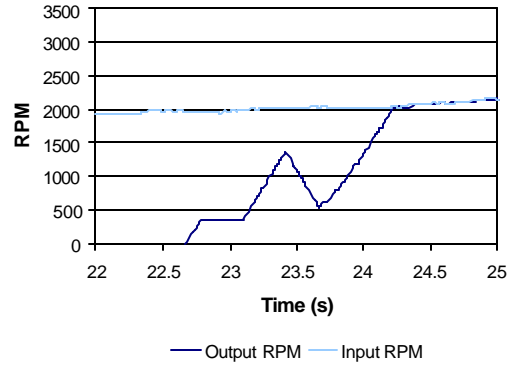
The following data shows the smoothness of engagement and the contact engagement for the Hoffco-Comet 4 inch go-kart clutch. The method used for gathering the data was the *RPM Contact Engagement Test Procedure*.



Test # BM0912C-E1
Contact Engagement Speed 2067 rpm

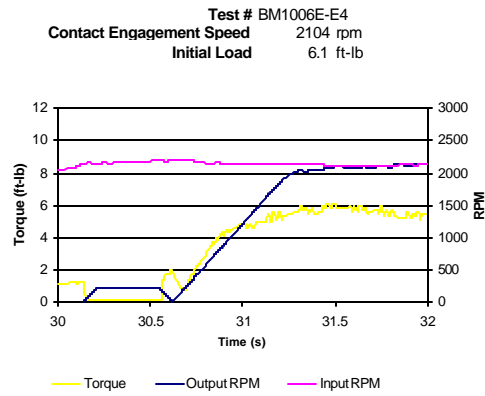
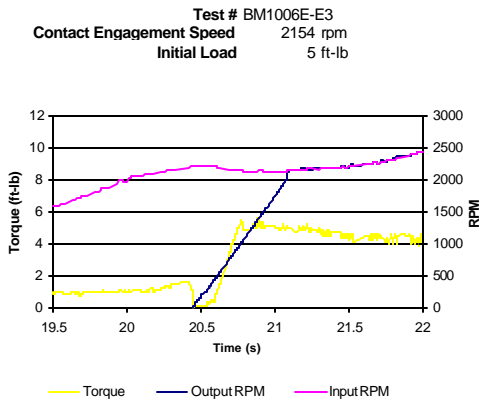
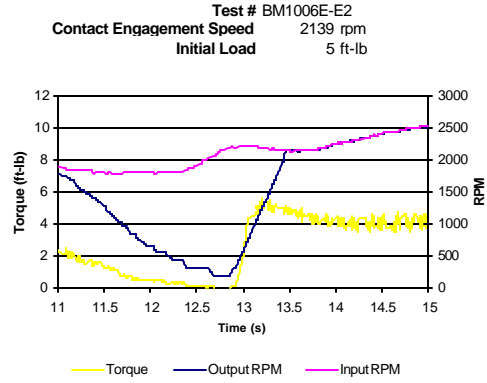
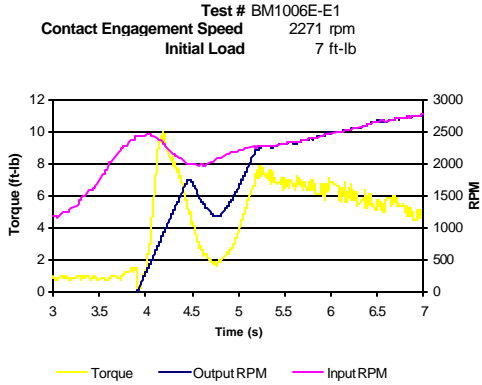


Test # BM0912C-E2
Contact Engagement Speed 2047 rpm



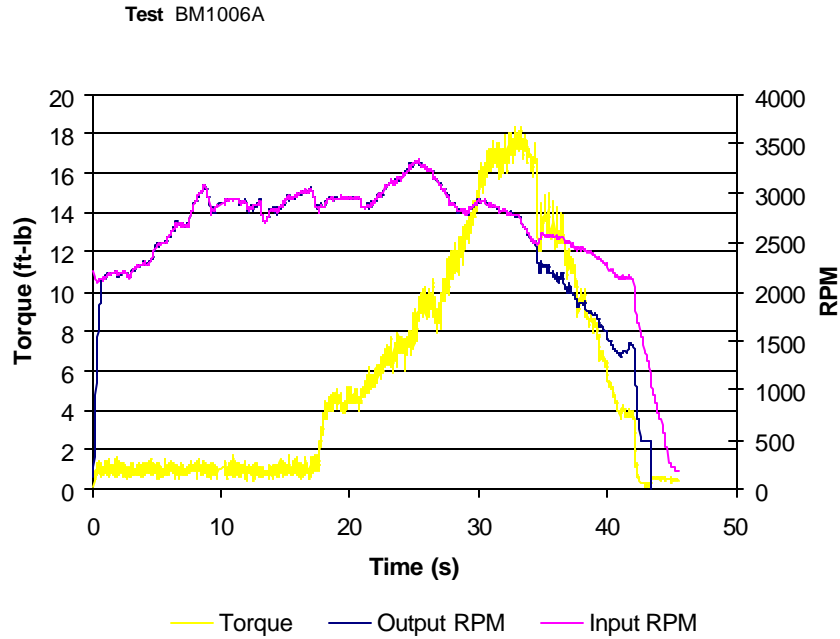
B.2.2 Benchmark Engagement Speed Data

The following data shows the smoothness of engagement and engagement speed for the Hoffco-Comet 4 inch go-kart clutch. The method used for gathering the data was the *RPM Engagement Test Procedure*.



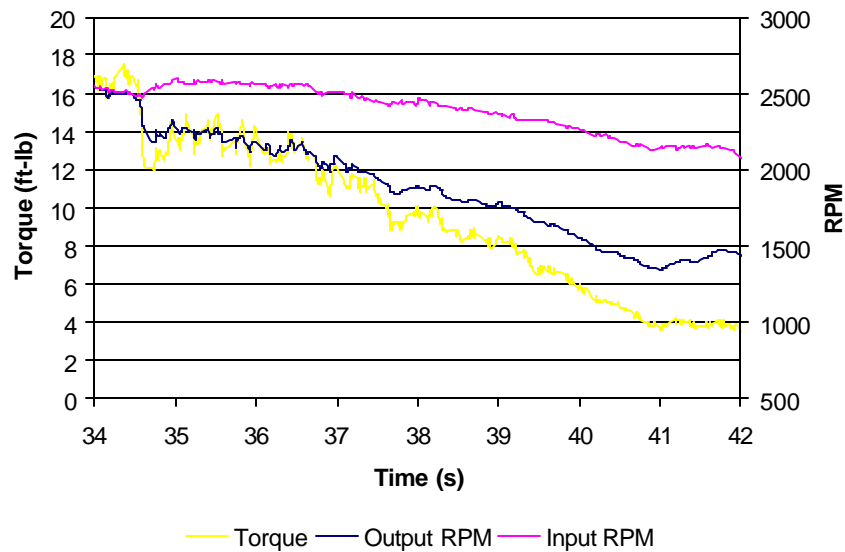
B.2.3 Benchmark Torque Capacity Data

The following data shows the torque capacity for the Hoffco-Comet 4 inch go-kart clutch. The method used for gathering the data was the *Torque Test Procedure*. Maximum torque capacity happens at point where the output shaft slips from the input shaft.

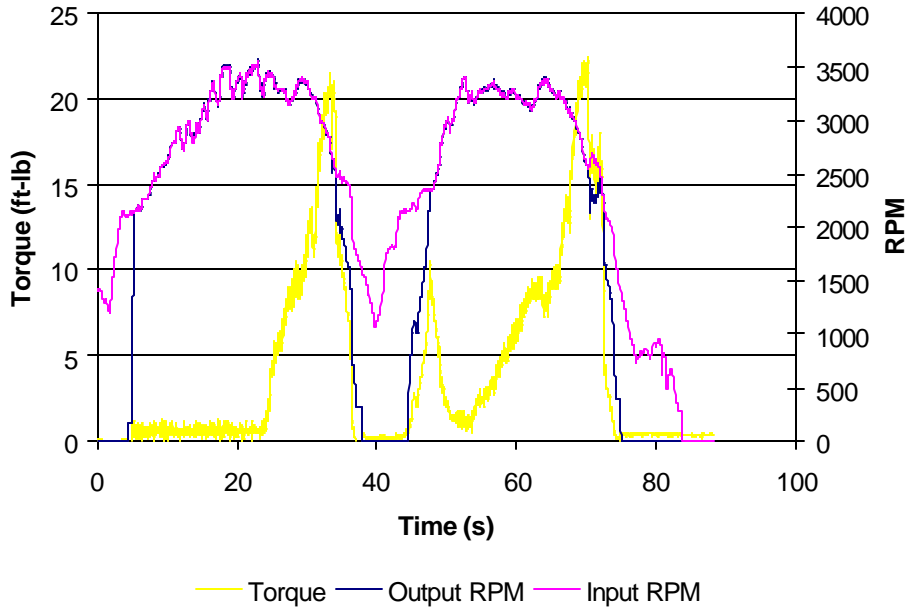


Test # BM1006A-T1

Eng	N/A	rpm
Torque	17.7 ft-lb at	2665 rpm
Slippage	14.4 ft-lb at	2474 rpm



Test BM1006A

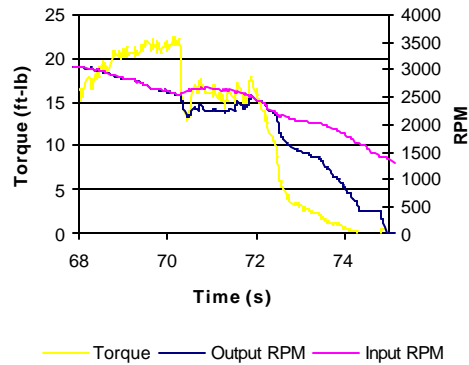
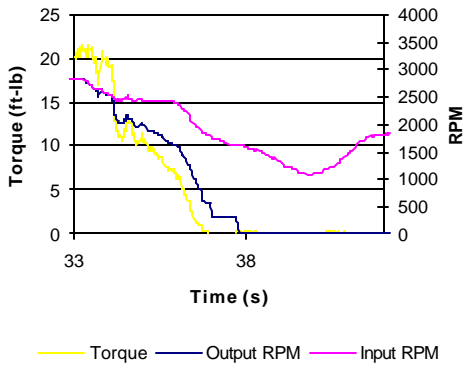


Test # BM1006B-T1
Eng N/A

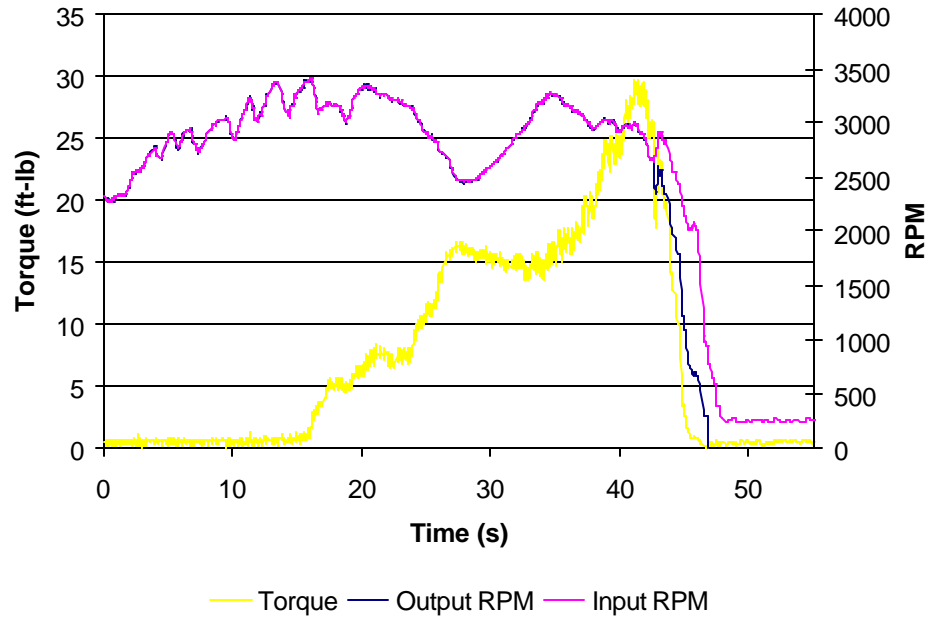
Torque	21.5 ft-lb at	2648 rpm
Slippage	18.7 ft-lb at	2494 rpm

Test # BM1006B-T2
Eng N/A

Torque	21.3 ft-lb at	2563 rpm
Slippage	21.3 ft-lb at	2563 rpm

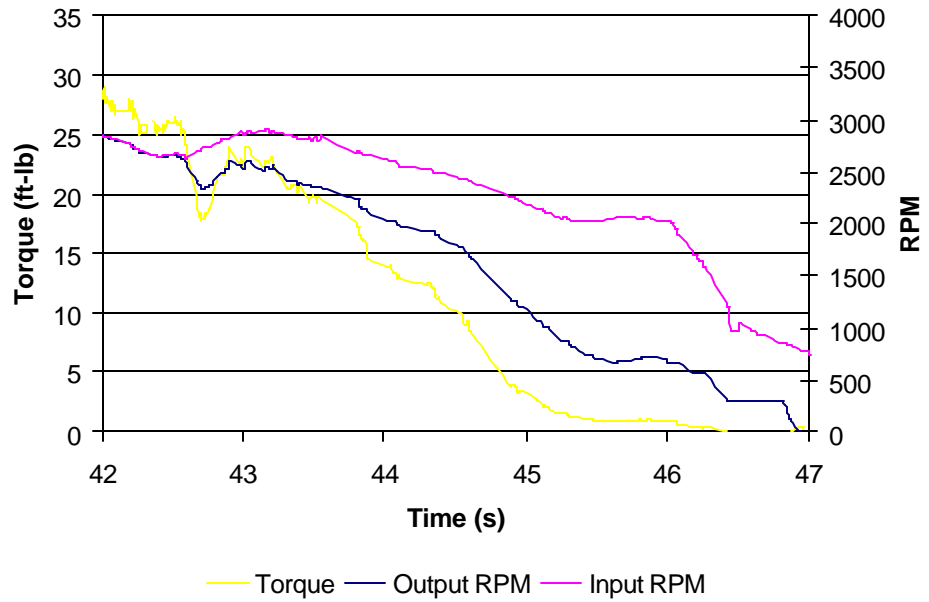


Test BM1006C

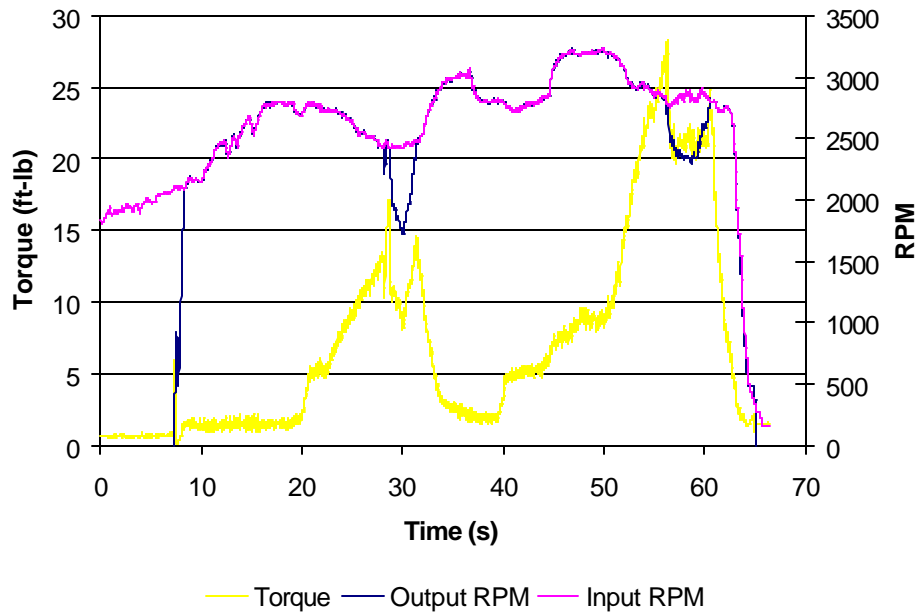


Test # BM1006C-T1

RPM	N/A	
Torque	29.7 ft-lb at	2994 rpm
Slippage	26.1 ft-lb at	2660 rpm

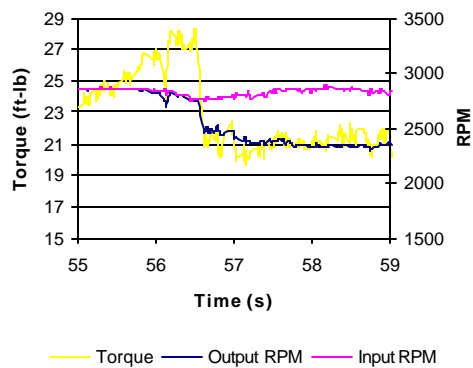
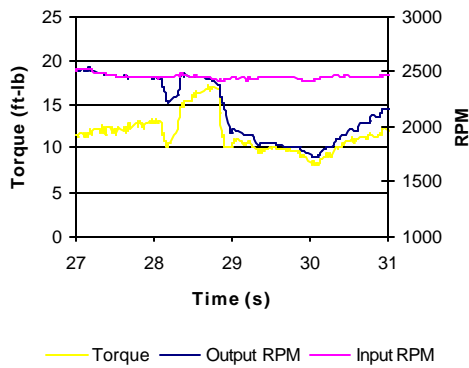


Test BM1006D



Test # BM1006D-T1
 RPM N/A
 Torque 16.5 ft-lb at 2422 rpm
 Slippage 16.5 ft-lb at 2422 rpm

Test # BM1006D-T2
 RPM N/A
 Torque 28.3 ft-lb at 2779 rpm
 Slippage 28.3 ft-lb at 2779 rpm



B.3 Multi-layer Floating Opposing Arm (MFOA) Clutch

B.3.1 MFOA Model Parameter Values

The following values are the model parameters for the (a) MFOA vA clutch and the the MFOA vB clutch that were fabricated and tested. The torque values are given for a μ of 0.42 and a r_{hubarm} of 0.95 inches.

INPUTS		
	Value	Units
n segments	3	segs
t _{clutch}	0.626	in
r _{hub}	0.750	in
r _{drum}	2.000	in
r _{clutch}	1.950	in
δ _{clearance}	0.050	in
t _{outer}	0.070	in
t _{inner}	0.070	in
l _{outer}	0.800	in
l _{inner}	0.700	in
W _{outer slot}	0.300	in
W _{inner slot}	0.100	in
r _{hub arm}	0.950	in
θ _{contact (high)}	10	deg
R _{outer round}	0.075	in
R _{inner round}	0.075	in
μ	0.42	unitless
ω _{operational}	3600	rpm
indent _{outer}	0.050	in
indent _{inner}	0.000	in
S _y	120000	psi
E	30000000	lb/in ²

OUTPUTS		
	Value	Units
ω _{contact eng}	2139.3	rpm
T _{operating}	584.6	in-lb
	48.7	ft-lb

(a)

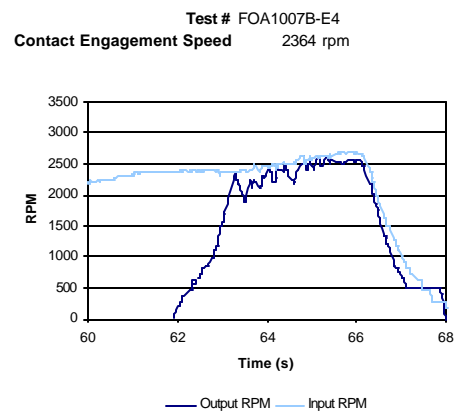
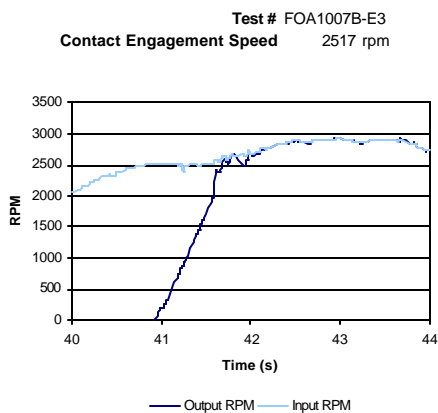
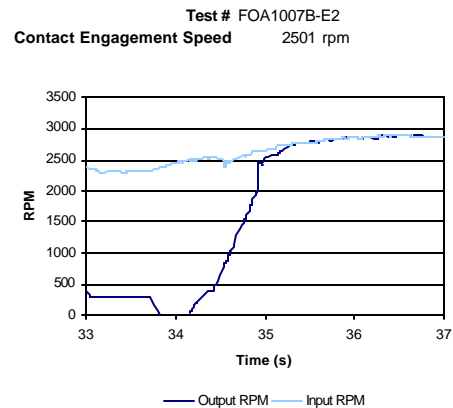
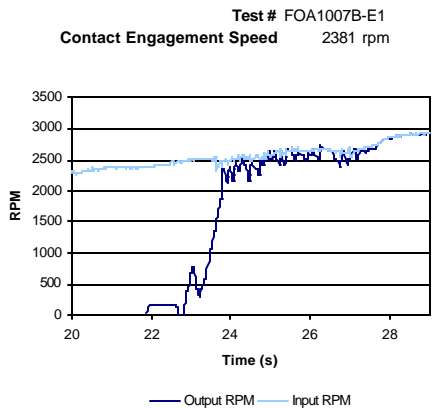
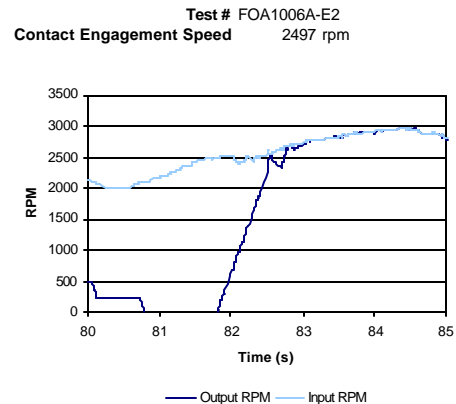
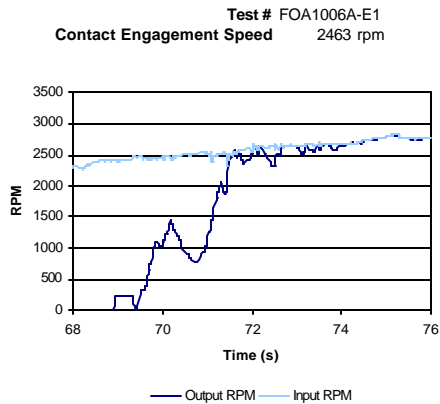
INPUTS		
	Value	Units
n segments	3	segs
t _{clutch}	0.626	in
r _{hub}	0.750	in
r _{drum}	2.000	in
r _{clutch}	1.950	in
δ _{clearance}	0.050	in
t _{outer}	0.067	in
t _{inner}	0.066	in
l _{outer}	0.900	in
l _{inner}	0.800	in
W _{outer slot}	0.300	in
W _{inner slot}	0.100	in
r _{hub arm}	0.950	in
θ _{contact (high)}	20	deg
R _{outer round}	0.075	in
R _{inner round}	0.075	in
μ	0.42	unitless
ω _{operational}	3600	rpm
indent _{outer}	0.050	in
indent _{inner}	0.000	in
S _y	120000	psi
E	30000000	lb/in ²

OUTPUTS		
	Value	Units
ω _{contact eng}	2011.6	rpm
T _{operating}	847.1	in-lb
	70.6	ft-lb

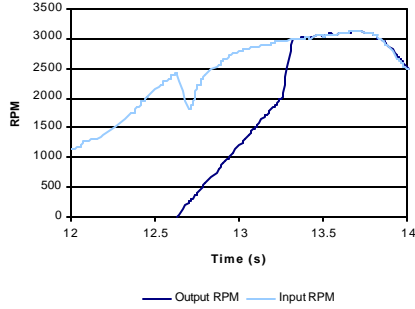
(b)

B.3.2 MFOA vA SHA Contact Engagement Speed Data

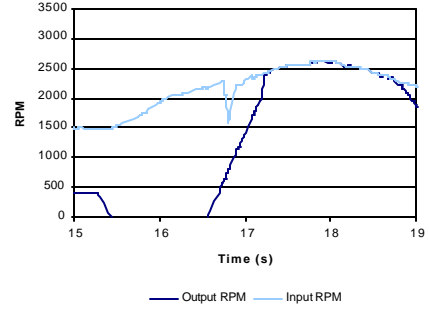
The following data shows the smoothness of engagement and the contact engagement for the MFOA vA clutch with the small hub arms (0.95 inches). The method used for gathering the data was the *RPM Contact Engagement Test Procedure*.



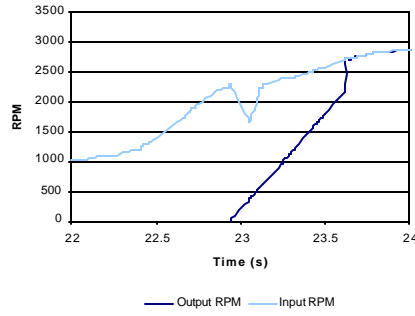
Test # FOA1007C-E1
Contact Engagement Speed 2410 rpm



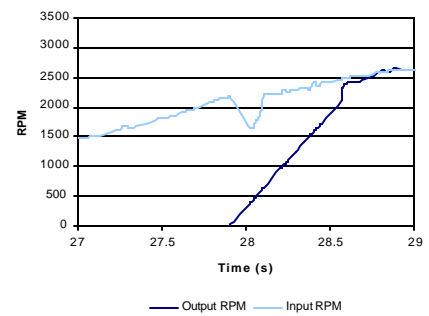
Test # FOA1007C-E2
Contact Engagement Speed 2273 rpm



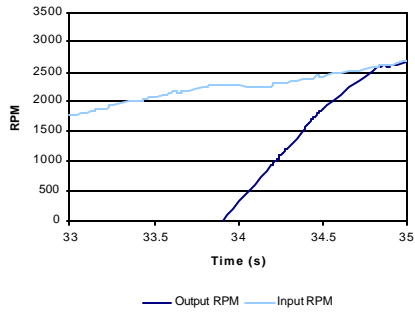
Test # FOA1007C-E3
Contact Engagement Speed 2235 rpm



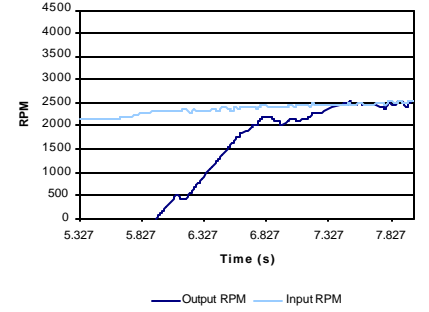
Test # FOA1007C-E4
Contact Engagement Speed 2171 rpm



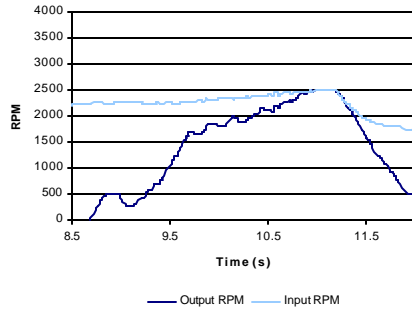
Test # FOA1007C-E5
Contact Engagement Speed 2264 rpm



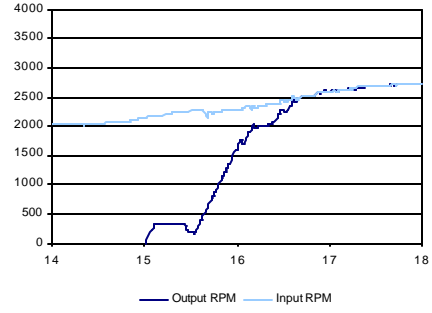
Test # FOA1008A-E1
Contact Engagement Speed 2308 rpm



Test # FOA1008B-E1
Contact Engagement Speed 2256

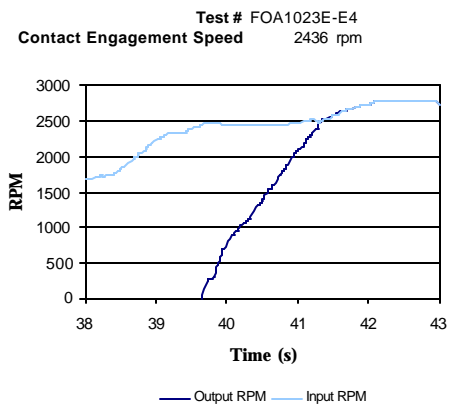
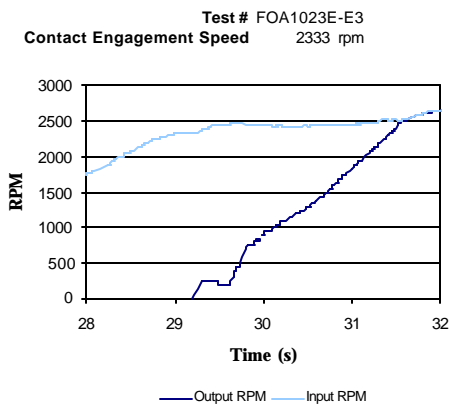
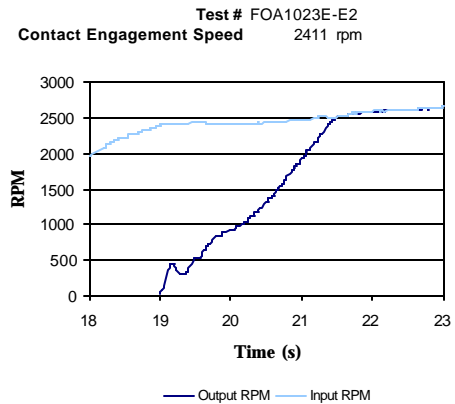
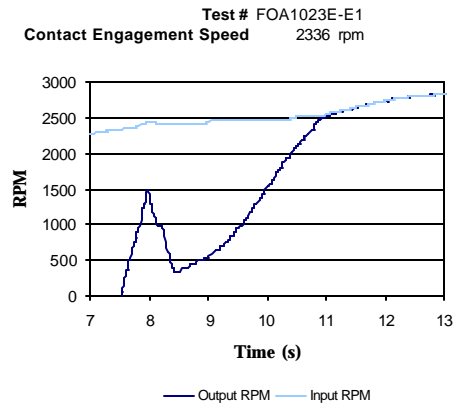


Test # FOA1008B-E2
Contact Engagement Speed 2175



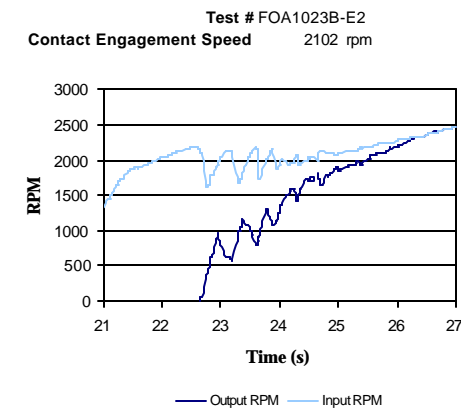
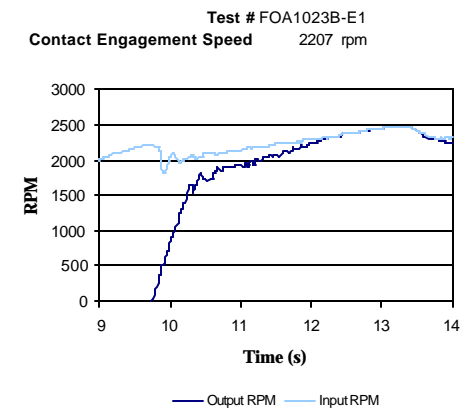
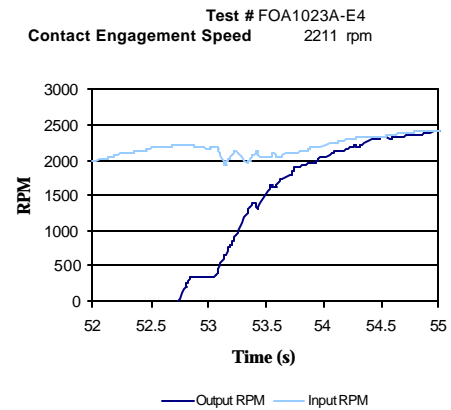
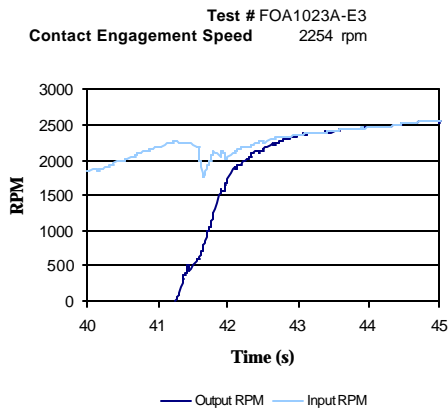
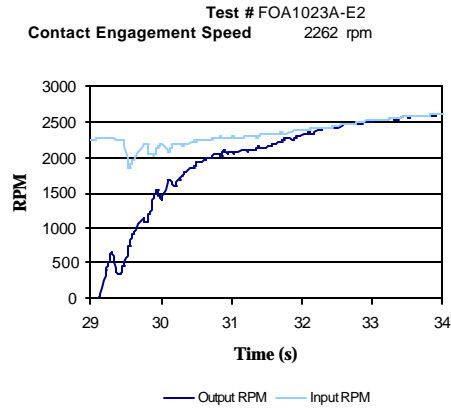
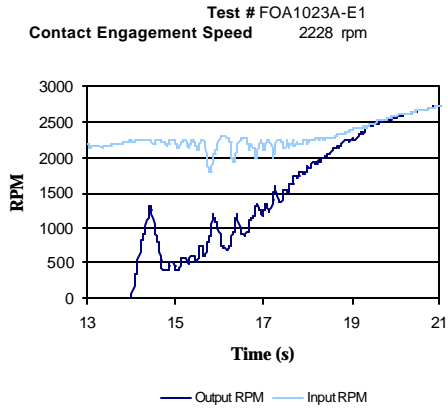
B.3.3 MFOA vA LHA Contact Engagement Speed Data

The following data shows the smoothness of engagement and the contact engagement for the MFOA vA clutch with the long hub arms (1.25 inches). The method used for gathering the data was the *RPM Contact Engagement Test Procedure*.

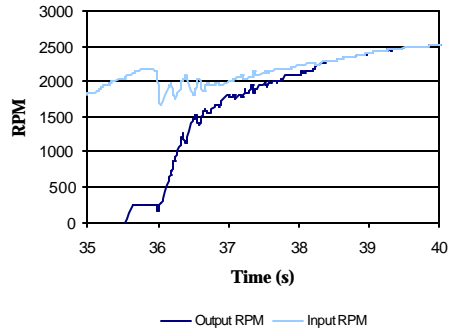


B.3.4 MFOA vB SHA Contact Engagement Speed Data

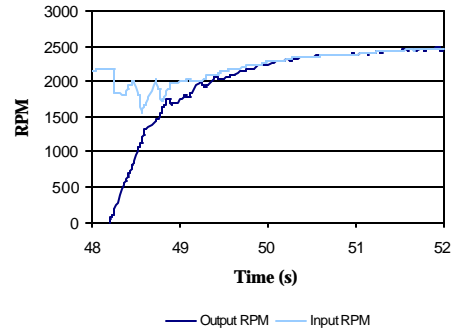
The following data shows the smoothness of engagement and the contact engagement for the MFOA vB clutch with the short hub arms (0.95 inches). The method used for gathering the data was the *RPM Contact Engagement Test Procedure*.



Test # FOA1023B-E3
Contact Engagement Speed 2066 rpm

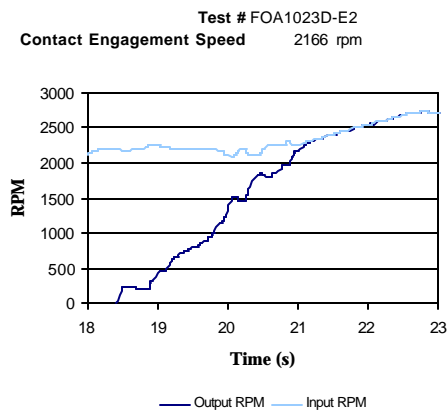
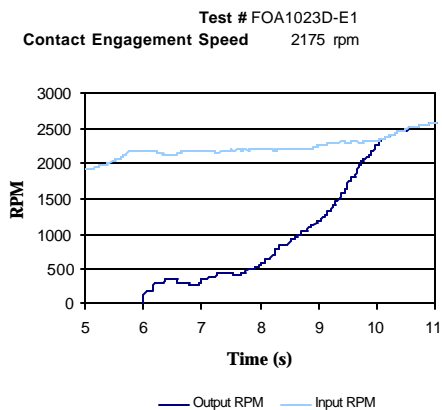
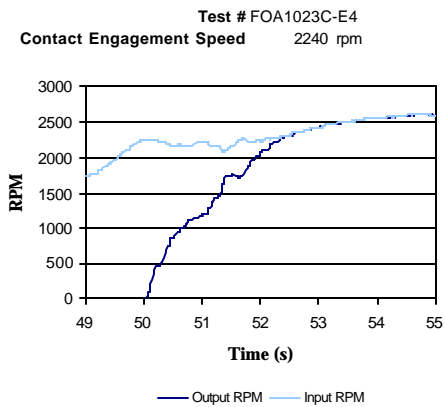
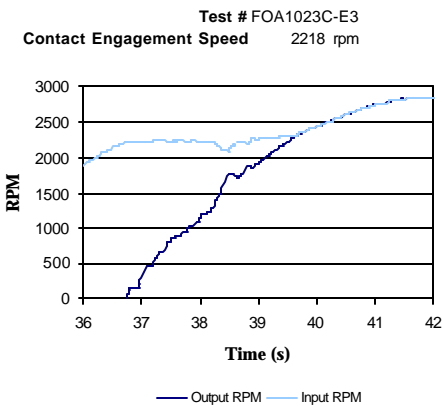
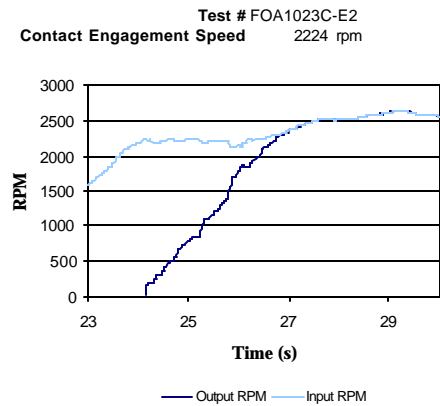
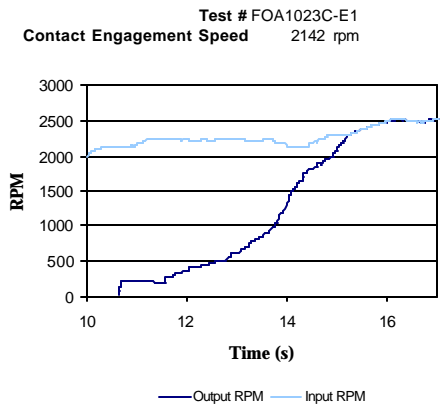


Test # FOA1023B-E4
Contact Engagement Speed 2165 rpm

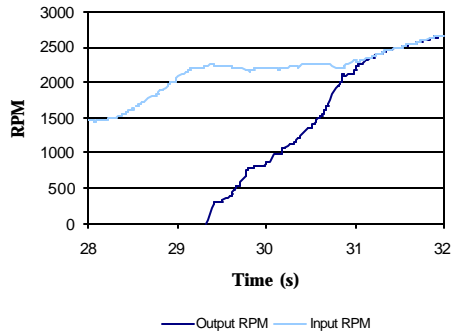


B.3.5 MFOA vB LHA Contact Engagement Speed Data

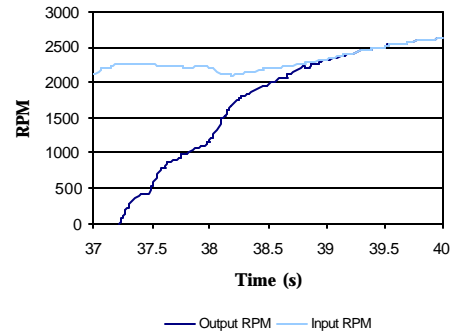
The following data shows the smoothness of engagement and the contact engagement for the MFOA vB clutch with the long hub arms (1.25 inches). The method used for gathering the data was the *RPM Contact Engagement Test Procedure*.



Test # FOA1023D-E3
Contact Engagement Speed 2228 rpm

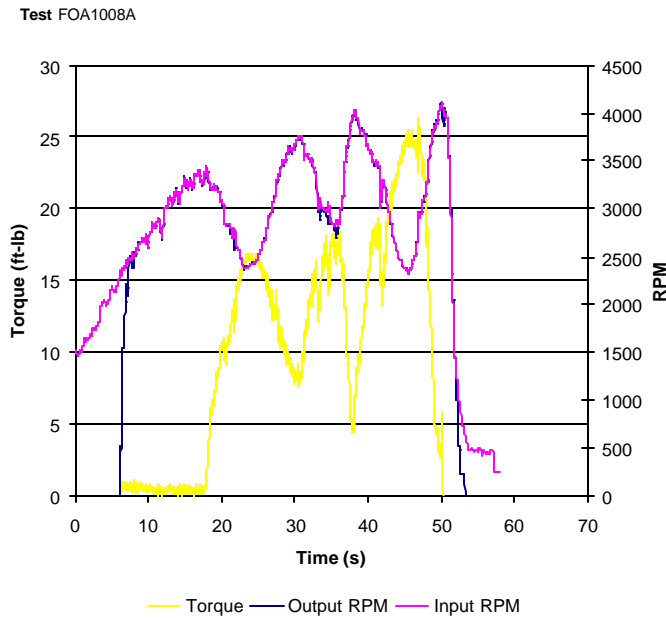


Test # FOA1023D-E4
Contact Engagement Speed 2251 rpm



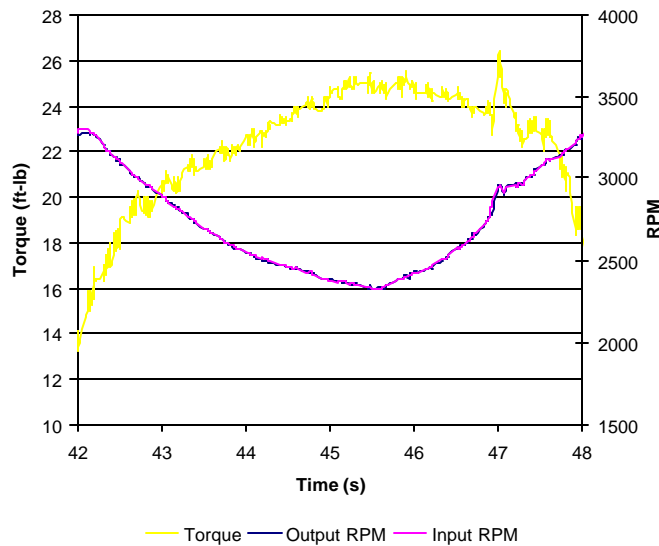
B.3.6 MFOA vA SHA Torque Capacity Data

The following data shows the torque capacity for the MFOA vA clutch with short hub arms (0.95 inches). The method used for gathering the data was the *Torque Test Procedure*. Maximum torque capacity happens at point where the output shaft slips from the input shaft.

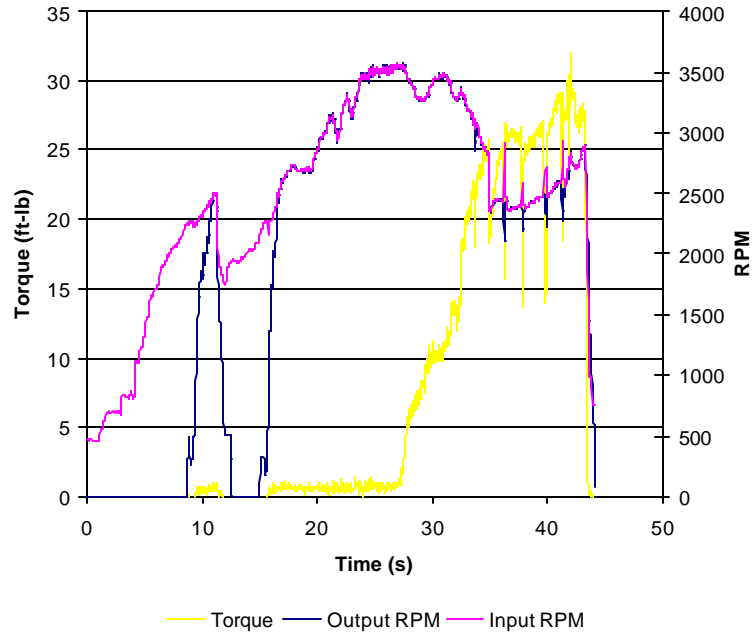


Test # FOA1008A

Eng	N/A	rpm
Torque	16.8 ft-lb at	2432 rpm
Torque	18.5 ft-lb at	2823 rpm
Torque	25.1 ft-lb at	2420 rpm

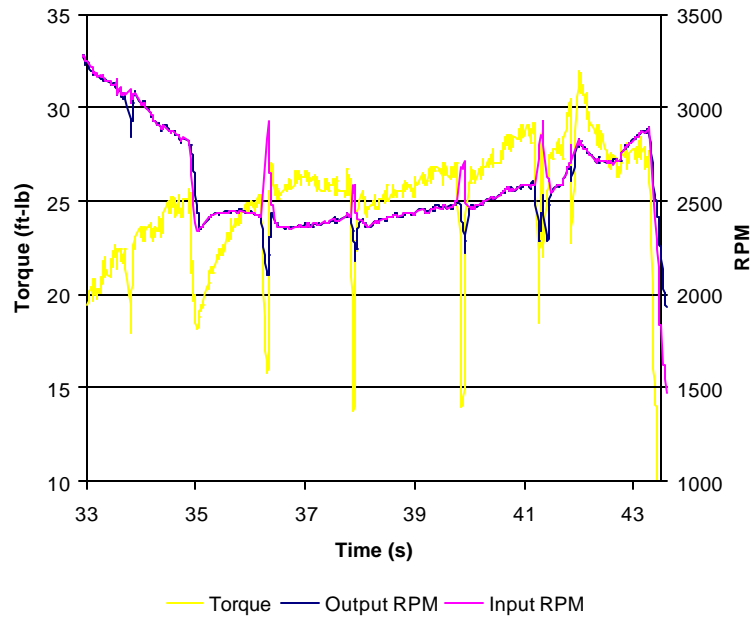


Test FOA1008B



Test # FOA1008B

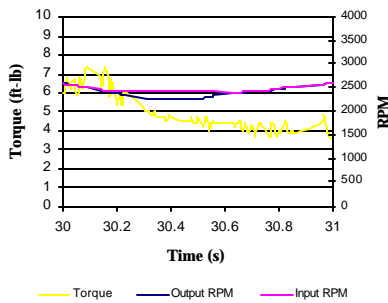
Eng	N/A	rpm	
Torque	25.4 ft-lb	at	2654 rpm
Torque	31.3 ft-lb	at	2776 rpm



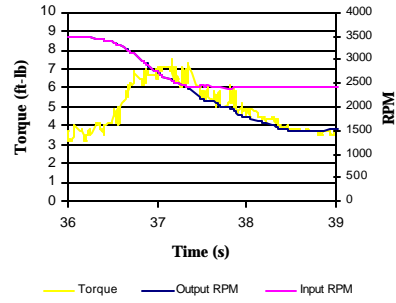
B.3.7 MFOA vB LHA Torque Capacity Data

The following data shows the torque capacity for the MFOA vA clutch with long hub arms (1.25 inches). The method used for gathering the data was the *Torque Test Procedure*. Maximum torque capacity happens at point where the output shaft slips from the input shaft.

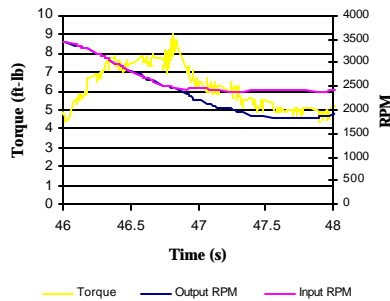
Test # FOA1023F-T1
Slippage 6.7 ft-lb at 2432 rpm



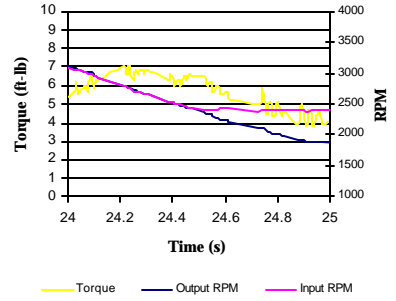
Test # FOA1023F-T2
Slippage 7 ft-lb at 2420 rpm



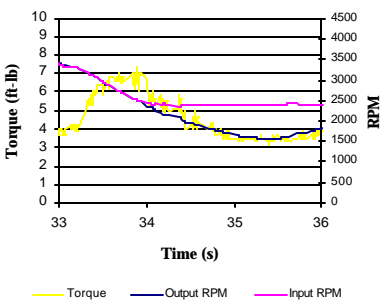
Test # FOA1023F-T3
Slippage 7 ft-lb at 2459 rpm



Test # FOA1023G-T1
Slippage 6.5 ft-lb at 2458 rpm



Test # FOA1023G-T2
Slippage 7 ft-lb at 2469 rpm



Test # FOA1023G-T3
Slippage 6.5 ft-lb at 2423 rpm

